Multiple-Phase Trajectory Optimization for Formation Flight in Civil Aviation

Master of Science Thesis

M.E.G. van Hellenberg Hubar

Technische Universiteit Delft

A350
A350
QATAR
A350 XWB Launch Customer
A350
A350
AIRBUS A350
Around the world
AIRBUS A350
A350

TU Delft

Cover photo: Copyright AIRBUS S.A.S. 2014 – photo by S.Ramadier
(http://aviationweek.com/blog/photo-airbus-a350-formation-flight)

Multiple-Phase Trajectory Optimization for Formation Flight in Civil Aviation

Master of Science Thesis

by

M.E.G. van Hellenberg Hubar

in partial fulfillment of the requirements for the degree of

Master of Science
in Aerospace Engineering

at the Delft University of Technology,
to be defended publicly on Tuesday July 19, 2016 at 2:00 PM.

Supervisor (Primary):	Dr. ir. H.G. Visser	
Supervisor (Secondary):	Dr. ir. S. Hartjes	
Thesis committee:	Dr. ir. H.G. Visser	TU Delft
	Dr. ir. S. Hartjes	TU Delft
	Dr. ir. E. van Kampen	TU Delft

This thesis is confidential and cannot be made public until July 19, 2016.

An electronic version of this thesis is available at http://repository.tudelft.nl/.

Delft
University of
Technology

Summary

In this research the focus is on developing a tool that can optimize multiple-phase trajectories for commercial formation flights for minimum fuel consumption. In the past years, research has been conducted into formation flight and trajectory optimization, but not as a combined entity. Researchers have investigated the aerodynamics behind formation flight and conducted flight tests to validate their results. The results show that a significant reduction in induced drag of 10-50% can be obtained for the trailing aircraft in a formation. Others, investigated the optimal routing for commercial aircraft and what the savings of formation flight could be when applied to certain flights. The trajectories of aircraft that join in formation, however, deviate from their optimal individual trajectories. What effect does formation flight have on the trajectories and where should the aircraft that will join in formation meet and split-up? These are questions that have not been answered yet.

The research conducted in this study focuses on answering these questions by developing a tool that optimizes the trajectories of each aircraft in a formation such that the total fuel consumption is minimal. This question leads to the following research objective:
"To minimize the overall fuel consumption or Direct Operating Cost (DOC) of commercial aircraft flying in formation by developing a multiple-phase optimal control formulation."

From this research objective, the following research question is derived:
"Is it possible to develop a tool that optimizes the multiple-phase trajectories for two or three commercial aircraft flying in formation weighing the reduced fuel consumption, due to induced drag reduction, versus economic factors using a dynamic optimization technique?"

When an aircraft flies through the sky it leaves an upwash behind it and when another aircraft flies through this upwash it experiences a reduction in induced drag, which leads to a reduction in fuel consumption. Different formation constellations and the relative positioning of the aircraft within the formation influence the amount of induced drag reduction. However, this study does not focus on this issue and during the experiments 25% reduction in induced drag is assumed for the trailing aircraft in a two-aircraft formation. There are multiple phases that are considered in the assembly and disassembly of a formation. For a two-aircraft formation, five phases are identified: the first two phases are from the departure points of both aircraft to the rendezvous point, the third is a joint phase from the rendezvous point to the split-up point and the fourth and fifth phases are from the split-up point to both destination airports. As the aircraft only fly in formation in phase 3, the reduction in induced drag is only valid for this phase.

The structure of the developed optimization tool can be divided into three parts, the optimization framework, the input and the output. The optimization framework allows optimizing for both minimum fuel burn and minimum DOC and uses a MatLab based optimization software called GPOPS that is able to solve multiple-phase optimal control problems using pseudospectral methods. The framework contains the differential-algebraic equations that define the aircraft model as well. The solo phases are represented by an intermediate point-mass dynamic model and the formation phases by a more simplified energy-state dynamic model. These dynamic aircraft performance models are linked to each other at the beginning and end of the phases. For the input, atmospheric data is required and three aircraft types are considered: the Boeing 737-300 (B733), the Boeing 747-400 (B744) and the McDonnell Douglas MD-11 (MD-11). When in formation, a formation flight induced drag fraction ϵ is implemented in the aircraft models. Several constraints are implemented in the tool as well (e.g. constraints on altitude, velocity, final weight, thrust level and duration of the formation segment). The output of the tool gives the state and control variables of all aircraft for all points in time and with these variables, the trajectories can be replicated and the fuel burn, distance flown and flight time per aircraft can be obtained. Furthermore, the implementation of schedule disturbances and wind contributed to make the tool more

realistic. The developed tool has been validated by comparing the results with the aircraft performance manuals of the manufacturers and by replicating a case study of other research reported in the literature and comparing the results.

Several experiments were conducted to investigate the benefits of formation flight. A common result all experiments showed is that in a formation the leading aircraft, due to the detour it must fly, consumes more than compared to its corresponding solo flight. Often, however, the reduction of the trailing aircraft is high enough to render the total fuel consumption for all aircraft in the formation lower than the total solo consumption. Also, the flight times and track distances increase when formation flight is applied. This is due to the fact that aircraft must fly a detour to meet-up. Existing scheduled flights have been replicated and the developed tool showed that combining two daily KLM flights, KLM can save over 1.2 million kilograms of fuel per year and when two SkyTeam flights (one KLM and one Delta) join in formation they can yearly save over 2.3 million kilograms of fuel. Furthermore, experiments demonstrated that combining different aircraft types in a formation affect the formation, and the sequence of the aircraft in a formation influences the results as well. The experiments showed that when combining a B744 with a MD-11, the aircraft will only join in formation when the B744 is the trailing aircraft. When the B744 is designated to lead the formation, the results showed that flying in formation is not beneficial. This is due to different performance characteristics of the aircraft. In another experiment, the results of departure delay for one of the aircraft in the formation are investigated. This revealed that not only the on-time aircraft slows down and the delayed aircraft speeds up, but the rendezvous point location shifts as well. The location of the rendezvous point shifts towards the split-up point, while it also shifts sideways towards the delayed flight. To investigate the effects of wind on the formation, another experiment was conducted. A wind-field was modelled across the North-Atlantic Ocean and a set of eastbound flights was compared with a set of westbound flights. The westbound flights, which encounter headwinds, divert North to encounter less wind and feature a larger formation segment (and a relatively larger reduction in fuel burn) compared to the eastbound flights. Finally, an experiment containing three aircraft in formation was conducted. The results of this experiment were not further discussed, but the experiment showed that the tool is able to optimize the trajectories for more than two aircraft joining in formation.

All experiments are optimized for minimum fuel consumption because it is less straightforward to determine the DOC, as it consists of costs that are different per airline and flight. A sensitivity analysis was conducted to explore the effect of shifting the optimization focus (from optimal for fuel to optimal for time) for a set of flights. This showed that, although the results are dependent of the flight properties (route, aircraft type, wind, etc.), compared to the corresponding solo flights, formation flight can offer significant reductions in fuel consumption without increasing the flight time. Another sensitivity analysis was conducted to investigate what the effect would be on the results, when the induced drag reduction due to formation flight is altered. For this analysis, the assumed reduction in induced drag on the trailing aircraft varied from 0-50% of the total induced drag. This resulted in a change in results in terms of trajectories (shift in rendezvous point location), fuel burn and flight time. However, these changes are as expected (a higher reduction in drag results in less fuel burn and vice versa), which means the developed tool is robust for different values of induced drag reductions.

In this study an optimization tool was developed to optimize the trajectories of multiple aircraft that join in formation for minimum fuel consumption or DOC. This tool can be developed further to enable, for example, airlines to explore the benefits of formation flight; on a greater scale including an entire flight schedule. Furthermore, the results of the performed experiments indicate that formation flight can lead to significant fuel reduction compared to flying solo. These results could prompt further development of aviation regulations to allow formation flight, as this can be a short-term fuel saving solution.

Acknowledements

A little less than one year ago, before I started my thesis, I was sceptic because I thought that this project would mean that I would have to spend almost a year, working all alone, on a subject that would not necessarily interest me. However, looking back on my last 10 months, I must admit, I had a good time. I am very glad I picked this project to finish my Masters at the faculty of Aerospace Engineering. I enjoyed the topic of my thesis, had great support from my supervisors and had a good time with my colleagues. Therefore, I would like to thank everybody who contributed to this project and/or supported me during this period. In particular, I want to thank:

My first supervisor during this project, Dr.ir. H.G. Visser. Dries, thank you for always making time for me every time I stopped by. Your enthusiasm for this research and for science in general, had a very motivating effect on me and your critical view on matters challenged me to improve my work. I hope I haven't stressed you too much by keeping a tight planning.

My second supervisor, Dr.ir. S. Hartjes. Sander, thank you for your time explaining GPOPS to me and for always sharing your thoughts and experience with me on my problems. Your positive and open attitude made it very easy to approach you, which I really appreciated.

My parents, for supporting me my whole life and especially throughout my study time. I know I took my time and I want to thank you for allowing me to do so. Thanks for always helping me out and for always taking care of me. Ma, thanks for making time to extensively read my work and give me feedback on it. Pa, thanks for sharing your experience with me.

My brothers and sister, for believing in me and motivating me. Thank you for distracting me from my studies when I needed it, while at the same time pushing me to finish. Fil, thanks for sharing your experience on things with me and keeping me sharp to stay on top of things. Steve, thanks for being a good roommate allowing me to study at home when necessary and thanks for all the good food you cook when I am home late. Carlot, thanks for being you and making me laugh at stupid things, I hope our sense of humour never changes.

Off course I want to thank Laura, for always being there for me and supporting me in stressed times. Thanks for always listening to me, even when you don't (want to) have an idea of what I am talking about. Even if I don't always show it, I really appreciate the way you always think a long with me.

My colleagues from the "broodjes smeren" group, who made me enjoy my time at the faculty. Thank you guys, for helping me to get started by pointing me in the right direction and thanks for the MANY coffee breaks, for the good talks and for exchanging thoughts.

Finally, all my friends from Delft (Club Gulden, my roommates from de Heeren van 9/11 and others), who made my time during the project very enjoyable. Thanks guys!

Everyone else, who is not mentioned but who contributed to this project or to my motivation over the last year, I appreciate it a lot, thanks!

M.E.G. van Hellenberg Hubar
Delft, Juli 2016

Contents

List of Figures **ix**

List of Tables **xi**

Nomenclature **xiii**

1 Introduction **1**
- 1.1 Formation Flight . . . 1
- 1.2 Research question . . . 2
- 1.3 Report Structure . . . 2

2 Literature Review **5**
- 2.1 Research Area . . . 5
- 2.2 Research Fields . . . 7
  - 2.2.1 Aerodynamic Benefits . . . 7
  - 2.2.2 Formations and Positioning . . . 8
  - 2.2.3 Fuel Burn . . . 9
  - 2.2.4 Flight Tests . . . 10
  - 2.2.5 Multiple Phases . . . 11
  - 2.2.6 Schedule Disturbances and Wind . . . 11

3 Formation Flight **13**
- 3.1 Benefits . . . 13
  - 3.1.1 Military Aviation . . . 13
  - 3.1.2 Airspace Capacity . . . 13
  - 3.1.3 Fuel Reduction and Lower emissions . . . 14
- 3.2 Drawbacks . . . 14
  - 3.2.1 Safety . . . 14
  - 3.2.2 Operational Complications . . . 14

4 Trajectory Optimization for Formation Flight **17**
- 4.1 Optimization Framework . . . 17
  - 4.1.1 Optimization Criteria . . . 18
  - 4.1.2 GPOPS . . . 19
  - 4.1.3 Multiple phases . . . 20
  - 4.1.4 Dynamic Aircraft Performance Models . . . 21
  - 4.1.5 Phase Linkages . . . 23
- 4.2 Formation Flight . . . 24
  - 4.2.1 Split the benefits during flight . . . 24
  - 4.2.2 Split the benefits post flight . . . 25
- 4.3 Input . . . 26
  - 4.3.1 Atmospheric Data . . . 27
  - 4.3.2 Aircraft Data . . . 27
  - 4.3.3 Constraints . . . 29
  - 4.3.4 Initial Guess . . . 34
- 4.4 Output . . . 34
  - 4.4.1 Optimal Trajectories . . . 35
  - 4.4.2 Results . . . 35
- 4.5 Delay . . . 35
- 4.6 Wind . . . 36

5 Validation **41**
5.1 Boeing 737-300 41
5.2 Boeing 747-400 42
5.3 McDonnell Douglas MD-11 43
5.4 Formation Flight 44

6 Experimental Set-up **47**

7 Results **49**
7.1 Two-Aircraft Formation Flight 49
7.1.1 Experiments 1 & 2: Standard Two-Aircraft Formation Flight 49
7.1.2 Experiments 3 & 4: Real-Life Scenarios 52
7.1.3 Experiments 5 & 6: Different Aircraft Types and Weights 55
7.1.4 Experiment 7: Delay 57
7.1.5 Experiment 8: Wind - Eastbound vs. Westbound 57
7.2 Experiment 9: Three-Aircraft Formation Flight 58
7.3 Experiment 10: Direct Operating Cost 60

8 Discussion **63**
8.1 Sensitivity Analysis 63
8.2 Results 65
8.2.1 Fuel Consumption 65
8.2.2 Distance Flown 65
8.2.3 Flight Time 65
8.2.4 Formation Trajectory. 65
8.2.5 Factors influencing the Formation. 66
8.3 Methodology 68
8.3.1 Jumps in the Results 69
8.3.2 Cost Function 69
8.3.3 Aircraft Dynamic Performance Models 69
8.3.4 Initial Guess 70
8.3.5 Aircraft Types 70
8.3.6 Wind 70

9 Conclusions & Recommendations **71**
9.1 Conclusions 71
9.2 Recommendations 73

A Polynomial representation of the wind field **75**

B Solo Flights for Benchmarking **77**

C Results for the KLM Scenario (Experiment 3) **81**

D Results for SkyTeam Scenario (Experiment 4) **85**

E Results for the experiment with Different Aircraft Weights (Experiment 6) **89**

F Results for the experiment with wind (Experiment 8) **91**

G Results for the Three-Aircraft Formation (Experiment 9) **93**

Bibliography **95**

List of Figures

2.1 Outboard wake upwash and inboard wake downwash leading aircraft [1] 7
2.2 Effect of upwash from leading aircraft on trailing aircraft [2] 8
2.3 Obtainable drag reduction in formation flight per aircraft [3] 8
2.4 Several three-aircraft formation configurations [4] 9
2.5 Contours of formation induced drag fractions for a two-aircraft echelon formation flight with a 20 wingspan streamwise separation [4] 9
2.6 Different aircraft types in close formation 10

3.1 Typical military transport formation [5] 13

4.1 Schematic overview of the optimization structure 17
4.2 Schematic overview of the horizontal flight paths of two aircraft with a common cruise segment [6] 20
4.3 A schematic representation of the vertical flight paths of a two-aircraft formation (five phases) 24
4.4 Induced drag fractions for different spanwise over wingspan (y/b) distance between leading and trailing aircraft [7] 25
4.5 Induced drag reduction for various lead and trail weight ratios [8] 26
4.6 Boeing 737-300 28
4.7 Boeing 747-400 28
4.8 McDonnell Douglas MD-11 29
4.9 Speed constraints in knots Calibrated Airspeed (CAS) 32
4.10 Mission profile for the standard mission of an individual aircraft with reserve option . . . 33
4.11 Mission profile for an individual aircraft that will join a formation with reserve option . . . 33
4.12 Example on how the initial or final time is fixed 34
4.13 Average delay per flight (all-causes) for departures [9] 35
4.14 Departure punctuality in January 2014 and 2015 [10] 36
4.15 U component of the wind on May 24^{th} 2016 (east-west windvector, which is positive in eastern direction) 39
4.16 V component of the wind on May 24^{th} 2016 (north-south windvector, which is positive in northern direction) 40

5.1 Horizontal flight paths for the validation of the Boeing 737-300 in combination with the intermediate point-mass and energy-state models. 41
5.2 Horizontal flight paths for the validation of the Boeing 747-400 in combination with the intermediate point-mass and energy-state models. 43
5.3 Horizontal flight paths for the validation of the McDonnell Douglas MD-11 in combination with the intermediate point-mass and energy-state models. 43
5.4 Maps showing the results of a case study performed on the optimal routing for formation flights [7] 45

6.1 Airspace of interest 47

7.1 Schematic overview of a two-aircraft formation (5 phases) 49
7.2 Horizontal flight paths of both solo flights for the Boeing 737-300 and Boeing 747-400 (as these are the same) 50
7.3 Horizontal Flight Paths of Aircraft A (London - Atlanta) and Aircraft B (Madrid - New York) when joining in formation and their corresponding optimal great circle paths 52

7.4 Results of the Boeing 737-300 two-aircraft formation from London to Atlanta and Madrid to New York City . . . 53
7.5 Results for the Boeing 747-400 two-aircraft formation from London to Atlanta and Madrid to New York City . . . 53
7.6 KLM seven wave system [11] . . . 54
7.7 Real KLM flights [12] . . . 54
7.8 Results for the SkyTeam experiment . . . 55
7.9 Small detour of aircraft A in Formation 2 for the SkyTeam experiment . . . 55
7.10 Different aircraft types in different lead-trail order (Experiment 5) . . . 56
7.11 Velocity profiles for the delay experiment (Experiment 7) . . . 58
7.12 The rendezvous point of the formation shifts when one of the aircraft is delayed (Experiment 7) . . . 59
7.13 Horizontal flight paths of an Eastbound and a Westbound formation (Experiment 8) . . . 60
7.14 Schematic overview of how the number of phases increases from a two-aircraft formation to a three-aircraft formation . . . 61
7.15 The horizontal flight path of a three-aircraft formation from Europe to North-America (Experiment 9) . . . 61
7.16 Direct Operating Cost: shift cost function from optimize for minimum total fuel consumption to optimize for minimum total flight time . . . 62

8.1 Shifting rendezvous point for two flights from Europe to North-America for different values of induced drag reduction . . . 63
8.2 Sensitivity analysis: fuel consumption . . . 64
8.3 Sensitivity analysis: flight time . . . 64
8.4 Change in induced and total drag due to formation flight, minimum total drag point shifts to bottom left . . . 66
8.5 Trajectory comparison of a flight from the SkyTeam formation experiment (Experiment 4) to its corresponding solo flight . . . 66
8.6 Shift of rendezvous point when aircraft A or B is delayed . . . 68
8.7 Examples of jumps in the results . . . 69

A.1 Considered wind-field for this research (May 24^{th} 2016) . . . 76

B.1 Results for solo flights 1 and 2 . . . 78
B.2 Results for solo flights 3 and 4 . . . 79

C.1 Results for Formation 1 of the KLM experiment (Experiment 3) . . . 82
C.2 Results for Formation 2 of the KLM experiment (Experiment 3) . . . 83

D.1 Results for Formation 1 of the SkyTeam experiment (Experiment 4) . . . 86
D.2 Results for Formation 2 of the SkyTeam experiment (Experiment 4) . . . 87

E.1 Horizontal flight paths of Formation 1 (solid line) and Formation 2 (dashed line) . . . 89
E.2 Results for the experiment with one empty (aircraft A) and one full (aircraft B) B744. Formation 1 has aircraft A as trailing aircraft (solid line) and Formation 2 where aircraft B is the trailing aircraft (dashed line). . . . 90

F.1 Horizontal flight paths of the set of eastbound flights. The dashed lines represent the optimal trajectories of the aircraft when flying solo and the solid green lines represent the optimal trajectories for the same flights that join in formation. . . . 91
F.2 Horizontal flight paths of the set of westbound flights. The dashed lines represent the optimal trajectories of the aircraft when flying solo and the solid green lines represent the optimal trajectories for the same flights that join in formation. . . . 92

G.1 Results for the three-aircraft formation experiment (Experiment 9) . . . 94

List of Tables

2.1 Summary of flight test results . . . 10

4.1 Specification of aircraft . . . 27
4.2 Boeing 737-300 High Speed Drag Polar . . . 28
4.3 Boeing 747-400 High Speed Drag Polar . . . 29
4.4 The McDonnell Douglas MD-11 High Speed Drag Polar . . . 29
4.5 Maximum altitudes for the different aircraft types . . . 30
4.6 Operating speeds of the Boeing 737-300, the Boeing 747-400 and the McDonnell Douglas MD-11 . . . 31
4.7 Values of R-squared for second- and fourth degree polynomials of the wind components 37

5.1 Block fuel per passenger for the Boeing 737-300[13] . . . 42
5.2 Results for a flight from Amsterdam to Madrid for a Boeing 737-300 . . . 42
5.3 Results for a flight from Paris to Buenos Aires for a Boeing 747-400 . . . 42
5.4 Results for a flight from London to Atlanta for a McDonnell Douglas MD-11 . . . 44
5.5 Optimization for a scenario based on a case study performed by Bower et al. [7] . . . 44

7.1 Solo flights from London to Atlanta and from Madrid to New York City for the Boeing 737-300 50
7.2 Solo flight from London to Atlanta and from Madrid to New York City for the Boeing 747-400 50
7.3 Initial and final fuel weights of the solo flights . . . 51
7.4 Results for two B733 aircraft from London to Atlanta and Madrid to New York city that join formation (Experiment 1) . . . 51
7.5 Results for two B744 aircraft from London to Atlanta and Madrid to New York city that join formation (Experiment 2) . . . 52
7.6 Results for two KLM flights, one from Amsterdam to Washington (aircraft A) and one from Amsterdam to New York City (aircraft B) flying solo and in formation (Experiment 3) . . . 53
7.7 Results for two SkyTeam flights from Amsterdam to New York City flying solo and in formation (Experiment 4) . . . 54
7.8 Fuel consumption of the formations with different aircraft types (Experiment 5) . . . 56
7.9 Results for formation flight for similar aircraft with different weights (Experiment 6) . . . 57
7.10 Results for formation flight when one aircraft has a delayed departure (Experiment 7) . . 57
7.11 Results for the Eastbound and Westbound flights (Experiment 8) . . . 58
7.12 Results for the three-aircraft formation (Experiment 9) . . . 60

8.1 Resulting fuel consumption for the experiment on which the influence of wind is taken into account (Experiment 8) compared with corresponding solo flights . . . 68

B.1 S1: Solo flight from London to Atlanta for the Boeing 737-300 with a payload of 3142kg 77
B.2 S2: Solo flight from Madrid to New York City for the Boeing 737-300 with a payload of 3142kg . . . 77
B.3 S3: Solo flight from London to Atlanta for the Boeing 747-400 with a payload of 63916kg 77
B.4 S4: Solo flight from Madrid to New York City for the Boeing 747-400 with a payload of 63916kg . . . 78

C.1 Results for the KLM experiment . . . 81

D.1 Results for the SkyTeam experiment . . . 85

G.1 Results for a three-aircraft formation flown by three B733 aircraft. Aircraft A from London to Atlanta, aircraft B from Amsterdam to New York City and aircraft C from Madrid to Toronto (Experiment 9) 93
G.2 Results for the aircraft in a three-aircraft formation relative to their corresponding solo flights (Experiment 9) 93

Nomenclature

(x/b)	Streamwise spacing between aircraft normalized by span	$[-]$
(y/b)	Spanwise spacing between aircraft normalized by span	$[-]$
α	Constant used in shifting of cost function	$[-]$
χ	Heading	$[^\circ]$
δ	Ratio pressure over pressure at sea level	$[-]$
$\dot{m}$	Fuel burn per unit time	$[kg/s]$
ϵ	Formation flight induced drag fraction	$[-]$
η	Engine control setting	$[-]$
γ	Flight path angle	$[^\circ]$
λ	Longitude	$[^\circ]$
μ	Roll angle	$[^\circ]$
Φ	Mayer term	$[-]$
ϕ	Latitude	$[^\circ]$
ρ	Air density	$[kg/m^3]$
θ	Ratio temperature over temperature at sea level	$[-]$
c_0	Fixed cost component of DOC	$[-]$
C_D	Drag coefficient	$[-]$
C_L	Lift coefficient	$[-]$
C_{D_0}	Zero-lift drag coefficient	$[-]$
C_{D_i}	Induced drag coefficient	$[-]$
c_{fuel}	Fuel cost component of DOC	$[-]$
c_{time}	Time cost component of DOC	$[-]$
CAS	Calibrated airspeed	$[m/s]$
D	Drag	$[N]$
DOC_i	Direct Operating Costs of aircraft i	$[€]$
E	Specific energy	$[J/kg]$
EAS	Equivalent airspeed	$[m/s]$
F_c	Fuel flow	$[kg/s]$
g_0	Gravitational acceleration	$[m/s^2]$
h	Altitude	$[m]$

J_c	Cost function	$[-]$
L	Lagrange term	$[-]$
L	Lift	$[N]$
M	Mach number	$[-]$
M_{MO}	Maximum operating Mach	$[-]$
n_a	Number of aircraft	$[-]$
p	Pressure	$[N/m^2]$
q	Dynamic pressure	$[N/m^2]$
R_e	Earth radius	$[m]$
S	Wing surface	$[m^2]$
T	Temperature	$[^\circ]$
t_0	Initial time	$[s]$
t_f	Final time	$[s]$
t_{detour}	Extra detour flight time	$[s]$
t_{flight}	Flight time	$[s]$
T_{max}	Maximum thrust	$[N]$
T_{min}	Idle thrust	$[N]$
TAS	True airspeed	$[m/s]$
$u(t)$	Control variable	$[-]$
V	Airspeed	$[m/s]$
V_{min}	Minimum operating airspeed	$[m/s]$
V_{MO}	Maximum operating airspeed	$[m/s]$
V_{sound}	Speed of sound	$[m/s]$
V_{Wind_U}	U wind component	$[m/s]$
V_{Wind_V}	V wind component	$[m/s]$
W	Aircraft gross weight	$[kg]$
W_{fuel}	Fuel weight	$[kg]$
x	Aircraft x-position in the national triangulation system	$[m]$
$x(t)$	State variable	$[-]$
x_0	Initial state variable	$[-]$
x_f	Final state variable	$[-]$
y	Aircraft y-position in the national triangulation system	$[m]$
z	Altitude	$[m]$

1

Introduction

In this chapter first the concept of formation flight will be introduced. Second, the research question and research goals will be elaborated upon and finally the structure of the report will be outlined.

1.1. Formation Flight

As the world becomes more connected and air travel becomes more accessible for everybody, every year more commercial flights are conducted to accommodate this increasing demand [14]. With the amount of flights increasing also more fuel is burned. For airlines, the fuel consumption of their aircraft is one of the main expenses and can reach up to over 30% of their total operating costs [15]. Next to high costs, a recent trend is that the environment should be kept in mind. The environmental footprint of the aviation industry should be brought down, while the number of flights increase. Every kilogram of fuel burned by aircraft contributes to the greenhouse gasses and therefore has a negative impact on the environment. The Intergovernmental Panel on Climate Change (IPCC) indicates, that aviation contributes to around 2% of man-made carbon dioxide (CO2) emissions and also that other aircraft emissions at high altitudes have additional climate impacts [16]. Modern aircraft already consume significant less fuel than older aircraft and also have much lower emissions, but airlines can not buy new aircraft everyday. With an average lifespan for aircraft of 25 years, this means that the aircraft will continue to fly for many years, despite the excessive fuel consumption. So, for airlines to renew their fleet would be optimal, but this is a long-term solution and therefore other solutions must be found.

This is where formation flight comes into play. The concept of formation flight is not very new. Research on formation flight started over 50 years ago, when the formation of a group of birds was observed [17]. Over the years a lot of research has been done in this field. The aerodynamics behind formation flight have been investigated [7][18] and also flight tests have been performed to back-up the results [1]. When flying in formation the trailing aircraft experience a reduction in induced drag, which results in a lower total drag. Less drag also means means that less thrust is required. And when the engines produce less thrust, less fuel is burned. Hence, formation flight leads to lower fuel consumption. With this in mind, researchers also conducted studies on optimal routing for a number of flights and on how this can be applied in civil aviation.

Another well investigated subject in the aviation industry, is the optimization of the trajectories of aircraft [19][20]. Knowing the optimal trajectories prior to departure can also lead to fuel savings. Not only is the most cost efficient path predefined (with regard to when and where to climb, cruise and descent), but also the amount of fuel taken on-board can be optimized.

However, no research has been done on the combination of these two subjects. When two aircraft are intended to join in formation, it would be interesting to know the optimal trajectories of both aircraft. As both aircraft will probably deviate from their own optimal path to join in formation, it is necessary to know where they should meet and where they should split up. From these trajectories it would then be possible to determine the fuel consumption of the aircraft. Furthermore, it will be interesting to explore what the effect of a reduction on induced drag on the trailing aircraft does for the trajectories of both aircraft. Finally, it could also be useful to assess the influences of, for example, the types of aircraft, size and sequence of the aircraft within the formation and the presence of wind on the trajectories and on the resulting fuel consumption. The research conducted in this study hopes to contribute to closing this gap in the body of knowledge.

1.2. Research question

In this section the research objectives and questions are discussed. This research will investigate the existing gap in the body of knowledge regarding ”trajectory optimization for commercial formation flight”.

Hence the **Research Objective** is as follows:
The objective of this research is to minimize the overall fuel consumption or Direct Operating Cost of commercial aircraft flying in formation by developing a multiple-phase optimal control formulation.

To simplify the research, we can split the objective up into sub-objectives or goals, these sub-objectives will play a major role in how the intended research will be set up. The sub-objectives are:

1. Determine from literature what factors influence the trajectory of formation flight.
2. Develop and validate a methodology to optimize the multiple-phase trajectory of a single aircraft with regard to relevant parameters such as fuel cost and Direct Operating Cost.
3. Develop and validate a methodology to optimize the multiple-phase trajectory of a two- and three-aircraft formation flight with regard to the same parameters.
4. Implement this methodology in the optimization framework and validate its correctness.
5. Perform a realistic case study optimizing the trajectories for aircraft flying in formation across the North Atlantic Ocean.
6. Assess whether it is feasible to implement formation flight for transatlantic routes.
7. Gain understanding of cost and benefits with variations in fuel consumption, and formation size.

The research objectives result in the following **Research Question**:
Is it possible to develop a tool that optimizes the multiple-phase trajectories for two or three commercial aircraft flying in formation weighing the reduced fuel consumption, due to induced drag reduction, versus economic factors using a dynamic optimization technique?

This research question can be divided into smaller more manageable questions. when all sub-questions are answered, it should also be possible to answer the main research question. The sub-questions are:

1. What are important factors regarding formation flight?
2. How can a multiple-phase two- or three-aircraft formation trajectory optimization for a realistic North Atlantic Route be formulated to minimize fuel or Direct Operating Cost and how can this be implemented in an optimization framework?
   (a) How does trajectory optimization work?
   (b) What are appropriate dynamic aircraft performance models for studying long-haul formation flight?
   (c) What optimization technique will be used?
   (d) What does this optimization framework look like?
   (e) How to formulate a single aircraft trajectory optimization?
   (f) What is the fuel consumption during flight for solo aircraft and for aircraft flying in formation?
   (g) What factors contribute to the Direct Operating Cost?
   (h) Which objectives and constraints are to be implemented?
   (i) How to keep the computational time within limits?
3. How to validate the tool?
4. How can the obtained results be compared to the real-life situation?
5. What can we conclude from all this and what are recommendations for future research?

1.3. Report Structure

This report actually concerns two main issues. The first being the development of a tool that is able to optimize multiple-phase trajectories for several aircraft that will join in formation to minimize the total fuel consumption. And secondly, when this tool is developed and validated, a couple of experiments will be conducted to investigate the benefits of formation flight and what influence several factors, like different aircraft types, delay and the presence of wind, may have on formation flight.

To start of, important background information on the concept of formation flight is presented in Chapter 2. The current state-of-the-art research will be explored and the concept of formation flight will be explained. Prior to the development of the tool, it is necessary to know how aircraft can benefit from formation flight and what influences these benefits. In addition to a possible reduction in fuel consumption, other advantages can be obtained from flying in formation, like increased airspace capacity and less pollution. However, some drawbacks exist as well, beginning with the increased safety risks. In Chapter 3 the benefits and drawbacks of formation flight are discussed. After discussing the concept of formation flight, the methodology on developing the optimization tool follows in Chapter 4. Here, the developed optimization tool is elaborated upon and the optimization framework containing the cost function, the optimization technique and the dynamic aircraft performance models is discussed. The required input and output of the tool are explained as well. In Chapter 5 the tool is validated and in chapter 6 the general set-up of the experiments that will be conducted is reviewed. The results of the experiments are presented in Chapter 7. These results are discussed more extensively in Chapter 8. Finally, in Chapter 9 the conclusions of this study are summarized and also recommendations for future research are given.

2

Literature Review

In this chapter the current research relating to multiple-phase trajectory optimization for commercial aircraft in formation will be reviewed. First the relevant research areas will be defined and subsequently all important subjects for this research will be addressed.

2.1. Research Area

A general search was conducted in order to get familiar with the concept of formation flight. It was encouraging to see that over the last years much research in this area has been done. However, research on formation flight started many years ago when in 1970 Lissaman et al. [17] studied the formations of birds in flight. Lissaman et al. suggested that, while the formation is sensitive to ambient winds, birds in formation could theoretically have an increase in range of about 70% compared to a lone bird. From that moment on more research was conducted on formation flight and now also for aircraft. As stated before, formation flight could possibly save energy without significant modifications of present aircraft. This fact together with the increasing fuel cost over the last years and the growing environmental awareness, has made formation flight a popular research area.

Research on formation flight for commercial flights emerged over the last two decades. Between now and then, many different aspects on formation flight for aircraft have been investigated. Below some studies that form the base for this research are reviewed in more detail.

In 1998 Blake et al. [21] analyzed the induced drag effects for close formation flight. During close formation flights aircraft fly within a few of wingspans of each other. They conclude that large reductions in induced drag are possible for close formation flights accompanied by changes in lift, side force and moments about all three axes. They state also that the optimum cruise altitude of aircraft in formation is higher than when an aircraft flies solo.

In the same year, but not related to the articles on formation flight, Sherzada Khan [22] published an article on flight track optimization. In this work Khan discusses different optimization techniques for different phases of flight and compares them with regard to each other to show their merits and limitations.

In 2003 Ribichini et al. [23] investigate how to plan formation flight. They want to show under which conditions two airplanes should join in formation. They present a ”greedy” decentralized approach in which the aircraft (pilots) can decide if they will join in a formation or not during flight. If they will join in a formation they will deviate from their path, but will have the benefit of flying in formation, thus the aircraft will only join in formation if the benefits outweigh the cost of the detour. The drawback of such a decentralized approach is that it will not lead to the optimal global energy consumption because all aircraft only keep in mind their own benefits.

A couple of years later, in 2006 Bangash et al. [24] evaluated the aerodynamic characteristics of aircraft in formation. They analyzed the results of wind tunnel tests to investigate the effects of spatial offset between aircraft in formation and of different formation constellations on the aerodynamic characteristics of aircraft in formation.

Different formation geometries lead to different amounts of formation induced drag reduction. In 2009 Bower et al. [7] predicted the induced drag of aircraft flying in four different geometries. They performed a case study for five FedEx flights joining in one two- and one three-aircraft formation. According to Bower et al. FedEx could save up to 700.000 gallons of fuel per year by only having these five daily flights fly in formation.

To investigate what the potential gains of formation flight could be for long-haul commercial flights, in 2011 Herinckx et al. [3] addressed the operational feasibility from a market demand and economic, as well as air traffic control perspective. They proved that there is sufficient demand for formation flight and that flying in formation is a possible solution to the impending regulations regarding the reduction in CO2 in aviation.

From 2011 to 2014 Ning et al. investigated the aerodynamics of extended formation flight for commercial aircraft at transonic speeds, focusing on the compressibility effects in formation flight [4][25]. During extended formation flights, the streamwise distance between the aircraft in formation is 10 to 50 wingspans. They conclude that compressibility-related drag penalties can be avoided by flying at slightly lower airspeeds at a fixed altitude or fixed lift coefficient and that larger streamwise separation between the aircraft allow for slightly higher cruise speeds in exchange for higher induced drag. Ning et al. also explored methods of determining where the ”sweet spot” is for the trailing aircraft [26]. The sweet spot is the optimal location for the trailing aircraft in formation flight.

In 2012 Xue and Hornby published an article in which they investigated what the potential savings would be from flying in formation in the National Airspace System (NAS) [8]. The NAS is the airspace, navigation facilities and airports of the United States along with their associated information, services, rules, regulations, policies, procedures, personnel and equipment [27]. As there are many different aircraft types in the NAS, Xue and Hornby state that it is important to know the effect on the change in induced drag for different aircraft types in a formation. They developed a model that calculates the change in induced drag for heterogeneous formations. The results of their model will be used in this research.

From 2012 to 2014 Xu et al. [6][28] investigated the fuel and cost benefits of applying extended formation flight to commercial airline operations. The design of the framework is a combination of aircraft performance and aerodynamics with aircraft scheduling. To increase the efficiency of their optimization they used heuristic filters in order to eliminate unlikely formations after which they use gradient-based optimization to reduce the computational cost. They used the Breguet range equation for the cruise segment. In different case studies Xu et al. find large reductions in Direct Operating Cost (DOC). By merely implementing formation flight, they find a reduction of 2% in DOC for a 31-flight case (South African Airlines) and a reduction of 2.6% in DOC for a larger 150-flight case (Star Alliance). For future work Xu et al. recommend an analysis of the influences of wind and delay on the optimal routing.

Parts of the research done by Kent et al. from 2012 to 2015 [29][18][30] form a solid base for this research. Kent et al. investigated the optimal routing for commercial formation flight. They use an extension of the Fermat-Torricelli problem [31][32] to find the optimal formations for a given list of routes. They compare two methods (nominal and differential rates) of computing fuel burn and assess the impact of wind on the optimal routes assuming a fixed flight altitude and a single ”layer” of predicted wind.

In the same period the earlier mentioned, Blake et al. [2][33] also investigated the optimal routing for extended formation flight. They looked at routes with either a common origin or a common destination where the lead aircraft does not deviate from its optimal path, use segments of great circle routes as the nominal flight segments and present a closed-form solution for the optimal routing.

In 2014 Visser and Hartjes [20] published an article on flight trajectory optimization for economic and environmental criteria. In this article they present a multiple-phase trajectory optimization for one aircraft flying between a city pair. The flight trajectory is split up into the horizontal and vertical flight path. For the horizontal flight path there are series of waypoint that are connected and for the vertical flight path there are 11 different phases which are to be optimized. Visser and Hartjes demonstrated the usefulness of the multiple-phase optimization tool in a case study of the Amsterdam-Munich city pair.

Besides theoretical research also some flight tests have been performed. In 2002 several flight tests have been performed with two F/A 18 aircraft in close formation. Ray et al. [34] and Wagner et al. [35] analyzed the results from these tests and both came to the conclusion that a significant fuel flow reduction for the trailing aircraft can be achieved. Ray et al. found that for the trailing aircraft values of more than 20% in drag reduction and over 18% in fuel flow reduction at flight conditions of Mach 0.56 and an altitude of 25000 ft. Wagner et al. found comparable results of 8.8% +- 5% savings in fuel flow flown at 300 KIAS and at an altitude of 10000 ft. Wagner et al. also had a second objective for these tests, which was to determine if the savings would increase with larger formations. They added an extra aircraft, however, the flight test data for this three-ship formation was inconclusive. More recent flight tests regarding formation flight were carried out in 2012. Two C-17 military aircraft which are equipped with an advanced formation flight system performed an extended formation flight. Pahle et al. [1] summarize the flight data gathered during this test. More on these flight tests and their results will follow later.

2.2. Research Fields

In this section, the aspects that are relevant to this research will be further addressed. First, the working principle of formation flight is reviewed and the different possible formations and their configurations are discussed. Then, the reasoning behind using multiple-phase optimization is explained and finally, the current research into the effects of schedule disturbances and wind for formation flight is presented.

2.2.1. Aerodynamic Benefits

It is important to have a good understanding of the working principle of formation flight. Over the years the mechanism behind drag reduction for formation flight has been investigated by many. When an aircraft flies through the air there is a pressure difference between the upper and lower side of the wing resulting in lift and at the wing tips vortices are formed. When the aircraft flies through the air it leaves behind regions of downwash inboard and regions of upwash outboard as shown in Figure 2.1.

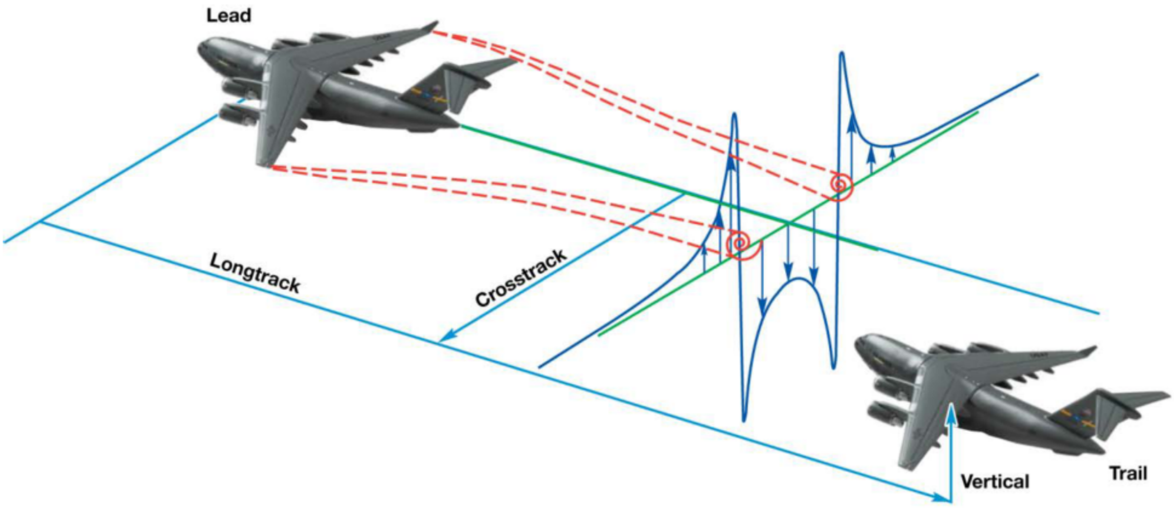

Figure 2.1: Outboard wake upwash and inboard wake downwash leading aircraft [1]

When another aircraft flies through the upwash wake of this leading aircraft, the local velocity vector changes compared to the local velocity vector of an aircraft performing a straight and level flight [2]. As shown in Figure 2.2, the upwash generated by the leading aircraft rotates the lift vector of the trailing aircraft forward and the drag vector upward which results in a reduction of thrust required for level flight.

When more aircraft are added to the formation the benefits increase (Figure 2.3). This looks promising for flying in large formations. However, up until now only two- and three-aircraft formations have been tested and the test results are somewhat lower than the results shown in Figure 2.3. Blake et al. [2] explain different items to which these disparities can be accounted. First of all, in theory an ideal lift distribution is assumed, which is unattainable in practice. Furthermore, it could be that the tests are not performed under optimal flight conditions or that the positioning of the trailing aircraft relative to the leading aircraft is not optimal.

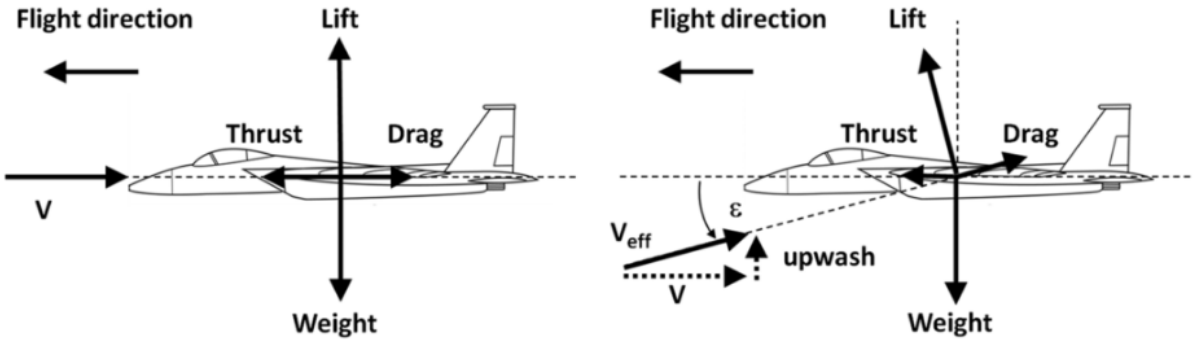

Figure 2.2: Effect of upwash from leading aircraft on trailing aircraft [2]

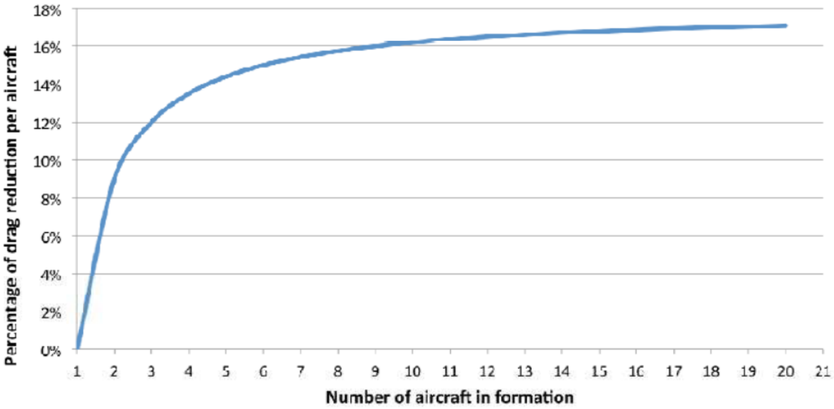

Figure 2.3: Obtainable drag reduction in formation flight per aircraft [3]

2.2.2. Formations and Positioning

Now that the working principle is clarified, different formation constellations and aircraft positioning within the formations are reviewed. Formation flight can be divided into two kinds of formations: close formations and extended formations. Close formation flight means that the aircraft fly within a few wingspans of each other. For birds this is no problem and even for small agile (e.g. military) aircraft this could be realized, but for commercial aircraft this would present an unacceptable high risk of collision and thus is not applicable. To reduce this risk of collision, further streamwise distances are introduced. So called extended formation flights are formations with streamwise separations of 10 to 50 wingspans between the leading and trailing aircraft. So even if aircraft in close formation gain more reduction in induced drag, due to safety issues commercial aircraft will likely only fly in extended formations.

Depending on the number of aircraft in a formation, different configurations are possible. For a two-aircraft formation the only beneficial configuration is an echelon formation. For three-aircraft formations several possible configurations exist that result in drag reduction (see Figure 2.4). When the formation size increases, the number of possible configurations increases too, but this study only two- and three-ship formations are considered.

The different formation configurations have their own characteristics and are slightly different from each other. There are a number of factors for which one formation configurations could be more beneficial than the other, factors like: aircraft weight, specific fuel consumption and the stage length. In the research done by Ning et al. up several advantages and disadvantages per configuration are outlined [4]. The inverted V, for example, has the advantage that the trailing aircraft has more symmetric loading conditions and thus need less aileron deflection to counteract the rolling moments of the upstream wash. Because of this and because the inverted V formation is insensitive to high levels of positioning uncertainty Bower et al. [7] conclude that this is the most attractive configuration for a three-aircraft formation. For this study the actual configuration is not really relevant as long as a realistic value for the drag reduction of two- and three-aircraft formations can be obtained.

Both the streamwise the streamwise distance between the aircraft and the configuration of the

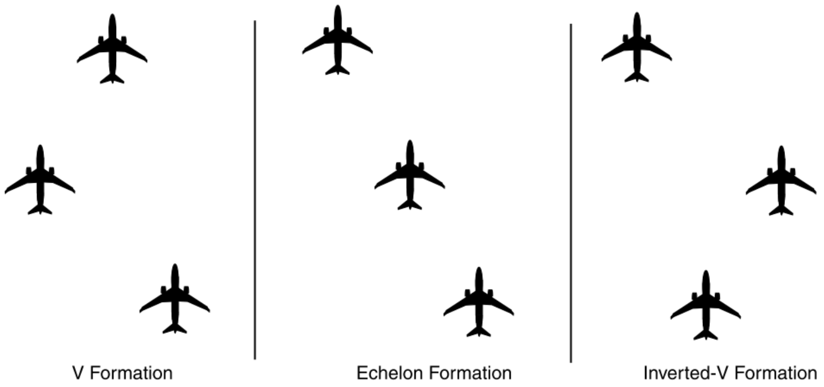

Figure 2.4: Several three-aircraft formation configurations [4]

formation, as well as the horizontal and vertical spacing between the trailing and the leading aircraft play an important role in the amount of induced drag reduction. In Figure 2.5 contours of the induced drag fraction for a two-aircraft echelon formation with a 20 wingspan separation are shown [4]. The induced drag fraction equals the total induced drag of all aircraft in-formation relative to all aircraft out-of-formation. For this formation, the optimum positioning for the highest reduction in induced drag occurs when the wingtip of the trailing aircraft slightly overlaps the vortex center. However, when flying more distant from the vortex center, the drag savings vary less, which results in a lower induced rolling moment. Lower induced rolling moments require less aileron deflection to trim the aircraft, leading to less induced drag. At the outboard positions the contours are close to circular and thus the sensitivity for vertical and horizontal positioning is pretty much equal. Therefore, the best position for the trailing aircraft is sensitive to many factors and is not fixed. The contours for other aircraft formations might vary compared to Figure 2.5, but these conclusions generally remain true.

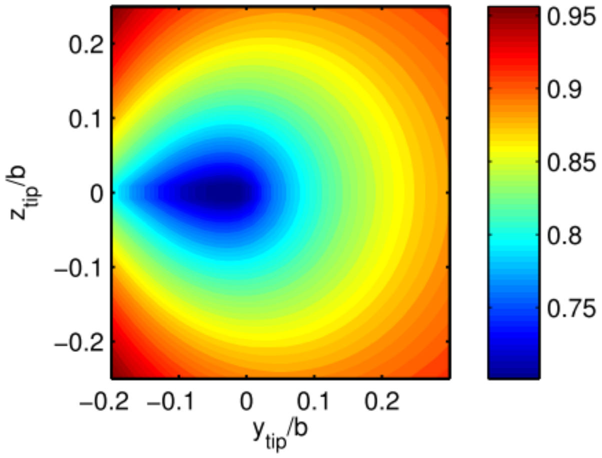

Figure 2.5: Contours of formation induced drag fractions for a two-aircraft echelon formation flight with a 20 wingspan streamwise separation [4]

2.2.3. Fuel Burn

To model the aircraft fuel burn Kent et al. [30] use a rearrangement of the Breguet range equation. When the aircraft fly in formation they implement a discount factor on the drag. This method is not very accurate, but it offers a fast and effective framework to find optimal formations for large numbers of flights. Furthermore, they assume an additional 10% reserve fuel for aircraft flying in formation compared to aircraft flying solo. This is due to the fact that aircraft in formation must most likely fly a detour in order to meet each other and for safety reasons the aircraft must carry enough fuel to be able to fly this detour solo (in case something goes wrong and the other aircraft doesn't show up).

Bower et al. calculate the fuel burn assuming linear variation in the range factor over all cruise segments [7]. Based on the weights of the aircraft at the beginning and end of the formation cruise segment, the induced drag fraction of each aircraft is calculated. A few iterations are typically required to converge to the correct weights and induced drag fractions at the end of the formation cruise segment. For climb, an additional time to climb and an additional fuel burn increment based on the cruise altitude and speed are calculated. An additional time is calculated to descend as well, but no fuel savings are allocated. In the engine model, they are able to capture change in the specific fuel consumption for different throttle settings. This is important for the rear aircraft in the three-aircraft formation where there can be up to a 50% reduction in total drag.

Visser and Hartjes [20] use an intermediate point-mass model to estimate the fuel burn during different flight segments. This method is more complex, but also more accurate as they investigate the optimal flight trajectories for a single flight instead of for a large number of flights. In their model the weight is a state variable, which is a function of the fuel flow, that changes with time. The total fuel burn is determined by subtracting the final weight from the initial weight of the aircraft.

2.2.4. Flight Tests

As previously stated, besides the theoretical research that has been performed, in the course of the years also several flight tests have been conducted. Tests have been performed in 1998 with small jet aircraft in close formation and more recently, in 2012, with large C-17 military aircraft in extended formation. The latter tests are very interesting for this research, because the C-17 aircraft is similar to commercial aircraft. Apart from the reduction in drag, and thus thrust and fuel flow, some problems emerged from the tests. First of all, it is hard to predict where the wake location will be, so it is difficult for the pilots to know where to fly in order to gain the most beneficial upwash of the leading aircraft. Secondly, the current flight systems are still not accurate enough to control the desired position behind the leading aircraft. Even for the pilots, flying the United States Air Force C-17 Globemaster III which features a very advanced formation flight system (far more advanced than normal commercial aircraft), it was difficult to maintain position. Hence, although formation flight is regarded as a short-term solution for fuel savings by some[6][30], current commercial aircraft are not capable to fly in formation yet and thus need to be modified to safely and efficiently fly in formation. In Table 2.1 some of the found flight test results are summarized.

Figure 2.6: Different aircraft types in close formation

Table 2.1: Summary of flight test results

Lead Aircraft	**Trail Aircraft**	**Average fuel flow benefit on trail**	**Reference**
F/A-18B	F/A-18A	18%	Ray et al. [34]
T-38A	T-38C	9%	Wagner et al. [35]
C-17A	C-17A	7%	Pahle et al. [1]

It is interesting to see that the tested fuel flow reduction for the C-17 is only 7% for the trailing aircraft, thus only 3.5% for the total fuel flow of the two aircraft. This is significantly lower than the theoretically achievable reduction. Pahle et al. however, conclude in their research that although their data is incomplete, it suggests that it is possible to gain a fuel flow reduction for the trailing aircraft of over 10% [1].

2.2.5. Multiple Phases

There are various reasons to split a flight up into different phases [20]. When, for example, the entire flight envelope from take-off to landing, the aircraft goes through different flight modes (take-off, climb, cruise, descend and landing). During these flight modes the aircraft will have different configurations (landing gear in or out, flaps and slats, thrust settings, etc.), which leads to several aircraft dynamic models. Secondly, there could be different constraints (for example constraints imposed by Air Traffic Management (ATM), safety or operational constraints) for different airspaces. Another reason could be that with different phases, different performance optimization criteria can be implemented. These are all good reasons to implement multiple phases, but for this research the main reason to use multiple phases is because there are multiple aircraft flying simultaneously and there is a flight segment in which the aircraft fly in formation and thus have a different fuel flow compared to the aircraft flying solo.

2.2.6. Schedule Disturbances and Wind

As mentioned before, several significant investigations have been conducted in the field of formation flight. However, the combination of formation flight with schedule disturbances and the effects of wind on the formation flights and the corresponding optimal routes have not really been investigated yet. Most research, which is based on optimal routing, indicates a reduction in fuel consumption. However, as stated by Xue et al., these studies have one significant shortcoming, which is that the formations investigated are scheduled ahead of time, which makes them vulnerable to uncertainty in flight departure times [8]. They state that when an aircraft is delayed, the other aircraft in the pre-scheduled formation has to wait at the rendezvous point, which wipes out the benefits of formation flight.

Kent et al. did some initial investigation to examine what the effects of wind would be on the fuel savings of formation flight [18]. When accounting for wind on the route of the aircraft (which is nearly always present), the aircraft will deviate from its original great circle path. It is beneficial for aircraft to fly with tailwinds, but headwinds have a negative impact on the aircraft fuel consumption and flight time. This is why aircraft will deviate from their optimal geometric route when it is possible to fly another route with advantageous wind conditions. Kent et al. base their route optimization approach on the optimal geometric formation paths. They investigate how well this approach performs in the presence of wind by comparing the results with the results of wind optimal routes. They generate a random wind field, add the contribution of the wind to the cost function (which in their research is a function of the distance) and then evaluate all possible routes. They state that this is very time consuming, but in their research they evaluate large numbers of flights. When just examining the combination of two or three flights this is not an issue. However, they investigate the optimal routing problem and not the optimal trajectories of the aircraft. In this research, the focus is on the optimal trajectories and therefore another approach should be used.

3

Formation Flight

During the literature review, background information concerning formation flight was presented and some benefits of formation flight were reviewed. In this section the pros and cons of formation flight will be described in more detail.

3.1. Benefits

Apart from reducing the fuel consumption for aircraft, formation flight also offers other benefits. Military aircraft have been performing formation flights a long time before it became known that this might save fuel. And also from an airspace capacity point of view formations can have a great impact. These benefits are briefly described in this section.

3.1.1. Military Aviation

Formation flight for military aircraft started as early as World War 1 (WW1) and is still used by the military today. There are several reasons why the military flies in formation, including: aerial refuelling, coordinated drops, minimize interval between take-offs, communication, concentration of fire power and defensive purposes. Also military transport aircraft regularly fly in formation, because formation flight is used as an effective approach to move large numbers of aircraft safely [5]. A typical military transport aircraft formation has a lateral spacing of 0ft to 500ft and a longitudinal spacing ranging from 3000ft to 8000ft and the leader controls the formation (Figure 3.1).

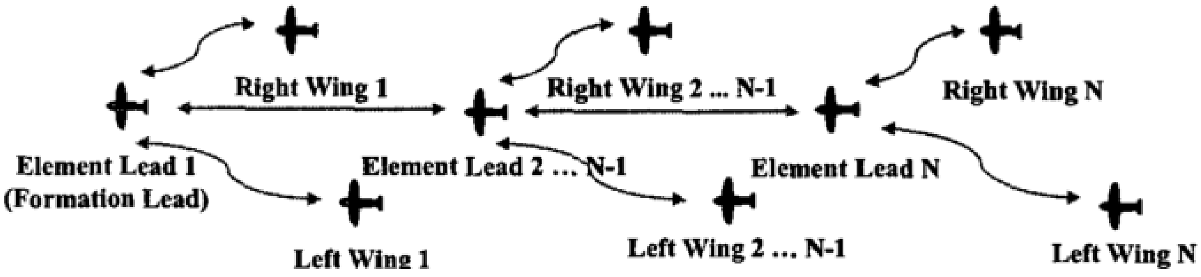

Figure 3.1: Typical military transport formation [5]

3.1.2. Airspace Capacity

With all the available airspace present and the relatively small amount of aircraft flying in this airspace, airspace congestion is still an increasing problem for the aviation industry worldwide. In some parts of the world the airspace is more crowded than other parts. The airspace above the North-Atlantic Ocean, which is the airspace that will be investigated in this research, accommodates air traffic between North America and Europe. Across the North-Atlantic Ocean there is no radar coverage and flights are prescribed to follow predefined oceanic tracks. As a result, aircraft often follow routes that are not optimal in view of their departure and destination points. This leads to an increase in aircraft cruising time and congestion level in continental airspace at input and output [36]. Also, as there is no radar coverage, specific safety separation rules are in place. One of these separation rules is that the in-trail aircraft spacing must be increased to compensate for delay and uncertainty in radio communication and navigation system positioning reporting. Reducing the aircraft separation distances can decrease the congestion and increase the airspace capacity as it increases the number of aircraft that can be on a specific segment of a track. Typical commercial aircraft that fly through zones without radar coverage should currently have a spacing of more than 25 nautical miles depending on the circumstances. When applying formation flight to commercial aircraft the spacing can be reduced allowing aircraft to fly within 2nm of each other. This will result in a much higher airspace capacity for these congested airspaces. For military formations the formation is pre-defined. This means that the pilots of all aircraft that join in the formation know what their role is and the whole flight is planned before take-off. For commercial aircraft this is not practical. For commercial aircraft procedures should be developed to form and dissolve formations. This could be done centralized by Air Traffic Control or decentralized by the aircraft crews themselves.

3.1.3. Fuel Reduction and Lower emissions

The most important reason for this research on commercial aircraft formation flight is the possible savings in fuel consumption. As many previous researchers already stated, aircraft flying in formation have less induced drag which results in a lower required thrust and thus a lower fuel consumption. The case study performed by Bower et al. [7] shows that for a set of 5 FedEx evening flights from northwest US to Memphis, which are flown 5 times per week and 52 weeks per year, formation flight can save 2.65 million litres of fuel per year. This study shows that a two-aircraft formation can save between 1.17% and 7.86% of fuel and a three-aircraft formation can save between 4.90% and 12.46% of fuel. Applying this to all air traffic could lead to major savings in fuel and thus cost.

Aircraft fuel burn also contributes to the amount of carbon dioxide CO2 (1 kilogram of jet translates into 3.15 kilograms of CO2 [16]) and other emissions to the atmosphere. Savings in fuel burn automatically leads to less emissions. As the aviation industry gets more and more regulated on noise and emissions and goals are set to decrease the CO2 footprint of aviation significantly by 2050, this issue is very important.

3.2. Drawbacks

As every advantage has its disadvantage, this is also the case for formation flight. It is not hard to imagine that when allowing aircraft to fly in the vicinity of each other this could lead to dangerous situations. Furthermore, as for every change in the aviation industry, there might be some issues in implementing formation flight considering the fact that splitting the savings over the participating aircraft is difficult. In this section these issues will be discussed.

3.2.1. Safety

As discussed above, military aircraft have already been flying in formation for many years, therefore (in theory) this should also be possible for commercial flights. It must not be forgotten, however, that military aircraft generally have much more advances equipment than commercial aircraft and military pilots are better trained in this aspect than normal pilots. Apart from having more advanced systems, military aircraft are more agile than typical commercial aircraft as well. When two or more commercial aircraft fly close to each other this causes an increased safety risk. For this reason, commercial aircraft should fly in extended formation with a separation of at least 10 wingspans. This significantly improves the safety, while maintaining most of the fuel savings achieved in close formations.

3.2.2. Operational Complications

In contrast to most fuel saving technologies, like improved engines or improved aerodynamics, formation flight mainly is an operational improvement that in theory could be implemented on existing flights. Hence, it could save fuel on the short term. Implementing new regulations in the aviation industry, however, is not done overnight. Currently, the International Civil Aviation Organization (ICAO) develops the principles and techniques of international air navigation [37]. Another operational complication is how to implement formation flight and how to split the savings. There are several approaches to plan formation flights. These approaches can be divided into centralized and decentralized approaches [38].

With the centralized approach formation flight is applied globally to optimize the fuel consumption. This means that every formation is planned before the flights take-off using the scheduled routes, departure and arrival times as well as specific formation benefits as parameters to generate a set of formations that optimizes the total fuel consumption. This is centrally coordinated process, hence the name centralized approach. The main advantage of this approach is that it provides the most fuel efficient solution globally, while its main disadvantages are that it requires very high computational efforts and does not provide a flexible solution in case of schedule changes or delays (non-robust solution). In the decentralized approaches, on the other hand, the formations are not planned before hand, but are considered as an en-route option. Based on in-flight collectible data, like flight plans and speeds of aircraft nearby, local optimizations are performed to determine if a formation should be formed or not. The main advantage of this is that aircraft are not dependent from other aircraft and thus are not sensitive for delays or schedule changes. On the other hand, however, with these decentralized approaches no total global fuel consumption is reached, but every aircraft (or airline) looks for the best solution for itself. Both approaches have their strengths and weaknesses. However, these approaches are not in the scope of this research. For more information on these network-wide approaches the works of Xu et al. [6] and Verhagen [38] can be consulted.

Yet another operational complication is how to split the benefits of formation flight. If only the trailing aircraft benefits from flying in formation, then why should an aircraft want to be the leading one? A solution can be to split the benefits of the formation between the two aircraft or to change position during flight so that all aircraft in the formation have a segment in which they are the trailing aircraft. Alternatively, the formations should only be performed with aircraft belonging to the same airline or airline alliance in order to keep the savings within the organization. This topic is not within the scope of this research, but it could be interesting to further investigate.

4

Trajectory Optimization for Formation Flight

The goal of this study is to develop a multiple-phase optimal control formulation to minimize overall fuel consumption or Direct Operating Cost. In other words, an optimization process is needed to optimize the trajectories of the aircraft that will join in formation. In Figure 4.1 a schematic overview of the optimization structure is shown. The blue parts represent the inputs, the yellow part the optimization framework and the green parts the outputs.
To start with, the optimal control problem that needs to be solved must be defined, this means that the cost functional, the differential-algebraic equations (DAE) and the boundaries must be specified as well as an initial guess for the solution. Then the initial trajectories and other inputs will be run through the tool, which will give a certain solution. If this solution satisfies all the criteria (if the solution lies within the constraints and is the optimal solution) the optimal trajectories are found, if not the tool will do iterations until they are (if the problem is feasible).

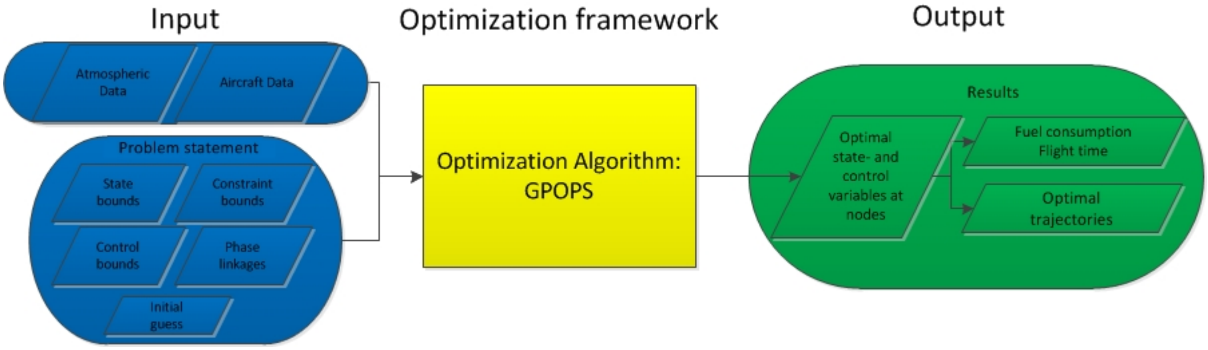
Input
Optimization framework
Output
Atmospheric Data
Aircraft Data
Problem statement
State bounds
Constraint bounds
Control bounds
Phase linkages
Initial guess
Optimization Algorithm: GPOPS
Results
Optimal state- and control variables at nodes
Fuel consumption Flight time
Optimal trajectories

Figure 4.1: Schematic overview of the optimization structure

In this chapter the optimization structure is reviewed. Firstly, the optimization framework is explained, secondly, the necessary modifications to this framework to implement formation flight are dealt with. Subsequently, the input and resulting output of the tool are discussed and, finally, also the implementation of delay and wind is examined.

4.1. Optimization Framework

In this section the optimization framework (the yellow part in Figure 4.1) is outlined in detail. The following items will be elaborated upon: optimization criteria, the optimization technique, the problem formulation, the dynamic aircraft performance models and the linkages between the different phases.

4.1.1. Optimization Criteria

From the previously explained research objective the cost function for this research can be derived. The research objective states that the overall fuel consumption or Direct Operating Cost (DOC) must be minimized. Xu et al. [6] and Visser and Hartjes [20] also used the optimization criteria to minimize the overall fuel consumption. They implemented the following objective function to optimize the fuel burn J_f for n aircraft:

$$J_f = min \sum_{i=1}^{n_a} (W_{1i} - W_{4i} + W_{fci}), \tag{4.1}$$

where, n_a is the number of aircraft, W_{1i} is the weight of aircraft i at the beginning of the cruise, W_{4i} is the weight of aircraft i and the end of the cruise and W_{fci} is the weight of aircraft i for the rest of the flight mission (taxi, take-off, climb, descent, landing and taxi). To determine the fuel burn for the entire trajectory of one aircraft the weight of the aircraft at the end of the cruise W_4 must be subtracted from the weight of the aircraft at the beginning of the cruise W_1 and an additional amount of fuel burn must be added to account for the fuel needed for the remainder of the mission W_{fc}. The function above minimizes the sum of the fuel burn of all aircraft. In other words, when looking at multiple aircraft (e.g. multiple aircraft that join in formation), the sum of the fuel burn for all aircraft that join in the formation must be minimized. This could result in some aircraft burning more fuel than they would normally do, but as other aircraft in the group have a larger reduction in fuel burn, the total fuel consumption is less.

The other optimization criterion, the DOC of an aircraft, is obtained differently. As the DOC of an aircraft depends on more than just the fuel consumption, this is more difficult to comprise. Usually the DOC is given by the following equation:

$$DOC = c_0 + c_{time} \cdot t_{flight} + c_{fuel} \cdot W_{fuel}, \tag{4.2}$$

where c_0, c_{time} and c_{fuel} are the cost components for fixed cost, time cost and fuel cost respectively, t_{flight} is the flight time and W_{fuel} is the amount of fuel burned. The fixed cost component c_0 of the DOC consists out of costs like: insurance, depreciation, maintenance per flight and landing fees. As these costs don't vary per flight hour or kg of fuel burned, the fixed cost component c_0 will not influence the optimization. The objective function for the DOC is modelled as:

$$J_c = min \sum_{i=1}^{n_a} DOC_i, \tag{4.3}$$

where, n_a is the number of flight and DOC_i is the DOC for flight i. However, it is difficult to find a value for the time cost component c_{time}, because this includes costs like: cabin and cockpit crew salary, extra aircraft maintenance cost and costs for passengers missing their connections. These costs can vary for different airlines and flights.

The performance index in this research is formulated in Bolza-form and consists of a Mayer term Φ and a Lagrange term L and is mathematically formulated as follows:

$$Minimize : J = \Phi(x_0, t_0, x_f, t_f) + \int_{t_0}^{t_f} L(x, u, t)dt, \tag{4.4}$$

where, the Mayer term Φ is a function of the initial and final state variables x_0 and x_f and the initial and final time t_0 and t_f and the Lagrange term L is a function of the state variables x, control variables u and time t. This formulation can also be extended to multiple-phase problems. In that case there is an initial cost term Φ_0 and each phase may have a final cost and a Lagrange cost. In the optimization framework in this research there are two options for optimization. The first one is to optimize only for fuel consumption and the second one is to optimize for flight time. These two options can be combined in order to optimize the DOC. This results in the following two cost functions:

$$\Phi_{fuel} = \sum_{i=1}^{n} \left(W_i(t_0) - W_i(t_f)\right) \tag{4.5}$$

and

$$\Phi_{DOC} = \alpha \cdot \sum_{i=1}^{n} t_{f_i} + (1-\alpha) \cdot \sum_{i=1}^{n} \left(W_i(t_0) - W_i(t_f)\right), \tag{4.6}$$

Equation 4.5 sums up the changes in weight for all aircraft and is used to optimize for minimum fuel consumption. Equation 4.6 optimizes the trajectories for a combination of minimum fuel and minimum flight time. Here α is a constant between 0 and 1 that allows shifting the cost function from optimizing for minimum fuel consumption ($\alpha = 0$) to optimizing for minimum flight time ($\alpha = 1$). α can be modified for different compositions of DOC. As explained before the DOC varies per aircraft, route and airline and should be seen as an additional option for the tool.

The two cost functions given in Equations 4.5 and 4.6 are the main focus of this research. Based on which of these two cost functions need to be optimized, Equation 4.5 or 4.6 should be implemented in the performance index (Equation 4.4). The Lagrange components are not required in this research, so the Lagrange component in the performance index is set to zero.

4.1.2. GPOPS

For this study a tool is required that can optimize multiple-phase problems. For trajectory optimization problems, the absence of discrete variables generally allows the use of optimal control theory based optimization algorithms [39]. One of the benefits of optimal control algorithms is that they make use of gradient information to determine both the search direction towards an optimal solution and a termination criterion to confirm an optimal solution has been found, which results in a relatively low computational time. Furthermore, optimal control theory also allows to implement complex constraints and composite performance indices (which in this research allows to optimize for a combination of fuel consumption and flight time). The optimization tool that will be used is ”GPOPS”. GPOPS stands for ”General Pseudospectral OPtimal Control Software” and is a MATLAB based general purpose software for solving multiple-phase optimal control problems using pseudospectral methods [40]; it does so using the Radau pseudospectral method [41]. It uses the technique of collocation at Legendre-Gauss points relying on gradient based algorithms. GPOPS is used in combination with ”IntLab” (Interval Laboratory) which is a third-party automatic differentiator, and with the non-linear programming solver ”SNOPT” (Sparse Nonlinear OPTimizer).

To solve an aircraft trajectory optimization control problem three mathematical objects must be combined: the control system differential equations, the state-control constraints and the cost function integration [42]. For this optimization a pseudospectral method is suitable as it is efficient in the approximation of all three mathematical objects. The optimisation routine enables the use of multiple-phase problem solving. Different phases are used for several reasons. They can describe different segments of the flight, different aircraft configurations or maybe different regulations during different altitudes or airspaces. The different phases of this study are discussed in the next subsection. Several MatLab functions are conceived in order to accurately specify the optimal control problem and should be defined independently of each other. In order to solve an optimal control problem like this one in GPOPS, several MATLAB functions should be defined. The MATLAB functions should define the following functions in each phase:

1. The cost functional.
2. The right-hand side of the differential equations and path constraints
3. The boundary conditions
4. The linkage constraints (how the phases are linked with each other)

Furthermore there are lower and upper limits on all components. This means that the following quantities cannot exceed specified limits:

1. Initial and terminal time per phase
2. The states at the following points in time:
    - Start of the phase

    - During the phase
    - End of the phase

3. The controls

4. The static parameters

5. The path constraints

6. The boundary conditions

7. The phase duration

8. The linkage constraints

Also the number of ”nodes” and ”intervals” per phase should be specified. The number of nodes represents the number of collocation points.

The problem is solved using the direct trajectory optimisation technique of collocation with non-linear programming (NLP). In this method, the trajectory dynamics are discretized in order to transform the optimal control problem into a NLP problem. The trajectory is divided into a specified number of time intervals, connected by node points (the number of nodes and intervals must be specified per phase). The system differential equations are discretized and transformed using implicit integration.

4.1.3. Multiple phases

GPOPS enables the optimization of a problem consisting of multiple phases. As mentioned before, there are several reasons to split the trajectories up into multiple phases. The question that rises now is: how many and which phases should be distinguished? The main interest in this research is to assess whether it is beneficial to fly in a formation or not. As the aircraft will not join in formation during the take-off and landing segments of the flight, these segments will remain the same for aircraft that will or will not join in formation. So the take-off and landing segments of the flights are of less importance than the cruise segments and will therefore not be included in this research. The more phases we distinguish in our optimization, the higher the computational time will be. This is why in this research a starting and final point for all flights will be taken at a certain altitude and airspeed and between these two points there is a climb, cruise and descent part in which the different aircraft can join in formation or not. When the aircraft join in formation there will be cruise segments before and after the formation, this is because the aircraft need to reach the rendezvous point from their starting point and they must reach their final points from the split-up point.

In this research the trajectories are determined as in Figure 4.2, every flight segment is a different phase. Thus for every flight we have an initial phase that is from the starting point (departure) to the rendezvous point, a formation phase that is the cruise in formation segment from the rendezvous point to the split-up point and a final phase that is from the split-up point (separation) to the end point (arrival). The formation phase, however, is a joint phase, meaning that this phase is a common phase of multiple aircraft. A two-aircraft (as seen in Figure 4.2) for example features five phases.

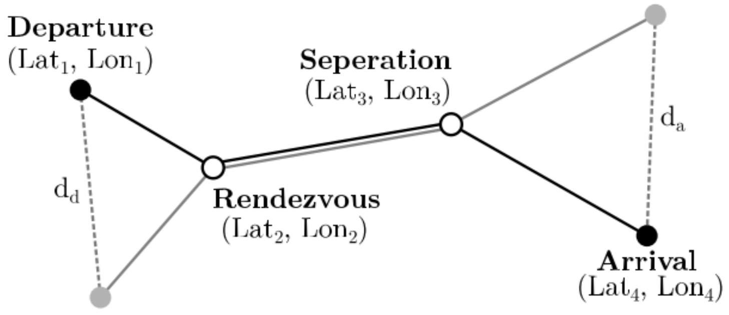

Figure 4.2: Schematic overview of the horizontal flight paths of two aircraft with a common cruise segment [6]

4.1.4. Dynamic Aircraft Performance Models

From literature different dynamic aircraft performance models can be found. Because the most important (most fuel consuming) segment of a flight is the cruise segment, the research will mainly focus on that particular segment (including some climb and descent, but no take-off and landing). Two models are combined in this research, the intermediate point-mass model and the energy-state model.

Intermediate Point-Mass Model

The first model that is investigated is the intermediate point-mass model. This model is a simplification of the dynamic full point-mass model (which in its turn is a simplification of the rigid-body model). The equations of motion commonly used for performance analysis are based on the assumption that the aircraft behaves as a point in time with a variable mass. For the full point-mass model (excluding the effect of wind) the equations of motion are:

$$\dot{x} = Vcos(\gamma)cos(\chi) \tag{4.7}$$

$$\dot{y} = Vcos(\gamma)sin(\chi) \tag{4.8}$$

$$\dot{h} = Vsin(\gamma) \tag{4.9}$$

$$\dot{V} = g_0\left[\frac{T-D}{W} - sin(\gamma)\right] \tag{4.10}$$

$$\dot{\gamma} = \frac{g_0}{V}\left[\left(\frac{L}{W}\right)cos(\mu) - cos(\gamma)\right] \tag{4.11}$$

$$\dot{\chi} = \frac{g_0}{Vcos(\gamma)}\frac{Lsin(\mu)}{W} \tag{4.12}$$

$$\dot{W} = -F_c, \tag{4.13}$$

where x, y and h are the position coordinates, V is the airspeed, γ is the flight path angle, χ is the heading, W is the aircraft gross weight, g_0 is the gravitational acceleration, T is the thrust, D is the drag, μ is the bank angle and F_c is the fuel flow, which is a function of altitude, velocity and thrust: $F_c = F_c(z, V, T)$. Visser and Hartjes apply this model to a 2-dimensional space in their research. They need to optimize the vertical flight path which follows a certain ground track[20]. This results in less state and control variables. However, this method can also be applied to a more complicated 3-dimensional problem. Visser elaborates on this further in other work as well [19]. The model described above is the full point-mass model and in this case it comprises seven state variables (the left-hand side in the equations above) and three control variables: the engine control setting η, the aerodynamic roll angle μ and the lift coefficient C_L. The engine control setting variable η has the following effect on the thrust of the aircraft:

$$T = (T_{max} - T_{min})\eta + T_{min}, \tag{4.14}$$

where T_{max} and T_{min} are the maximum and idle thrust of the engine respectively. The aerodynamic forces are the usual. For the lift:

$$L = C_L qS = C_L\frac{1}{2}\rho(z)V^2S, \tag{4.15}$$

where C_L is the lift coefficient, q is the dynamic pressure, ρ is the air density and S is the wing surface. And for the drag:

$$D = C_D(C_L)qS \Rightarrow D = D(z, V, C_L), \tag{4.16}$$

where C_D is the drag coefficient for which a parabolic drag polar will be assumed:

$$C_D = C_{D_0} + K(M)C_L^2, \tag{4.17}$$

which consists of two parts: the zero-lift drag C_{D_0} and the induced drag $K(M)C_L^2$. This shows that the lift coefficient control variable affects the lift and drag. By excluding the path angle dynamics, this model can be simplified to the intermediate point-mass model. In the intermediate point-mass model the flight path angle γ replaces the lift coefficient C_L as control variable. The intermediate point-mass model has six state variables x, y, h, V, χ and W and control variables η, μ and γ. As this study focuses on flights that cross the North-Atlantic Ocean the coordinate system will be changed to the ”World Geodetic

System" (WGS). This system is widely used for navigation and comprises a standard coordinate system for the Earth. The coordinate origin of this system is at the center of the Earth and the meridian of zero longitude is near Greenwich. Instead of the x, y and h position coordinates, in this research the position of the aircraft is given by latitude ϕ, longitude λ and altitude z. The altitude z is the altitude measured from the surface of the Earth and the distance from the center of the Earth to the surface R_E is approximately 6378km. The dynamics can now be expressed as:

$$x(t) = \begin{pmatrix} \phi \\ \lambda \\ z \\ V \\ \chi \\ W \end{pmatrix} \quad \text{and} \quad u(t) = \begin{pmatrix} \eta \\ \gamma \\ \mu \end{pmatrix} \tag{4.18}$$

$$\dot{\phi} = \frac{V cos(\gamma) sin(\chi)}{R_e + z} \tag{4.19}$$

$$\dot{\lambda} = \frac{V cos(\gamma) cos(\chi)}{R_e + z} \tag{4.20}$$

$$\dot{z} = V sin(\gamma) \tag{4.21}$$

$$\dot{V} = g_0 \left[\frac{T - D}{W} - sin(\gamma) \right] \tag{4.22}$$

$$\dot{\chi} = \frac{g_0}{V cos(\gamma)} \frac{L sin(\mu)}{W} \tag{4.23}$$

$$\dot{W} = -F_c \tag{4.24}$$

This order reduction simplifies the optimization of the trajectories and is therefore desirable. However, the aerodynamic drag is slightly underestimated; it is now evaluated as if the aircraft flies a quasi-linear path. Also, now the flight path angle γ is a control and no longer a state variable and this means that there can no longer be an initial and terminal boundary imposed on it. Also the flight path angle, being a control variable, is now allowed to vary discontinuously which also makes it less realistic.

Energy-State model

The intermediate point-mass model will be simplified further to the energy-state model, which is the second dynamic aircraft performance model used in this research. The energy-state model can be obtained by taking the order-reduction process one step further. Here the specific energy E is introduced. The specific energy is a function of velocity V and altitude z given by:

$$E = z + \frac{V^2}{2 g_0} \tag{4.25}$$

In the energy-state model the altitude dynamics are neglected, so:

$$\dot{z} = V sin(\gamma) = 0 \quad \Rightarrow \quad \gamma = 0 \tag{4.26}$$

When neglecting the altitude dynamics, the flight path angle γ can be removed from the problem (see Equation 4.26), while the altitude z is promoted from state variable to control variable. Hence, for the energy-state model the following state and control variables are left:

$$x(t) = \begin{pmatrix} \phi \\ \lambda \\ E \\ \chi \\ W \end{pmatrix} \quad \text{and} \quad u(t) = \begin{pmatrix} \eta \\ z \\ \mu \end{pmatrix}, \tag{4.27}$$

with the following equations for the state variables:

$$\dot{\phi} = \frac{V cos(\chi)}{R_e + z} \tag{4.28}$$

$$\dot{\lambda} = \frac{V sin(\chi)}{R_e + z} \tag{4.29}$$

$$\dot{E} = \frac{(T-D)V}{W} \tag{4.30}$$

$$\dot{\chi} = \frac{g_0}{V} tan(\mu) \tag{4.31}$$

$$\dot{W} = -F_c \tag{4.32}$$

Inspecting the equations above and the equations for the intermediate point-mass and full point-mass model, it can be seen that the effect of merely neglecting the flight path angle dynamics results into setting $cos(\gamma) = 1$, which is a reasonable approximation when an aircraft is in steady flight (e.g. cruise). In the energy-state model, the altitude z is promoted from state to control variable and therefore, has the same issue as the flight path angle γ had in the intermediate model, it can no longer be given an initial or terminal boundary.

However, due to the simplifications the energy-state model does has some drawbacks. This model does not allow to enforce the flight path angle γ to remain within specified boundaries, as it is ”vanished from the equations. Furthermore, as the altitude z is promoted to control variable, the rate of descent $\dot{z}$ no longer be constrained.

4.1.5. Phase Linkages

During the different phases the state variables are free, but at the moment when two phases meet, the terminal state variables of one phase should be equal to the initial state variables of the other phase. This is done by the linking terminal state variables of one phase with the initial state variables of the successive phase. In Figure 4.3 a schematic representation of the vertical flight path over five phases is shown. The red line represents aircraft A, the blue line aircraft B and the green line represents the common formation phase. These five phases are linked to each other by four links. For a two-aircraft formation the following four links are identified:

- Link 1: Connects phase 1 with phase 3
- Link 2: Connects phase 2 with phase 3
- Link 3: Connects phase 3 with phase 4
- Link 4: Connects phase 3 with phase 5

The first two links are:

$$Link_1: \begin{pmatrix} \phi_{f,1} \\ \lambda_{f,1} \\ z_{f,1} \\ V_{f,1} \\ \chi_{f,1} \\ W_{A_{f,1}} \end{pmatrix} \Rightarrow \begin{pmatrix} \phi_{f,1} \\ \lambda_{f,1} \\ E_{f,1} \\ \chi_{f,1} \\ W_{A_{f,1}} \end{pmatrix} = \begin{pmatrix} \phi_{0,3} \\ \lambda_{0,3} \\ E_{0,3} \\ \chi_{0,3} \\ W_{A_{0,3}} \end{pmatrix} \quad \text{and} \quad Link_2: \begin{pmatrix} \phi_{f,2} \\ \lambda_{f,2} \\ z_{f,2} \\ V_{f,2} \\ \chi_{f,2} \\ W_{B_{f,2}} \end{pmatrix} \Rightarrow \begin{pmatrix} \phi_{f,2} \\ \lambda_{f,2} \\ E_{f,2} \\ \chi_{f,2} \\ W_{B_{f,2}} \end{pmatrix} = \begin{pmatrix} \phi_{0,3} \\ \lambda_{0,3} \\ E_{0,3} \\ \chi_{0,3} \\ W_{B_{0,3}} \end{pmatrix}, \tag{4.33}$$

where $E_{f,1} = z_{f,1} + \frac{V_{f,1}^2}{2g_0}$, $E_{f,2} = z_{f,2} + \frac{V_{f,2}^2}{2g_0}$ and the subscripts of the state variables indicate the number of the phase and whether it is the initial state or the terminal state of that phase (e.g. $\phi_{f,1}$ is the terminal latitude of phase 1 and $W_{B_{0,3}}$ is the initial weight of aircraft B in phase 3). Links 3 and 4 are given by:

$$Link_3: \begin{pmatrix} \phi_{f} \\ \lambda_{f,3} \\ E_{f,3} \\ \chi_{f,3} \\ W_{A_{f,3}} \end{pmatrix} = \begin{pmatrix} \phi_{0,4} \\ \lambda_{0,4} \\ E_{0,4} \\ \chi_{0,4} \\ W_{A_{0,4}} \end{pmatrix} \Rightarrow \begin{pmatrix} \phi_{0,4} \\ \lambda_{0,4} \\ z_{0,4} \\ V_{0,4} \\ \chi_{0,4} \\ W_{A_{0,4}} \end{pmatrix} \quad \text{and} \quad Link_4: \begin{pmatrix} \phi_{f,3} \\ \lambda_{f,3} \\ E_{f,3} \\ \chi_{f,3} \\ W_{B_{f,3}} \end{pmatrix} = \begin{pmatrix} \phi_{0,5} \\ \lambda_{0,5} \\ E_{0,5} \\ \chi_{0,5} \\ W_{B_{0,5}} \end{pmatrix} \Rightarrow \begin{pmatrix} \phi_{0,5} \\ \lambda_{0,5} \\ z_{0,5} \\ V_{0,5} \\ \chi_{0,5} \\ W_{B_{0,5}} \end{pmatrix}, \tag{4.34}$$

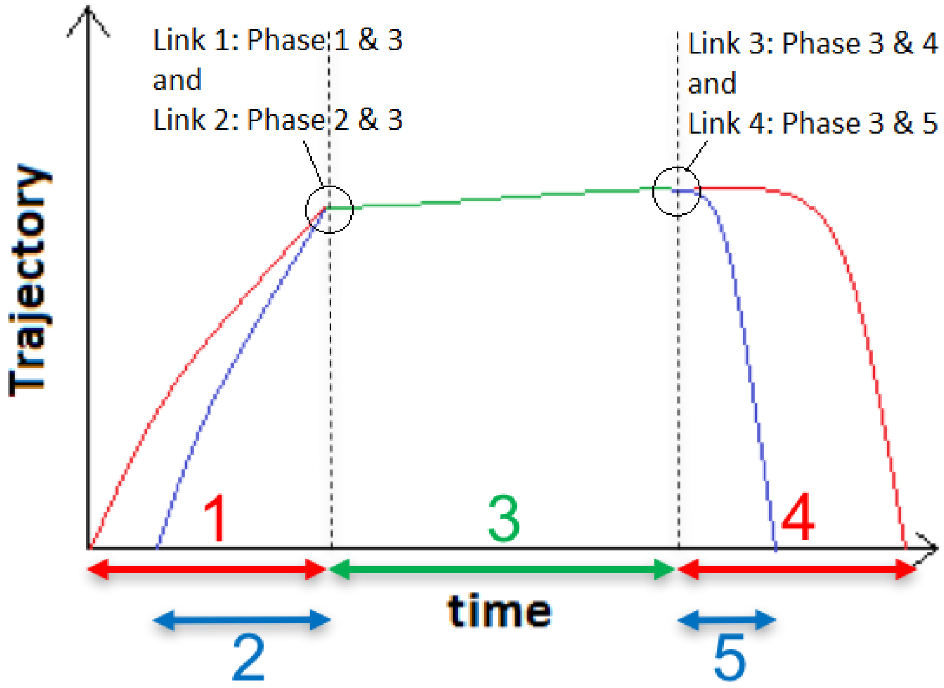

Figure 4.3: A schematic representation of the vertical flight paths of a two-aircraft formation (five phases)

where $E_{0,4} = z_{0,4} + \frac{V_{0,4}^2}{2g_0}$ and $E_{0,5} = z_{0,5} + \frac{V_{0,5}^2}{2g_0}$. To link phases with an intermediate point-mass model to phases with an energy-state model the specific energy E must be equal. As shown earlier, however, the specific energy is a function of altitude z and speed V. This means that at the link, where the initial specific energy in phase 3 is equal to the terminal specific energy of phases 1 and 2, the altitude and speed can still jump. For the final results in terms of fuel consumption and DOC this does not have a significant effect, but when looking at the trajectories of the individual aircraft this is not realistic. In order to keep this within limits some extra constraints might be needed. This problem will be discussed at a later stage.

4.2. Formation Flight

The next step in the development of the tool is to account for the reduction in fuel consumption due to formation flight. As it is clear from literature, the reduction in fuel consumption due to formation flight is a result of a reduction in induced drag. There are different approaches to implement this formation flight induced drag reduction. In this research the following two approaches are briefly investigated: the aircraft equally split the benefits during the flights and the aircraft split the benefits post flight.

4.2.1. Split the benefits during flight

One way to approach the benefits of formation flight in the research is to split the reduction in induced drag evenly over all aircraft flying in the formation. This means that the leading aircraft and the trailing aircraft both profit from flying in formation. This is easy to implement because in this approach, it is irrelevant which aircraft flies in front and which aircraft flies behind. To implement this for a two-aircraft formation, the induced drag reduction of for example 10% that would count for the trailing aircraft will be equally split over the two aircraft, resulting in 5% induced drag reduction for both aircraft. From an operational point of view this would be good, because this means that all aircraft in formation benefit and if aircraft from different operators (airlines) fly together they don't need to discuss what the sequence of the formation will be. However, this method is not realistic because, as mentioned before, the aircraft leading the formation does not experience a reduction in induced drag.

Another way to split the reduction is to have the aircraft switch position during the flight. This way all aircraft in the formation get to benefit in turns. In general, the formation is most beneficial when the trailing aircraft has the highest fuel consumption (which most likely is the heaviest aircraft). This means that relative to the leading aircraft, the trailing aircraft of the formation will become heavier over time and therefore the total savings are higher. If the sequence changes during formation, the lighter aircraft will become the trailing aircraft and thus the resulting fuel consumption will not be optimal. Therefore, even if this method seems fair, it is not the optimal solution.

4.2.2. Split the benefits post flight

In reality the leading aircraft does not gain anything from flying in formation. As a matter of fact, it has to fly a detour in order to join in formation. This means that it must not only fly an extra distance, but also has to take extra fuel on board, which results in a heavier aircraft during the flight and thus a higher fuel consumption. The trailing aircraft also has to fly a detour, but when in formation this aircraft benefits from a reduction in fuel flow. From an operational point of view, however, this method presents some complications, which are described in Chapter 3. The approach, in which the trailing aircraft remains in this position (with the related benefits), offers the highest reduction and will be applied in this research. To implement this, the formation flight induced drag fraction ϵ is introduced. ϵ is the fraction of induced drag due to formation over induced drag when not in formation. Different values for the reduction in induced drag are found by researchers. For a two-aircraft formation the reduction in induced drag of the trailing aircraft can be between 10% and 70% and for a three-aircraft formation the reduction ranges from 20% to 90%.

The results in Figures 4.4a and 4.4b, which are obtained by Bower et al. [7], show the induced drag fraction as a function of the spanwise position of the trailing aircraft relative to the leading aircraft, for a streamwise distance of $(x/b) = 5$ (a streamwise distance of five times the wingspan) and for a lift coefficient of $C_L = 0.5$. In Figure 4.4a the induced drag fraction for different spanwise distances for a two-aircraft formation is presented. In the figures y represents the spanwise distance and b is the wingspan of the leading aircraft. This figure shows that the aircraft, depending on their spanwise position, can reach a formation induced drag fraction of 0.65 (a reduction in induced drag of 35%). This is for the formation as a whole while, as mentioned before, the leading aircraft has no reduction, which means that according to Bower et al. the trailing aircraft can reach a reduction of 70% in induced drag. Figure 4.4b shows the same for three configurations of a three-aircraft formation. The formations V, inverted-V and echelon are represented by the colors red, black and blue, respectively. The different types of lines represent the left, middle and right aircraft. For echelon formation the aircraft in the middle has the same formation induced drag fraction as the trailing aircraft in the two-aircraft formation and the trailing aircraft of the three-aircraft formation can reach fraction of 0.3 (a reduction of 70%). Flying in the inverted-V formation the middle aircraft can reach even higher induced drag reductions. However, these values are for a streamwise distance of five wingspans. In civil aviation this would be much more.

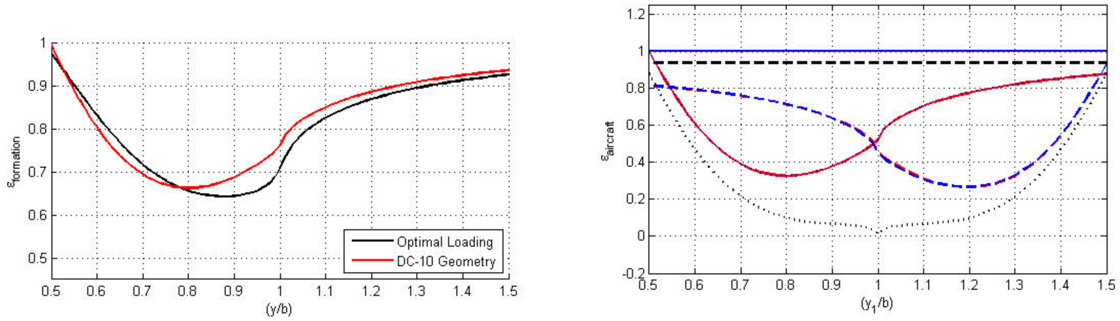

(a) Fraction of induced drag on the formation for a two-aircraft formation

(b) Fraction of induced drag per aircraft for a three-aircraft formation

Figure 4.4: Induced drag fractions for different spanwise over wingspan (y/b) distance between leading and trailing aircraft [7]

When different aircraft with different weights are joining together, this can influence the amount of reduction. Logically, when a small Boeing 737-300 flies in front of a fully loaded Airbus A380, the effect on the trailing A380 is lower compared to what the effect would be on the B733 when an A380 flies in front it. Xue et al. investigated this and developed a model that calculates the reduction in total drag and induced drag for aircraft with various lead and trail weight ratios [8]. The results of this model are shown in Figure 4.5.

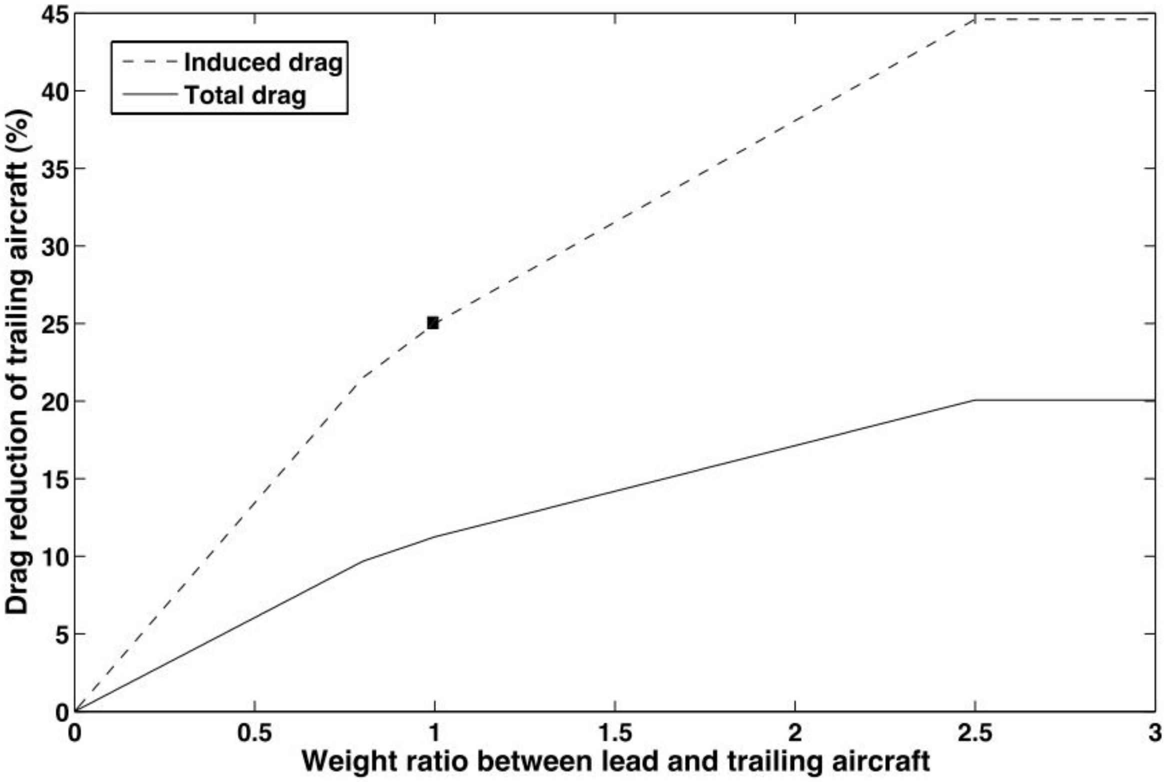

Figure 4.5: Induced drag reduction for various lead and trail weight ratios [8]

Figure 4.5 indicates that the reduction in induced drag is larger when the trailing aircraft is lighter than the leading aircraft. Hence, when two different aircraft join in formation it would make sense to have the heavier aircraft fly in front. On the other hand, the heavier aircraft probably has a higher fuel consumption compared to the lighter aircraft, which means that a reduction of a couple percent in fuel flow for the heavy aircraft results in more fuel savings than when a couple of percent is gained on the fuel flow reduction of the lighter aircraft. Therefore, the ideal formation sequence is not only based on the weights of the aircraft, but also on the aircraft types.

In this study mainly identical aircraft are investigated. A conservative value in induced drag reduction of 25% ($\epsilon = 1 - 0.25 = 0.75$) is assumed for the trailing aircraft of a two-aircraft formation and, respectively, 25% ($\epsilon = 0.75$) and 50% ($\epsilon = 0.5$) for the second and third aircraft in a three-aircraft formation. The formation flight induced drag fraction ϵ acts on the induced drag:

$$C_D = C_{D_0}(M) + \left(K(M) * C_L^2\right) * \epsilon, \tag{4.35}$$

where $C_{D_0}(M)$ is the zero-lift drag of the aircraft and $\left(K(M) * C_L^2\right)$ is the aircraft induced drag. As the leading aircraft does not experience a reduction in induced drag, the formation flight induced drag fraction ϵ on this aircraft is equal to one.

4.3. Input

In order to obtain the desired output, inputs are required. In Figure 4.1 these are presented in blue. The atmospheric data and aircraft data do not need to be changed per experiment once they are implemented correctly. The constraints and initial guess, however, should be adjusted for different experiments.

4.3.1. Atmospheric Data

As for all calculations in the aviation industry, the atmospheric data is of great importance. Aircraft fly at different locations and altitudes and therefore the atmospheric conditions changes. The atmospheric data necessary for the optimization tool to function properly are the following:

1. Temperature T
2. Temperature derivative over altitude $\frac{dT}{dz}$
3. Ratio temperature over temperature at sea level θ
4. Pressure p
5. Pressure derivative over altitude $\frac{dp}{dz}$
6. Ratio pressure over pressure at sea level δ
7. Air density ρ
8. Air density derivative over altitude $\frac{d\rho}{dz}$
9. Speed of sound V_{sound}
10. Speed of sound derivative over altitude $\frac{dV_{sound}}{dz}$

These parameters vary only with altitude and can be derived for all altitudes. Commercial aircraft usually have a cruise altitude of around 11000 meters and a service ceiling that is not much higher. Therefore, for this study mainly the altitude in the troposphere is of importance.

4.3.2. Aircraft Data

During this study three types of aircraft are considered. The short- to medium-range Boeing 737-700 (narrow-body aircraft), the long-range Boeing 747-400 (wide-body aircraft) and the medium- to long-range McDonnell Douglas MD-11 (wide-body aircraft). In the following sections they will be briefly reviewed and in Table 4.1 some specifications, which are also implemented in the aircraft models, are summarized.

Table 4.1: Specification of aircraft

Aircraft	**B733**	**MD-11**	**B744**
Wing Surface [m^2]	105.4	338.87	541.16
MTOW [kg]	62820	274655	362874
OEW [kg]	32700	128808	178756
MLW [kg]	51700	195048	260362
MZFW [kg]	48410	181440	242672
Max fuel [kg]	18000	117356	163396
Max payload [kg]	15710	52632	63917

Boeing 737-300

The Boeing 737-300 is a twin engine short- to medium-range aircraft. It has two CFM563 engines and is originally developed as a shorter low-cost version of the Boeing 707 and 727.

As mentioned above the 737-300 usually is not meant to fly long distances. It reaches its service ceiling at around 11278m and with a standard configuration (150 passengers) it has a maximum range of around 5000km. However, when the aircraft has a ”business” configuration (fewer passengers and higher fuel capacity) its range can increase up to 10000km, enabling it perform transatlantic flights.

The high-speed drag polar for the aircraft is parameterized as follows:

$$C_D(M, C_L) = C_{D_0}(M) + K(M)C_L^2, \tag{4.36}$$

and the drag coefficient of the B733 is given in Table 4.2.

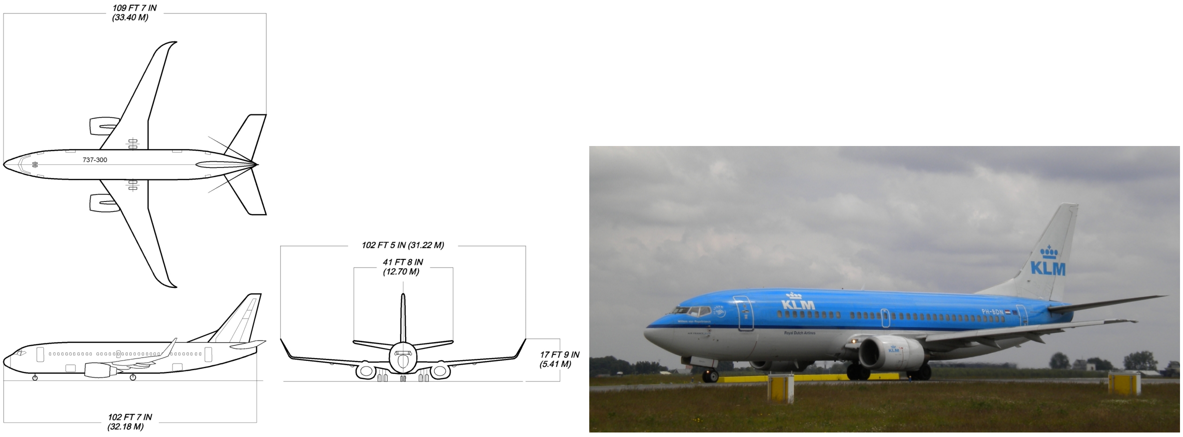
109 FT 7 IN
(33.40 M)
737-300
102 FT 5 IN (31.22 M)
41 FT 8 IN
(12.70 M)
17 FT 9 IN
(5.41 M)
102 FT 7 IN
(32.18 M)
KLM

(a) Boeing 737-300 dimensions

(b) Boeing 737-300 aircraft operated by KLM

Figure 4.6: Boeing 737-300

Table 4.2: Boeing 737-300 High Speed Drag Polar

M	0.3	0.5	0.6	0.7	0.78	0.78	0.8	0.82
$CD_0(M)$	0.0210	0.0210	0.0210	0.0215	0.0220	0.0332	0.0230	0.0270
$K(M)$	0.0425	0.0425	0.0425	0.0425	0.0450	0.0600	0.0700	0.0800

These values are interpolated and two second order polynomials are derived to represent the $C_{D_0}(M)$ and K(M):

$$C_{D_0}(M) = 0.0375M^2 - 0.0362M + 0.0288 \tag{4.37}$$

$$K(M) = 0.3167M^2 - 0.3066M + 0.1089 \tag{4.38}$$

Boeing 747-400

The Boeing 747-400 is a four-engine wide-body aircraft designed to fly long distances. It has four PW4056 engines and can fly 14200km carrying its maximum payload.

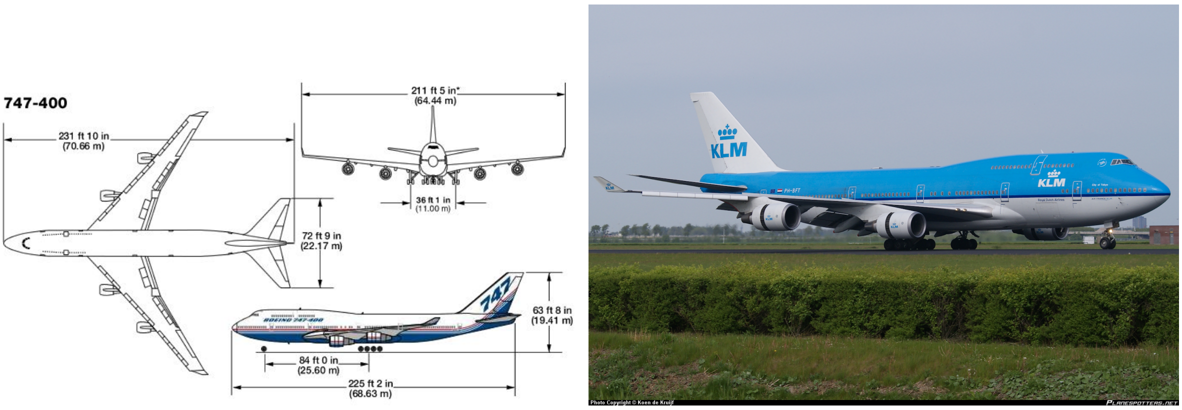
747-400
231 ft 10 in
(70.66 m)
211 ft 5 in*
(64.44 m)
36 ft 1 in
(11.00 m)
72 ft 9 in
(22.17 m)
63 ft 8 in
(19.41 m)
84 ft 0 in
(25.60 m)
225 ft 2 in
(68.63 m)
KLM

(a) Boeing 747-400 dimensions

(b) Boeing 747-400 aircraft operated by KLM

Figure 4.7: Boeing 747-400

Also the table of drag coefficients for the B744 is available in Table 4.3.

As done for the B733 these values are interpolated and two second order polynomials are obtained to represent the $C_{D_0}(M)$ and K(M):

$$C_{D_0}(M) = -0.0010M^2 + 0.0006M + 0.0125 \tag{4.39}$$

$$K(M) = 0.0975M^2 - 0.0846M + 0.0705 \tag{4.40}$$

Table 4.3: Boeing 747-400 High Speed Drag Polar

M	0.3	0.5	0.6	0.7	0.8	0.85
$CD_0(M)$	0.012564	0.02100.012469	0.012423	0.012443	0.012367	0.012173
$K(M)$	0.053463	0.05373	0.05474	0.058231	0.064035	0.070273

McDonnell Douglas MD-11

The McDonnell Douglas MD-11 is a three-engine wide-body aircraft that is designed to fly medium to long distances. It has three PW4460 engines and can fly around 12600km carrying its maximum payload.

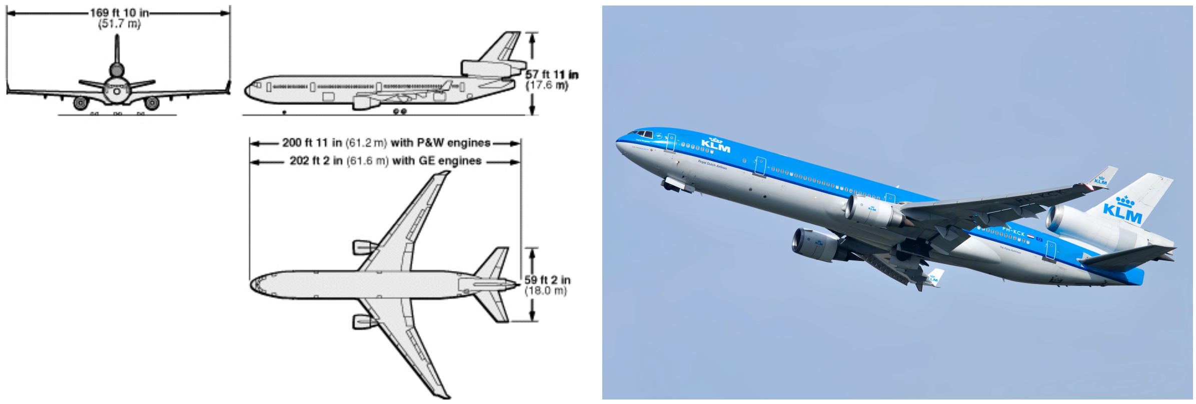
169 ft 10 in (51.7 m)
57 ft 11 in (17.6 m)
200 ft 11 in (61.2 m) with P&W engines
202 ft 2 in (61.6 m) with GE engines
59 ft 2 in (18.0 m)
KLM

(a) The McDonnell Douglas MD-11 dimensions (b) The McDonnell Douglas MD-11 operated by KLM

Figure 4.8: McDonnell Douglas MD-11

The table of drag coefficients for the MD-11 is shown in Table 4.4. Two second order polynomials are derived to represent the $C_{D_0}(M)$ and K(M):

$$C_{D_0}(M) = 0.0186M^2 - 0.0236M + 0.0235 \tag{4.41}$$

$$K(M) = 0.3608M^2 - 0.4686M + 0.1902 \tag{4.42}$$

Table 4.4: The McDonnell Douglas MD-11 High Speed Drag Polar

M	0.5	0.6	0.7	0.75	0.80	0.82	0.84	0.86	0.88
$CD_0(M)$	0.0163	0.0163	0.0163	0.0164	0.0165	0.0166	0.0167	0.0170	0.0176
$K(M)$	0.0431	0.0432	0.0433	0.0430	0.0428	0.0429	0.0456	0.0511	0.0690

4.3.3. Constraints

To make the developed tool more realistic, constraints are added. For this study there are two kinds of constraints: ”path” constraints and ”event” constraints. Path constraints are valid during a phase, excluding the final point of the phase (e.g. the climb rate during a climb phase may not be below 0 m/s), while event constraints are valid only for the initial or final point of the phase (e.g. the altitude at the final phase of a descend phase should be 3000 meters). In this section the active constraints will be briefly discussed.

Thrust Level

One of the three control variables in both dynamic aircraft performance models is the thrust level η. The thrust of the aircraft is determined by the following equation:

$$T = (T_{max} - T_{min})\eta + T_{min}, \tag{4.43}$$

where T_{max} is the maximum thrust and T_{min} is the idle thrust. When the engine is idle the thrust level η is zero and when the engine is at maximum thrust the thrust level η is 1. So the thrust level η must be:

$$0 < \eta < 1 \tag{4.44}$$

This constraint applies to all aircraft that join in the formation during all phases, but during formation the control variable η is only valid for one aircraft (aircraft A). The control variable η_A is an input for the aircraft model and from this aircraft model the thrust and fuel flow of aircraft A are determined. As the weight and maybe other aircraft characteristics of the second aircraft in the formation (aircraft B) are not the same as for aircraft A, the thrust level is different as well. But as it flies next to aircraft A, it has the same state variables except for the weight. As input for the aircraft model it uses the $\dot{E}$ to get the required thrust level η_B needed to keep up with aircraft A.

$$T_B = \frac{\dot{E} \cdot W_B}{V} + D_B \tag{4.45}$$

and

$$\eta_B = \frac{T_B - T_{min}}{T_{max} - T_{min}} \tag{4.46}$$

For this thrust level (and when more aircraft join the formation this applies also for them) the constraint remains the same; η_B must be between 0 and 1.

Altitude

The earlier mentioned service ceiling of the aircraft considered, constrains the maximum altitude of the trajectories. Furthermore, the initial and final states of the aircraft are determined beforehand. The altitude at which the experiments will start and end is set at 10000ft (3048m). This will also be the minimum altitude constraint during the experiments. This leads to the following constraint for the altitude:

$$z_{min} \leq z \leq z_{max}, \tag{4.47}$$

where the minimum altitude z_{min}, which is equal for all aircraft, is set to 3048m and the maximum altitude z_{max} depends per aircraft type. The maximum altitudes are given in Table 4.5.

Table 4.5: Maximum altitudes for the different aircraft types

Operating speeds	**B733**	**B744**	**MD-11**
z_{max} [m]	11278	13747	13000

Speed

The minimum and maximum operating speeds of the aircraft must also be constraint. The maximum speed of the aircraft is given by two terms: V_{MO} and M_{MO}. V_{MO} is in knots Calibrated Airspeed (CAS). The CAS is strictly a measure of dynamic air pressure, hence the relationship between CAS and TAS (True Airspeed) varies with the altitude (air density). As the altitude increases, the air density decreases and if the TAS remains constant, the CAS decreases. On the other hand there is the maximum operating Mach number M_{MO} for the aircraft, which has the following relation with the TAS.

$$TAS_{max} = M_{MO} * V_{sound}, \tag{4.48}$$

where the speed of sound V_{sound} is dependent of the temperature T ($V_{sound} = \sqrt{RT\gamma}$). As the altitude increases, the speed of sound also increases and the TAS decreases for a constant Mach.

This leads to the following speed constraints:

$$TAS_{min} \leq TAS \leq TAS_{max}, \tag{4.49}$$

for which the minimum and maximum operating speeds for all three aircraft can be found in Table 4.6. The maximum operating speed of the MD-11 actually changes with the fuel quantity in the wing tip tanks, but this will be left out of consideration. The maximum operating speed is determined by the slower of the two (at altitude above 10000m the M_{MO} is always limiting).

In Figures 4.9a, 4.9b and 4.9c the design speeds of the three aircraft are displayed. The velocity of the aircraft must be on the right side of the red line and on the left side of the blue and green lines.

Table 4.6: Operating speeds of the Boeing 737-300, the Boeing 747-400 and the McDonnell Douglas MD-11

Operating speeds	**B733**	**B744**	**MD-11**
V_{min} [kts]	195	195	195
V_{MO} [kts]	340	365	360
M_{MO}	0.82	0.9	0.88

Specific energy

The specific energy E is a function of the altitude z and speed V (see Equation 4.25). Therefore, the specific energy must always be larger than the altitude.

$$E - z > 0 \tag{4.50}$$

Final weight

To optimize the flights for fuel consumption it is important not to take too much fuel on board for the flight if it is not necessary. Therefore, to minimize the fuel consumption the flight should ideally end with zero fuel. However, in normal circumstances, aircraft take enough fuel on board for the flight plus a reserve. This reserve usually consists of contingency fuel and a final reserve fuel. The final reserve fuel is the minimum fuel required to fly for 30 to 45 minutes at 1500ft at holding speed above the destination or alternate aerodrome (Figure 4.10). Contingency fuel is carried to account for additional fuel consumption during the scheduled flight caused by for example wind, ATM restrictions or changes in route. In general this is around 5% of the normal trip fuel. Aircraft that join in formation will have to deviate from their optimal solo route, resulting in an increase of the distance covered. In addition, the aircraft must also take into account that the other aircraft with which it will join, might not show-up (due to technical problems, delay, etc.). This means that the aircraft should carry enough fuel to fly the detour distance solo (see Figure 4.11).

In order to apply this into the tool, a constraint is introduced that fixes the final weight of the aircraft. For aircraft flying solo (i.e. aircraft that won't join in formation) and therefore flying their optimal route, the final weight of the aircraft ($W_{solo}(t_f)$) is the sum of the Operational Empty Weight (OEW) the payload ($W_{payload}$) and a fuel reserve of 5% of the total fuel capacity (W_{FC}):

$$W_{solo}(t_f) = OEW + W_{payload} + 0.05 \cdot W_{FC} \tag{4.51}$$

These weights differ per aircraft and can be found in Table 4.1. With the final weight of the flight fixed, the tool will optimize the initial weight to give the optimal results for one of the cost functions. The required fuel, for the same aircraft that will perform a flight from the same origin to the same destination but as the trailing aircraft in a formation, will be less than the fuel required for the individual flight. However, as it will fly a detour and must carry enough fuel to safely fly this increased distance solo, the initial fuel of the aircraft should be more than for the individual flight. For the formation flight, the initial weight of the aircraft is fixed instead of the final weight. The initial weight of the aircraft joining in formation will be the initial weight of the corresponding solo flight plus an extra reserve to overcome the extra distance that it must be able to fly also on its own:

$$W_{formation}(t_0) = W_{solo}(t_0) + t_{detour} \cdot \dot{m}, \tag{4.52}$$

where t_{detour} is the extra flight time (due to the detour) that the aircraft will have compared to the corresponding solo flight and $\dot{m}$ is the fuel burn per second for the aircraft. However, the extra flight time is not known beforehand because the trajectories depend on the carried amount of fuel. To derive this extra distance an extra iteration is necessary. In the tool this is implemented as follows. First, aircraft A is labelled as the aircraft that will receive the reduction in induced drag. This means that for aircraft B, which will fly a detour without a reduced induced drag, the final weight is still fixed just as it is for the solo case above. Aircraft B therefore optimizes the initial weight for a fixed final weight. The initial weight for aircraft B will be higher than it was for the solo case because it flies over a longer distance.

For aircraft A this is not so simple, because when optimizing this for a final weight it will automatically optimize for the flight with a lower drag and thus lower fuel flow. In the aircraft dynamic performance models an extra state variable is added, called W_n, which represents the pseudo weight of aircraft A. It

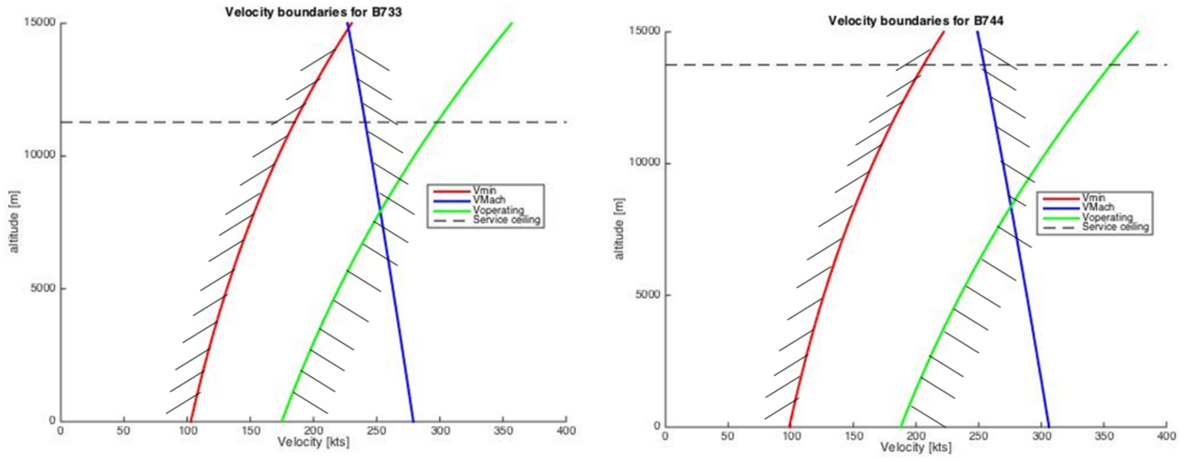

(a) Velocity boundaries for the Boeing 737-300

(b) Velocity boundaries for the Boeing 747-400

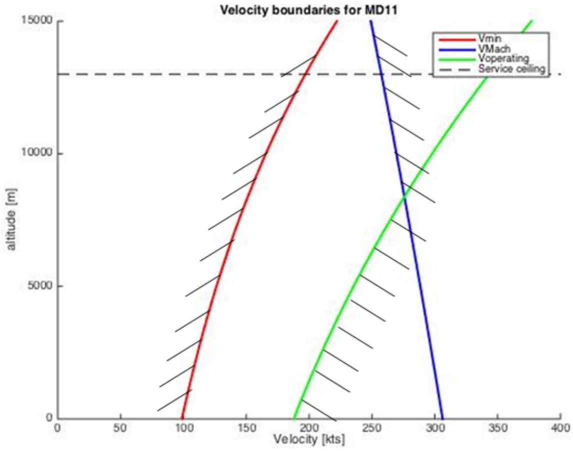

(c) Velocity boundaries for the McDonnell Douglas MD-11

Figure 4.9: Speed constraints in knots Calibrated Airspeed (CAS)

is the weight of aircraft A, but on the evolution of this variable there will be no influence of formation flight. As W_n is only necessary for aircraft A, it is only implemented in phases 1, 3 and 4 for a two-aircraft formation. This means that the number of state variables for these phases increase by one. This state is linked between these phases, just for like the real weight of aircraft A, W_A. What happens next, is that the tool still optimizes for the real weight of the aircraft, but in the meanwhile also records a fixed final weight for W_n, which is the same as it was for the solo flight. Now another constraint is introduced which equals the real initial weight of aircraft A with the initial pseudo weight:

$$W_{A_0} = W_{n_0} \tag{4.53}$$

This constraint enforces that the final weight of aircraft A is optimized for a fixed initial weight, with which it can also fly the (longer) formation route on its own in case the other aircraft does not show up.

Maximum fuel consumption

Besides fixing the final weight to get the optimal initial weight for a flight as described above (in Equation 4.51), there must also be a constraint on the total fuel consumption. The total fuel consumed by an aircraft during a flight cannot exceed the available fuel. Therefore the following constraint is added that limits the maximum fuel consumption for the flight per aircraft:

$$0 \leq \delta W \leq 0.95 \cdot W_{FC}, \tag{4.54}$$

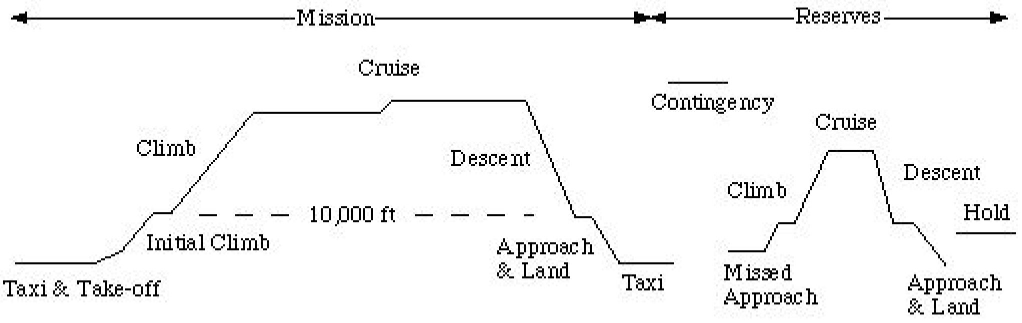
Mission
Reserves
Cruise
Contingency
Cruise
Climb
Descent
Climb
Descent
10,000 ft
Hold
Initial Climb
Approach
& Land
Taxi
Missed
Approach
Approach
& Land
Taxi & Take-off

Figure 4.10: Mission profile for the standard mission of an individual aircraft with reserve option

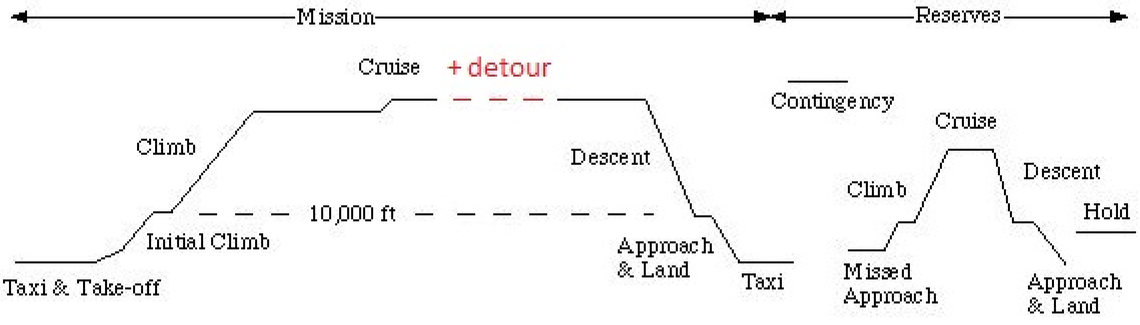
Mission
Reserves
Cruise
+ detour
Contingency
Cruise
Climb
Descent
Climb
Descent
10,000 ft
Hold
Initial Climb
Approach
& Land
Taxi
Missed
Approach
Approach
& Land
Taxi & Take-off

Figure 4.11: Mission profile for an individual aircraft that will join a formation with reserve option

where δW is the change weight over the entire flight and W_{FC} is the total fuel capacity. As the final weight of the aircraft includes 5% of the total fuel capacity, the maximum available fuel is 95% of the total fuel capacity. The total fuel capacity depends on the type of aircraft and is given in Table 4.1.

Forced Formation

When the tool is set to optimize the trajectories for aircraft that will join in formation, the tool forces the aircraft to fly together (at least for 5 seconds) even if it is not beneficial.

$$t_{formation} \geq 5, \tag{4.55}$$

where $t_{formation}$ is the flight time of the formation phase. When the results show that the total fuel consumption of the flights in formation is higher than the sum of the consumption of the corresponding solo flights or when the formation flight time $t_{formation}$ is only five seconds, it means that the formation in that case is not favourable.

Altitude and Velocity

During the different phases, different dynamic aircraft performance models are used. As mentioned before, these models have different state and control variables which must be linked to each other. However, linking the final points of the two initial solo phases to the initial point of the formation phase may lead to complications. The linkages (as described in Section 4.1.5) state that the specific energy at the end of phases 1 and 2 are equal to the specific energy at the start of phase 3:

$$E_{f,1} = E_{f,2} = E_{0,3} \tag{4.56}$$

This indicates that the specific energies are equal, but as the specific energy is a function of altitude z and velocity V, and these are not state variables in the energy-state model (phase 3), these can still vary. In the intermediate point-mass model, however, the altitude and velocity are state variables and can be constrained to be equal:

$$z_{f,1} = z_{f,2} \tag{4.57}$$

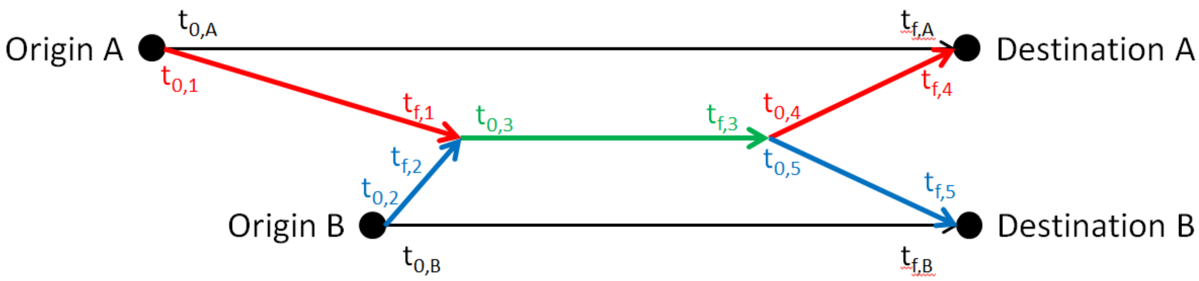

Figure 4.12: Example on how the initial or final time is fixed

and

$$V_{f,1} = V_{f,2} \tag{4.58}$$

The same is done for phases 4 and 5 (as the intermediate point-mass model is implemented also on these phases):

$$z_{0,4} = z_{0,5} \tag{4.59}$$

and

$$V_{0,4} = V_{0,5} \tag{4.60}$$

Initial or Final Time

The developed tool optimizes a certain cost function and consequently computes the departure and arrival times that result in the lowest cost. However, when neither the arrival nor the departure times are fixed, there is no point of reference for the optimization tool and the tool will have difficulties solving the problem. Therefore, during all experiments at least one of the departure or arrival times of the flights must be fixed. To fix one of these times, without negatively affecting the optimization, the origin and destination locations of the flights should be examined. When two or more aircraft will join in formation, all aircraft have a solo phase before and after the formation. Based on these origins and destinations, it can be estimated which of those solo phases covers the largest distance. Depending on whether this phase is before or after the formation phase, the initial or final time for this phase will be fixed. If this phase is before the formation, the initial time of the phase will be fixed at $t = 0$ and if this phase is after the formation the final time of this phase will be fixed at $t = 100000$.

In Figure 4.12, an example is shown on how a departure or arrival time will be chosen to fix as a reference point for the optimization. In this figure, the time duration of phase 1 ($t_1 = t_{f_1} - t_{0,1}$) is larger than that of the other solo phases. So, for this example $t_{0,1}$ should be fixed at $t_{0,1} = 0$

4.3.4. Initial Guess

The final input for the optimization tool is an initial guess. The initial guess must contain the same amount of phases as the experiment. And also the number of variables for all phases of the initial guess must be equal in the experiment. For this study the initial guess is of great importance, because the convergence behaviour and computational time of the optimization are heavily depending on it. An initial guess that is far off may result in a non-converging solution or in a very large computational time. During this study, the output of an earlier performed optimization is often used as initial guess. When a very different experiment is performed the initial guess may be entered manually to steer the tool in the correct direction. Sometimes this is a process of trial-and-error.

4.4. Output

When all of the above is implemented correctly the developed tool can be ran. The results from the optimization, will be in the form of a set of optimal trajectories for all phases and the minimum cost, which depends on the cost function to be optimized: minimum total fuel consumption or minimum total Direct Operating Cost.

4.4.1. Optimal Trajectories

As the problem is optimized, the state and control variables for all nodes (points in time) in the problem are known. From these variables all desired data can be obtained. The flight trajectory of the aircraft during all phases is relevant for this study. With the latitude ϕ, longitude λ and altitude z known at all time instances a 4 dimensional trajectory can be constructed. The 4 dimensional trajectories show the optimal routes per aircraft when flying solo and when flying in formation.

4.4.2. Results

The other relevant output for this study is the resulting cost. For this study two cost functions were established. One cost function concerns the total fuel consumption, while the other concerns the Direct Operating Cost, which is a combination of the fuel consumption and flight time. When an optimal solution is found for one of these cost functions, a variety of data on the flight development can be obtained. The results of interest are the following:

1. Fuel consumption per aircraft
2. Total fuel consumption
3. Flight time per aircraft
4. Total flight time
5. Distance flown per aircraft
6. Total distance flown

The total fuel consumption can be determined by the difference in weight of the aircraft (which is a state variable) from the initial point to the final point. These results then allow comparison with the flight time, fuel consumption and distance flown for the corresponding solo flights and give insight to the benefits of formation flight.

4.5. Delay

Every day many flights are delayed. According to EUROCONTROL many flights are delayed even before taking off [9]. A flight is officially delayed when it has a delay on departure of 5 minutes or higher. According to EUROCONTROL during the last quarter of 2015 approximately 37% of all flights had a delay on departure. Figure 4.13 shows the average delay per flight (for all causes) for departures over the last years. As can be seen the average delay does not change significantly over the years.

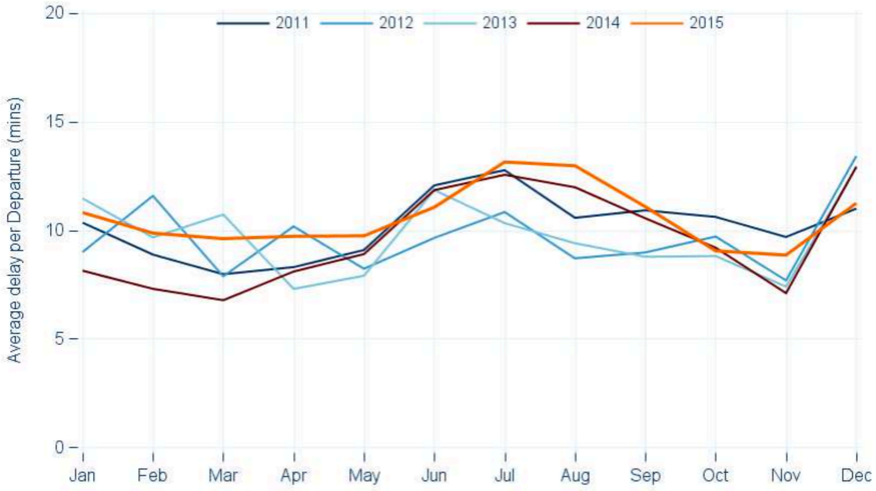

Figure 4.13: Average delay per flight (all-causes) for departures [9]

This delay could be due to several reasons. EUROCONTROL states that reactionary delays contributed the most to these delays, followed by airline-related delays. Reactionary delay is delay caused by late arrival of aircraft or crew from a previous journey. Of the 37% of delayed flights, it might also be interesting to know the distribution of the departure punctuality.

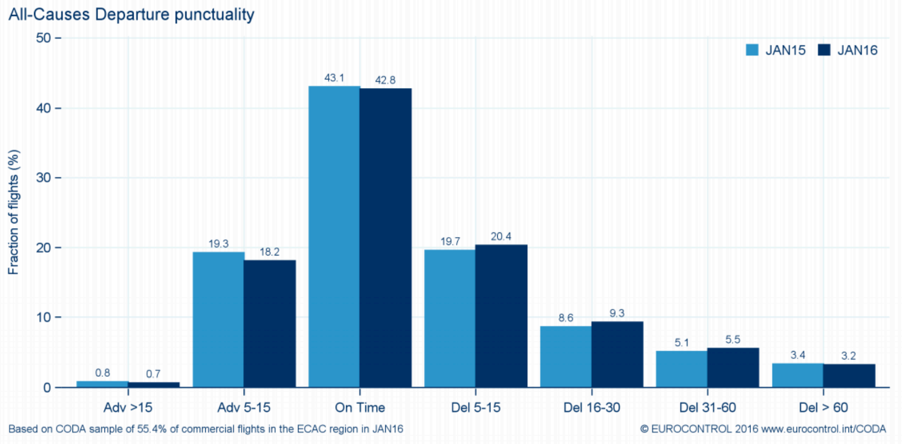

Figure 4.14: Departure punctuality in January 2014 and 2015 [10]

In Figure 4.14 the departure delay is split up into several groups. The percentage of delays in January 2016 is slightly more than the percentage in January 2015 (38.4% vs. 36.8%), but still around the earlier mentioned 37%. From the figure it can be seen that only a few flights (around 8.5%) have a delay on departure of more than 30 minutes. This means that the majority of the flights (91.5%) will depart within 30 minutes of the scheduled departure time.
For this research it might be interesting to see what happens with the formation if one aircraft in the formation has a delay. Not much research has been done to investigate what the effects of delay could be on the formation. Currently the state-of-the-art research on trajectory optimization is not focused on what happens when one of the aircraft joining the formation is delayed. Most research into formation flight is focused on how to solve the optimal routing problem. For example, when Kent et al. [18] implement delay in their model, the rendezvous point location changes, but it is assumed that this location shifts along the optimal predefined route. In this study, the effects of delay on formation flight will be investigated further.

So, when two aircraft are supposed to meet at a certain rendezvous point, but one of the two aircraft is delayed, what does this mean for the rendezvous point and the achievable benefits? In the developed model, the initial time for all aircraft can be altered to simulate a delay. First, the departure times of the optimal trajectories are found and then one of the aircraft will be given a departure delay. These results can be compared making the effects of delay visible.

4.6. Wind

In reality, aircraft almost never follow the great circle path from their origin to their destination, although it is geometrically the optimal route. This is because aircraft always have to take into account the weather conditions and especially the wind conditions. In the presence of wind, aircraft will deviate from the optimal path in order to avoid areas with large headwinds and even to search for areas with favourable tailwinds. Flying with tailwinds can reduce the flight time and fuel consumption significantly. Due to the presence of wind, North-Atlantic Tracks (NAT) are published daily. The NAT represent a structure of routes between Europe and North-America and they make sure that aircraft are separated above the ocean where radar coverage is limited. Every day, six eastbound and six westbound tracks are published, they are optimized to provide the Minimum Time Route (MTR) for the aircraft based on minimizing headwinds and maximizing tailwinds.

In this research, the developed tool does not take into account the NAT, but the effects of wind on the aircraft trajectories are taken into account by adding the wind to the atmospheric data input. On Canadian Government website [43], the Meteorological Service of Canada makes a GRIB2 format database available containing data from analysis systems along with output from Canadian Meteorological Centre's Numerical Weather Prediction (NWP) models, which is free to use. Here, atmospheric data is made available for a lat - lon grid at a 0.6 x 0.6 degrees resolution, which corresponds to approximately a 66km resolution. The Global Deterministic Forecast System (GDPS) data is vertically covered by 28 isobaric levels distributed over an altitude from approximately 100m to 19300m. In this research, as take-off and landing are not considered, the aircraft will fly at an altitude between 3000m and 13500m, therefore the atmospheric data for this range is required. However, to keep the computational time within limits, it is assumed that the wind will not vary with altitude. The average wind over the altitude range between 5000m to 15000m will be used for this study. Besides, the evolution of the wind over time has been disregarded to keep computational time within limits. Furthermore, the vertical wind vector has been neglected because it is expected that vertical wind will not impact the rendezvous and split-up point locations and therefore, is not truly relevant for this research. From this data, the wind is extracted and used as input for the tool. The wind is split-up in two components:

1. The U Wind Component V_{Wind_U}, which represents the east-west windvector, where wind in eastern direction is positive.

2. The V Wind Component V_{Wind_V}, which represents the north-south windvector, where wind in northern direction is positive.

For each of these two components, a 301 x 601 x 28 grid (latitude x longitude x altitude) is obtained, which covers the entire surface of the Earth. As indicated, first, the wind will be averaged over all altitudes. The pressure levels and corresponding altitudes that are included in this averaging process are between 4900m and 15800m. Now that the wind is constant over altitude, a 301 x 601 lat x lon grid remains. This grid covers the entire Earth and can thus be reduced to a smaller grid that contains only the area of interest. In this study, the area of interest is the North-Atlantic area, which in this research covers the North-Atlantic Ocean, the east-coast of North-America and the west-coast of Europe.

To obtain continuous functions for describing the wind components over this North-Atlantic area, the data points from this grid have to be fitted. This is done by polynomial interpolation. Piecewise or linear interpolation would be too heavy a burden for the tool and in the end, for this research, it is not crucial that the interpolation gives a perfect reproduction of the real wind-field. The main interest is to explore the effect of the wind on formation routing. Although the polynomials can be expanded to any desired degree, in this study the wind speed was fitted to second and fourth order polynomials which should be able to capture the wind speed variations over the North-Atlantic. With the MatLab ”Curve Fitting Toolbox” the unknown coefficients of the polynomial functions are found. Once these coefficients are estimated, the polynomial functions can be evaluated at any point within the area of interest. For this polynomial interpolation two options were examined: a polynomial with a degree of two and a polynomial with a degree of four. In Figures 4.15a and 4.16a the real wind-field components U and V are plotted. These plots represent the wind on May 24^{th} 2016. The second- and fourth degree polynomials for the wind components were also plotted in order to see how they resemble the real wind components. The second-degree polynomials gave oversimplified results, but the fourth-degree polynomials show some resemblance with the real wind components. The resulting U and V wind components of the fourth-degree polynomials are presented in Figures 4.15b and 4.16b, respectively.

So visually, the higher degree polynomial seems like the better option. Also, according to the coefficients of determination of the polynomials (Table 4.7), the fourth-degree polynomial gives better results. A further increase of the degree of the polynomial, increases the R-squared even more, but it also leads to more inaccurate values, especially near the edges of the area. The polynomials get very sensitive near the edges resulting in lowest and highest values of the polynomials which are, respectively, much lower and much greater than the original data.

Table 4.7: Values of R-squared for second- and fourth degree polynomials of the wind components

Approach	**Value** R^2
Second-degree polynomial wind component U	0.2533
Second-degree polynomial wind component V	0.04178
Fourth-degree polynomial wind component U	0.6278
Fourth-degree polynomial wind component V	0.4255

Based on the reasons mentioned above, the fourth-order polynomials have been chosen for this research. The polynomials for the wind components in east-west and south-north directions can be found in Appendix A. If the U and V wind components are combined, a wind-field is created. This wind-field is from May 24^{th} 2016 and is presented in Appendix A.

It should be noted, that the atmospheric data originally was a function of the altitude only. However, the magnitudes of the U and V wind components don't vary per altitude, but per location. Hence, with the inclusion of the influence of wind, the atmospheric data is not merely a function of the altitude anymore, but also of latitude and longitude.

The wind components are incorporated in the dynamic aircraft performance models. The modified equations of motion for the intermediate point-mass model become:

$$\dot{\phi} = \frac{V cos(\gamma) sin(\chi) + V_{Wind_V}}{R_e + z} \tag{4.61}$$

$$\dot{\lambda} = \frac{V cos(\gamma) cos(\chi) + V_{Wind_U}}{R_e + z} \tag{4.62}$$

and the modified equations of motion for the energy-state model become:

$$\dot{\phi} = \frac{V sin(\chi) + V_{Wind_V}}{R_e + z} \tag{4.63}$$

$$\dot{\lambda} = \frac{V sin(\chi) + V_{Wind_U}}{R_e + z} \tag{4.64}$$

Note that when the wind is not taken into account (for most experiments) the wind components V_{Wind_V} and V_{Wind_U} are set to zero in Equations 4.61 - 4.64.

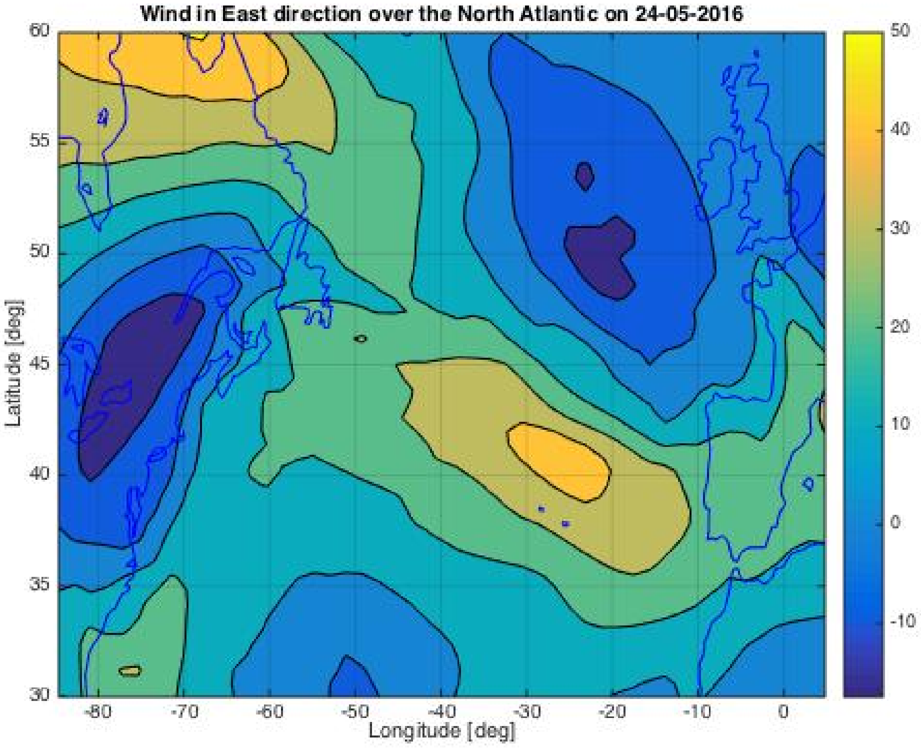
Wind in East direction over the North Atlantic on 24-05-2016
Latitude [deg]
Longitude [deg]
60
55
50
45
40
35
30
-80
-70
-60
-50
-40
-30
-20
-10
0
50
40
30
20
10
0
-10

(a) The real U wind component $[m/s]$

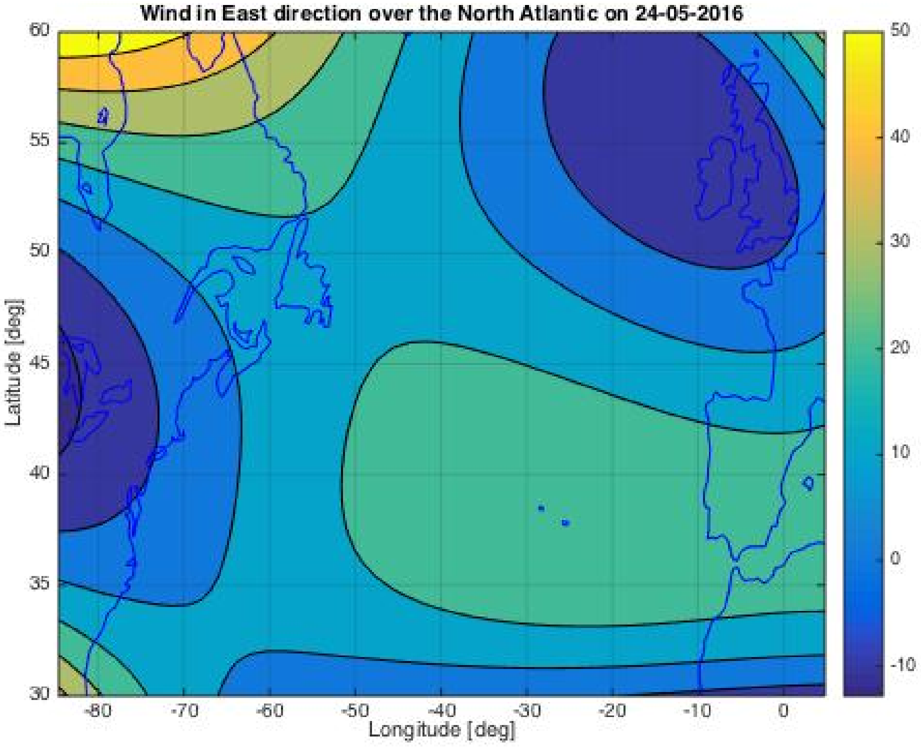
Wind in East direction over the North Atlantic on 24-05-2016
Latitude [deg]
Longitude [deg]
60
55
50
45
40
35
30
-80
-70
-60
-50
-40
-30
-20
-10
0
50
40
30
20
10
0
-10

(b) The fourth-order polynomial representing the U wind component $[m/s]$

Figure 4.15: U component of the wind on May 24th 2016 (east-west windvector, which is positive in eastern direction)

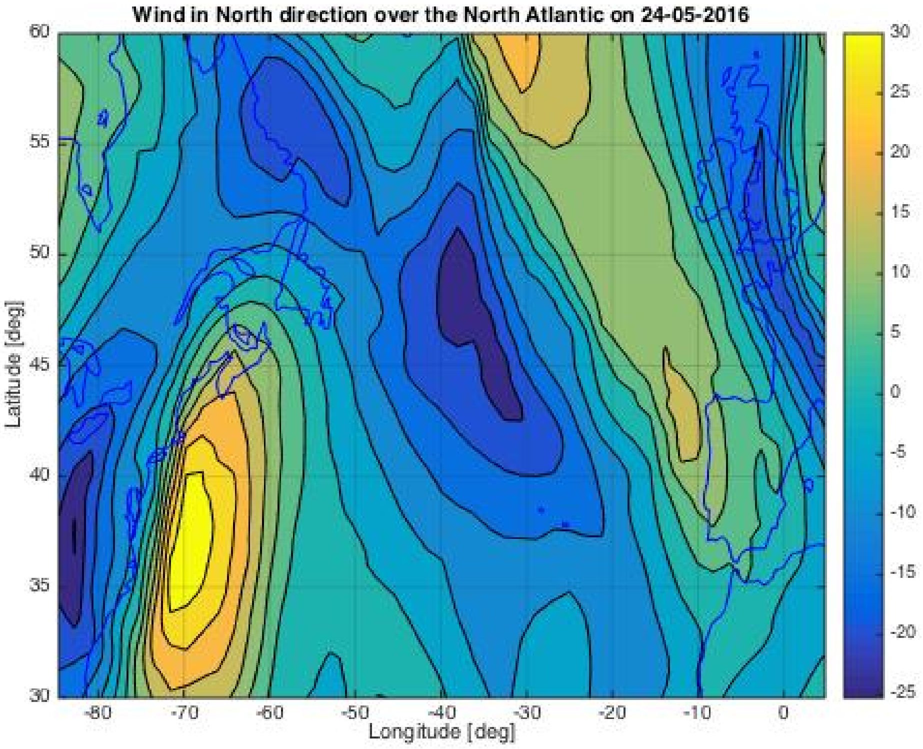
Wind in North direction over the North Atlantic on 24-05-2016
Latitude [deg]
60
55
50
45
40
35
30
-80
-70
-60
-50
-40
-30
-20
-10
0
Longitude [deg]
30
25
20
15
10
5
0
-5
-10
-15
-20
-25

(a) The real V wind component $[m/s]$

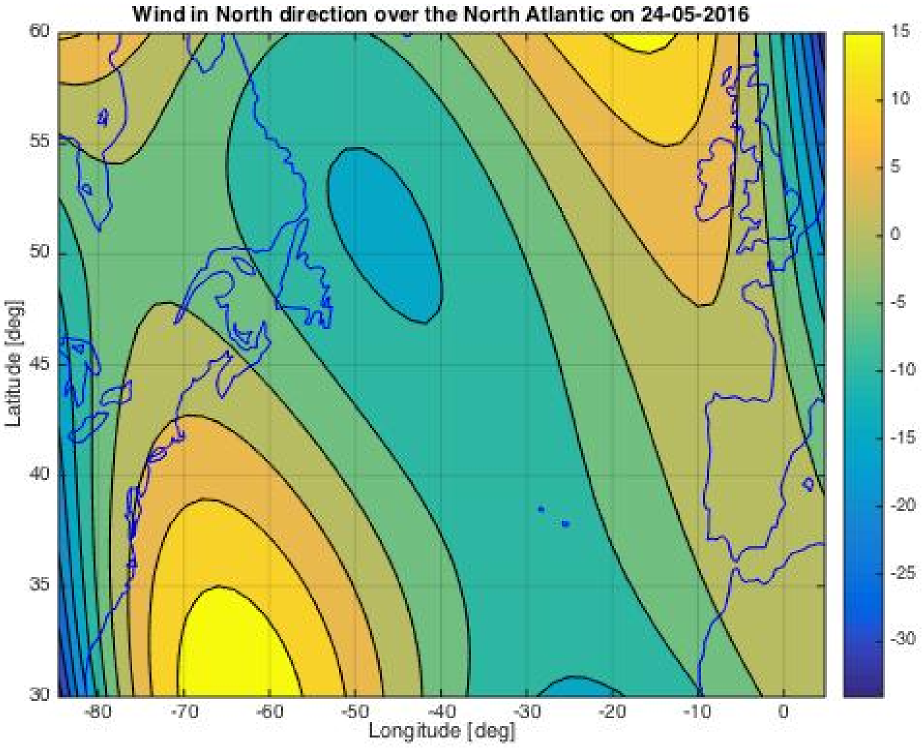
Wind in North direction over the North Atlantic on 24-05-2016
Latitude [deg]
60
55
50
45
40
35
30
-80
-70
-60
-50
-40
-30
-20
-10
0
Longitude [deg]
15
10
5
0
-5
-10
-15
-20
-25
-30

(b) The fourth-order polynomial representation of the V wind component $[m/s]$

Figure 4.16: V component of the wind on May 24^{th} 2016 (north-south windvector, which is positive in northern direction)

5
Validation

Before continuing with the experimental set-up, it is important to validate the accuracy of the developed multiple-phase optimization tool. The intermediate point-mass model and energy-state model will be validated in combination with the three aircraft types. In order to do this, a solo flight without wind will be optimized for a standard route for the Boeing 737-300, the Boeing 747-400 and the McDonnell Douglas MD-11. The resulting fuel consumptions of these optimizations will be compared to the fuel consumption given by the manufacturer's aircraft performance manuals and an online fuel planner [44], while the resulting horizontal flight paths will be compared with the great circle routes between the origins and destinations. When these models are validated, the tool will be validated against a set of aircraft that join in formation as well.

5.1. Boeing 737-300

The Boeing 737-300 is designed for short- to medium-range flights. A typical flight for this aircraft would be from Amsterdam to Madrid. Without the effects of wind, the optimal trajectory of the aircraft is the great circle path between Amsterdam and Madrid. In Figure 5.1 the original great circle path and the resulting optimal horizontal flight paths from the intermediate point-mass and energy-state models are shown. As can be seen, the optimal horizontal flight paths coincide with the great circle route.

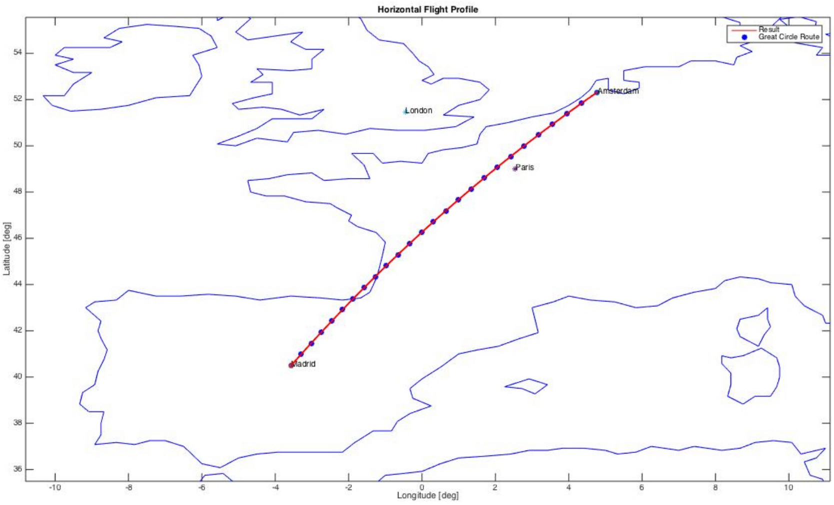

Figure 5.1: Horizontal flight paths for the validation of the Boeing 737-300 in combination with the intermediate point-mass and energy-state models.

To compare the fuel consumptions from the point-mass and energy-state models with the fuel consumption from the aircraft performance manual, the latter must be converted into the fuel consumption for this flight. From Boeing's performance manual for the 737-300 [13] the block fuel per passenger is given (Table 5.1), which is valid when carrying 126 passengers on-board.

Table 5.1: Block fuel per passenger for the Boeing 737-300[13]

Range [nmi]	Range [km]	Block fuel [kg/pax]	Total fuel [kg]
500	926	25.7	3238
1000	1852	46.3	5834
790	1460	37.8	4763

The distance from Amsterdam to Madrid is approximately 1460km. Assuming the block fuel per passenger increase linearly from 926km to 1852km, the block fuel per passenger from Amsterdam to Madrid is approximately 37.8kg per passenger. To obtain the total fuel consumption for this flight, this block fuel must be multiplied by 126 (number of passengers). The results from the performance manual, online fuel planner and the point-mass and energy-state models for this flight are summarized in Table 5.2. The difference between the minimum and maximum block fuel per passenger is caused by a different amount of fuel carried by the aircraft for the flight.

Table 5.2: Results for a flight from Amsterdam to Madrid for a Boeing 737-300

Method	Block fuel [kg/pax]	Total fuel [kg]
Performance manual	37.8	4763
Online flight planner	43.4	5468
Intermediate point-mass	32.9 - 38.3	4147 - 4820
Energy-state	32.9 - 38.3	4146 - 4832

The results in Table 5.2 that the block fuel per passenger from the aircraft manual is within the range of the results of the tool for the different models. The online flight planner, however, gives a higher fuel consumption, but still in the same order of magnitude. This higher fuel consumption can be assigned to the fact that the developed tool does not incorporate the taxiing, take-off and landing of the flight and the fuel planner does. In general, the amount of fuel that is burned during take-off is significant, especially for short flights. On short flights, as much as 25% of the total fuel consumed is used during take-off [45], while for medium- to long-distance flights this is in the order of 8% to 15% [46]. Assuming 15% of the total fuel consumption for this flight is consumed during taxi, take-off and landing, the resulting total fuel of the online flight planner is 4650kg, which is in line with the results from the tool for the different the models.

5.2. Boeing 747-400

The Boeing 747-400 is designed for long distances. A typical flight for this aircraft would be from Paris to Buenos Aires. The great circle route for this flight and the optimal horizontal flight paths resulting from the point-mass and energy-state models are presented in Figure 5.2. As can be seen, these routes coincide.

The block fuel per passenger for a flight of 11000km is found in Boeing's aircraft performance manual [47]. The distance from Paris to Buenos Aires is around 11100km, this means that the results from the tool can be compared with the data from the manual for validation. In Table 5.3 the results are summarized. The block fuel per passenger is valid for 416 passengers on-board.

Table 5.3: Results for a flight from Paris to Buenos Aires for a Boeing 747-400

Method	Block fuel [kg/pax]	Total fuel [kg]
Performance manual	296.7	123427
Online flight planner	339.9	141412
Intermediate point-mass	307.1	127760
Energy-state	307.0	127720

Compared with the aircraft performance manual, both the intermediate point-mass model and the energy-state model for the Boeing 747-400 are off by a few percent, which this is acceptable. The online

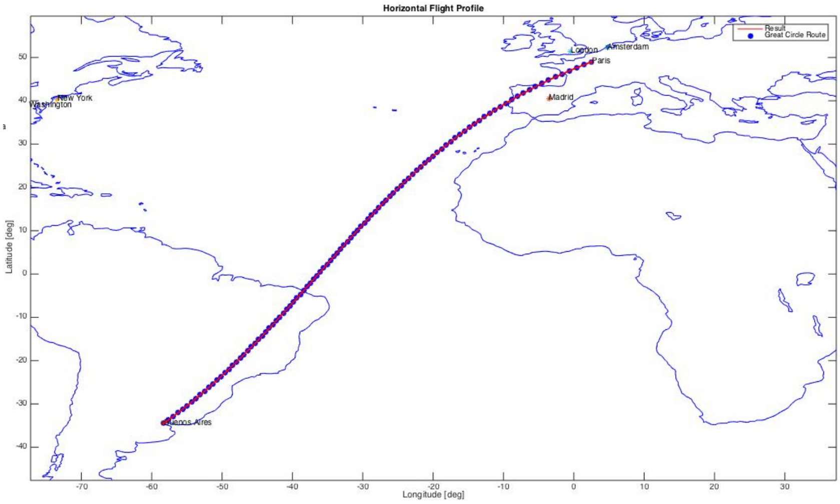
Horizontal Flight Profile
Result
Great Circle Route
London
Amsterdam
Paris
Madrid
New York
Washington
Buenos Aires
50
40
30
20
10
0
-10
-20
-30
-40
Latitude [deg]
-70
-60
-50
-40
-30
-20
-10
0
10
20
30
Longitude [deg]

Figure 5.2: Horizontal flight paths for the validation of the Boeing 747-400 in combination with the intermediate point-mass and energy-state models.

fuel planner has a higher fuel consumption than the results from the tool, this can be due to the same reasons that were mentioned for the B733 validation. Assuming 10% of the total fuel consumption given by the flight planner is burned during take-off and landing, this results in a total fuel consumption of 127271kg for the cruise segment. This result is in line with the results of the intermediate point-mass and the energy state models for the Boeing 747-400.

5.3. McDonnell Douglas MD-11

The McDonnell Douglas MD-11 is designed for medium- to long-distances. A typical flight for this aircraft would be from London to Atlanta. The great circle route for this flight and the resulting horizontal flight paths from the intermediate point-mass model and energy-state model coincide and are presented in Figure 5.3.

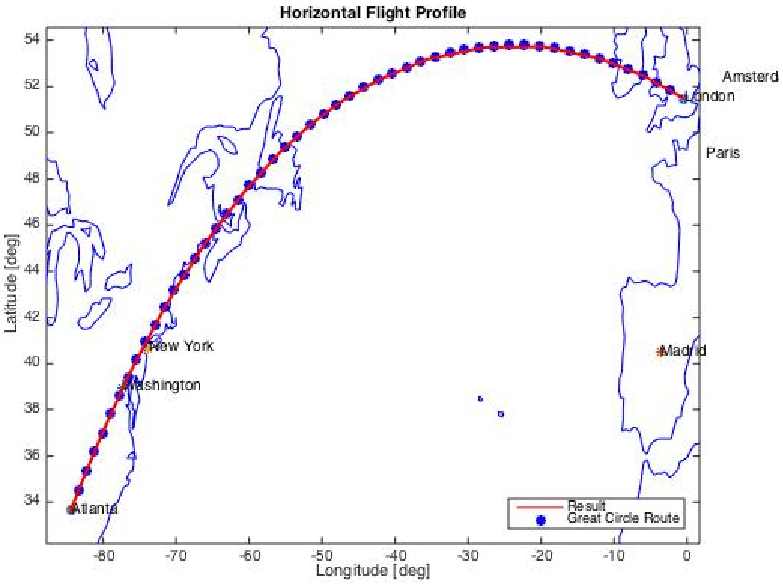
Horizontal Flight Profile
Amsterd
London
Paris
Madrid
New York
Washington
Atlanta
Result
Great Circle Route
54
52
50
48
46
44
42
40
38
36
34
Latitude [deg]
-80
-70
-60
-50
-40
-30
-20
-10
0
Longitude [deg]

Figure 5.3: Horizontal flight paths for the validation of the McDonnell Douglas MD-11 in combination with the intermediate point-mass and energy-state models.

For the MD-11 no performance manual is found and this aircraft will therefore be validated by comparing the results of the intermediate point-mass model and energy-state model with the online flight planner only. In Table 5.4 the results are summarized. Again, the online fuel planner shows a higher fuel consumption than the results from the tool. As the flight performed by this aircraft lies between the previous two cases in terms of range, 11% of the total fuel consumption is assumed to be needed for the taxi, take-off and landing segments. This results in a total amount of fuel burn of 56020 kg for the flight planner, which is in line with the results from the tool.

Table 5.4: Results for a flight from London to Atlanta for a McDonnell Douglas MD-11

Method	**Total fuel [kg]**
Online flight planner	62945
Intermediate point-mass	55973
Energy-state	55908

5.4. Formation Flight

As no other research on the optimal trajectories for aircraft joining in formation has been performed yet, it is difficult to validate the developed multiple-phase optimization tool. However, Bower et al., who studied formation geometries and route optimization for commercial aircraft, have performed a case study in which they selected a set of five FedEx flights from the Northwest US to Memphis for a route optimization study [7]. They considered five flights and made these flights join in one two-aircraft formation and one three-aircraft formation. The two-aircraft formation is flown with two identical aircraft (Boeing 727-200). The results of this case study are shown in Figures 5.4a and 5.4b, where the green lines in the Figures represent the two-aircraft formation of the case study. Figure 5.4a shows the results for a pessimistic scenario and Figure 5.4b the results for an optimistic scenario. These results are coherent with the positioning of the aircraft relative to each other, which has an effect on the reduction in induced drag and therefore on the fuel burn as well.

Bower et al. find that for this FedEx case the two-aircraft formation can save between 1.17% and 7.85% of fuel, depending on the positioning of the aircraft. To validate the outcome of the developed tool for a two-aircraft formation, this FedEx experiment will be replicated. As in this study the Boeing 727-200 is not considered, the aircraft type that is most similar it will be considered:

1. Flight A: A B733 from Great Falls International Airport (GTF) to Memphis International Airport (MEM)
2. Flight B: A B733 from Casper-Natrona County International Airport (CPR) to Memphis International Airport (MEM)

As Bower et al. have different spanwise positioning resulting in a pessimistic and an optimistic scenario, the set of flights will be optimized for different formation flight induced drag fractions ϵ. The fraction chosen to replicate the pessimistic scenario is 0.9, while the fraction chosen to replicate the optimistic scenario is 0.5. For comparison, the two flights are optimized to fly solo as well. The results are summarized in Table 5.5.

Table 5.5: Optimization for a scenario based on a case study performed by Bower et al. [7]

Results	Solo	$\epsilon = 50\%$	$\epsilon = 90\%$
Total fuel consumption [kg]	11046	10198 (-7.68%)	10926 (-1.09%)

A comparison of the results of the FedEx case study performed by Bower et al., with the results generated by the developed tool, shows that both are quite similar. Bower et al. demonstrate fuel savings between 1.17% and 7.85% and the tool shows fuel savings between 1.09% and 7.68%.

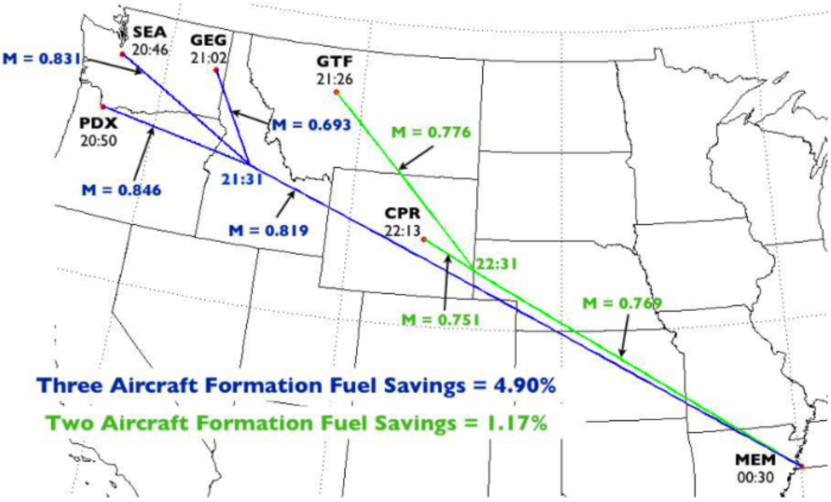
SEA
20:46
GEG
21:02
GTF
21:26
M = 0.831
PDX
20:50
M = 0.693
M = 0.776
M = 0.846
21:31
M = 0.819
CPR
22:13
22:31
M = 0.769
M = 0.751
Three Aircraft Formation Fuel Savings = 4.90%
Two Aircraft Formation Fuel Savings = 1.17%
MEM
00:30

(a) Pessimistic aircraft spacing, no time buffer

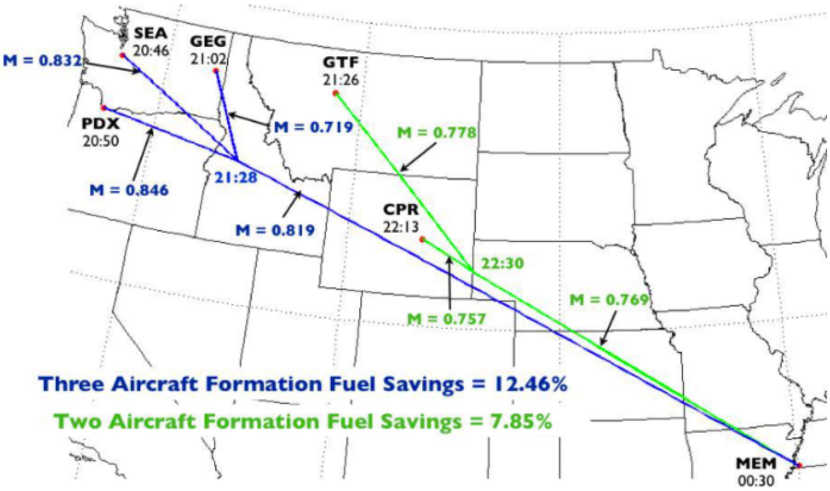
SEA
20:46
GEG
21:02
GTF
21:26
M = 0.832
PDX
20:50
M = 0.719
M = 0.778
M = 0.846
21:28
M = 0.819
CPR
22:13
22:30
M = 0.769
M = 0.757
Three Aircraft Formation Fuel Savings = 12.46%
Two Aircraft Formation Fuel Savings = 7.85%
MEM
00:30

(b) Optimistic aircraft spacing, no time buffer

Figure 5.4: Maps showing the results of a case study performed on the optimal routing for formation flights [7]

6

Experimental Set-up

Several different experiments are set-up, which have much in common. In this chapter the experimental set-up will be reviewed briefly. First of all, the cost function that will be optimized minimizes the total fuel burn for all aircraft participating in the experiment. When a different cost function will be optimized, this will be mentioned explicitly. Secondly, the selected geographic area in which the experiments will take place is the North-Atlantic airspace. In this research, mainly flights between Europe and North-America are of interest. In Europe the cities London (LHR), Amsterdam (AMS), Paris (CDG) and Madrid (MAD) and in North-America the cities Atlanta (ATL), New York City (JFK), Washington (IAD) and Toronto (YYZ) are considered. The airspace for this research is shown in Figure 6.1. All experiments will be conducted in westbound direction, unless stated otherwise.

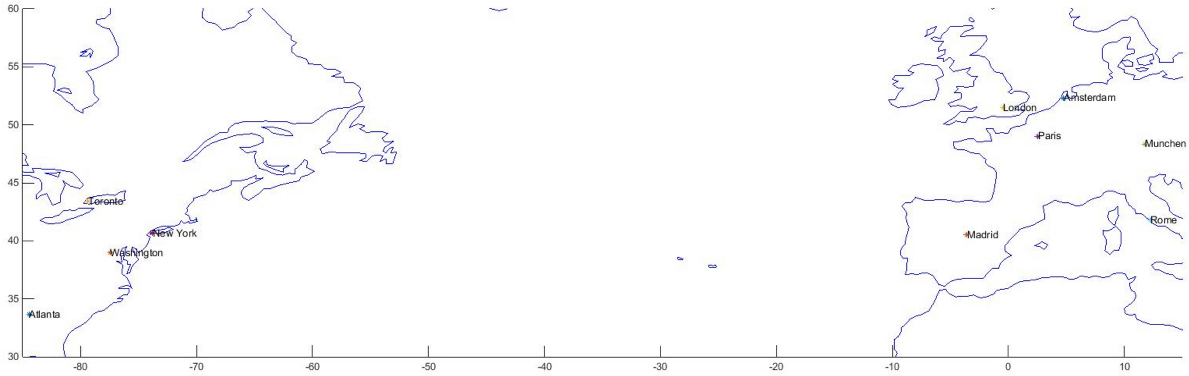

Figure 6.1: Airspace of interest

This study focuses on the optimal trajectories of aircraft in formation during the cruise phase. The starting and end points of the flights will be at an altitude of 3048 meters (10000 feet) and an airspeed of 250 knots true airspeed (TAS). The rendezvous and split-up points are not fixed, which means that the model optimizes these for every experiment. The take-off and landing segments of the flights will not be considered in the experiments as the aircraft will only fly in formation during cruise. Also, as the cruise segment of aircraft usually is steady, the number of nodes and intervals per phase can be low. For all phases, two intervals are specified and there are ten nodes per interval. As the phases are not of the same length, but contain the same amount of nodes, the time step per phase can be different per phase. As mentioned before, three aircraft types are selected: the short-haul Boeing 737-300, the long-haul Boeing 747-400 and the medium- to long-haul McDonnell Douglas MD-11. For all experiments the solo segments of the flights will be modelled with the intermediate point-mass model and the formation segments will be modelled with the energy-state model. During all experiments, the aircraft are constrained to join in formation for at least five seconds even when this is not beneficial. Furthermore, it is essential to mention that, unless stated otherwise, the departure and arrival times, as well as the rendezvous and split-up point times are not fixed during the experiments (aside from the constraint covered in Section 4.3.3).

Finally, a standard formation flight induced drag fraction of $\epsilon = 0.75$ will be implemented (on the trailing aircraft) when two identical aircraft types join in formation. When different aircraft types or aircraft with significant different weights join in formation, the formation flight induced drag fraction deviates from this standard and will be extracted from the graph shown earlier in Figure 4.5.

7

Results

In this chapter several experiments will be performed. First, several standard two-aircraft formation trajectories will be optimized and some real-life scenarios will be investigated. Next, the effects of different aircraft types, delay and wind on formation flight will be examined. Finally, a three-aircraft formation will be optimized to demonstrate that the tool is able to optimize larger formations. The results of the experiments will be discussed in more detail in the next chapter.

7.1. Two-Aircraft Formation Flight

In this section, experiments with two aircraft joining in formation are conducted. During these experiments five phases are distinguished. Both aircraft have an initial phase from their origins to the rendezvous point (RV), followed by a phase of both aircraft flying in formation from the rendezvous point to the splitting point (SU) and finally, are there are two more phases from the splitting point to both destinations. This is schematically shown in Figure 7.1.

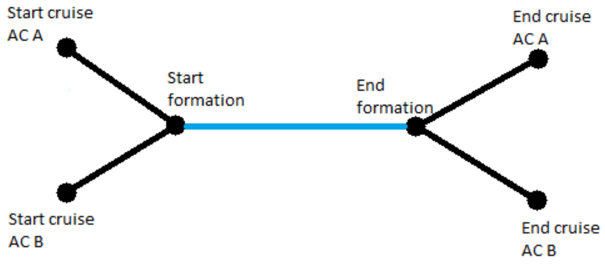

Figure 7.1: Schematic overview of a two-aircraft formation (5 phases)

7.1.1. Experiments 1 & 2: Standard Two-Aircraft Formation Flight

The first experiments involve two aircraft flying from Europe to North-America. To benchmark the results of formation flight, solo flights are optimized with which they can be compared to.

Solo Flights

Two solo flights from Europe to North-America are optimized for the Boeing 737-300 and for the Boeing 747-400:

1. Solo 1 (S1): A B733 from London to Atlanta
2. Solo 2 (S2): A B733 from Madrid to New York City
3. Solo 3 (S3): A B744 from London to Atlanta
4. Solo 4 (S4): A B744 from Madrid to New York City

These routes are chosen because they are both high frequency routes that have a similar direction, which makes them good candidates for joining in formation. In Figure 7.2 the horizontal flight paths of the solo flights are presented. The resulting horizontal flight paths of the solo flights for both aircraft are the same and they also coincide with the optimal great circle routes (GCR) between the cities.

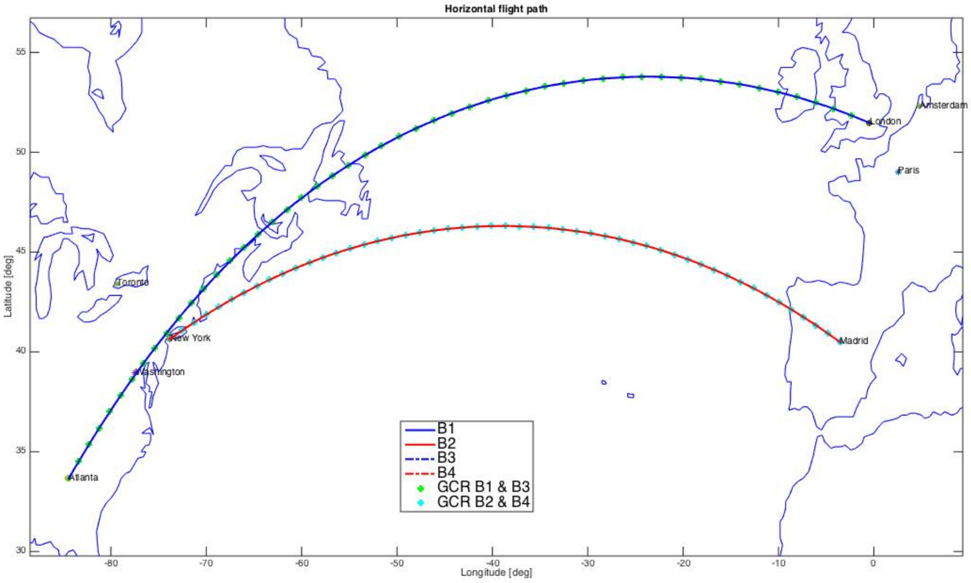

Figure 7.2: Horizontal flight paths of both solo flights for the Boeing 737-300 and Boeing 747-400 (as these are the same)

As mentioned before, the B733 is not a long-haul aircraft, but occasionally it is used for long-distance flights in a business configuration, which in this scenario is assumed to be the case. The assumed payload is 3142kg, which is 20% of the total maximum payload. The Boeing 747-400 flies the same routes with a full payload, which is 63916kg. In Tables 7.1 and 7.2 the results for the solo flights are summarized.

Table 7.1: Solo flights from London to Atlanta and from Madrid to New York City for the Boeing 737-300

Results	**S1: London - Atlanta**	**S2 Madrid - New York**	**Total**
Payload [kg]	3142	3142	6284
Fuel consumption [kg]	16588	13798	30386
Flight time [s]	37489	31889	36378
Flight time [hr]	10.41	8.86	19.27
Distance [km]	6778	5776	12554

Table 7.2: Solo flight from London to Atlanta and from Madrid to New York City for the Boeing 747-400

Results	**S3: London - Atlanta**	**S4: Madrid - New York**	**Total**
Payload [kg]	63916	63916	127832
Fuel consumption [kg]	79181	66331	145512
Flight time [s]	28458	24400	52858
Flight time [hr]	7.91	6.78	14.69
Distance [km]	6778	5776	12554

The results in Tables 7.1 and 7.2 are obtained by running the model twice per solo flight. Once with the intermediate point-mass model and once with the energy-state model. The results presented in Tables 7.1 and 7.2 are the average of the two per flight. The results for the solo flights are presented in more detail in Appendix B.

Experiment 1: Boeing 737-300 from London to Atlanta and from Madrid to New York City

For the first experiment, the trajectories of two Boeing 737-300 that join in formation will be optimized:

1. Aircraft A: A B733 from London to Atlanta
2. Aircraft B: A B733 from Madrid to New York City

The formation flight induced drag fraction ($\epsilon = 0.75$) applies to the trailing aircraft, therefore is most beneficial to have the heavier aircraft as the trailing aircraft. The initial and final fuel weights of the earlier optimized solo flights are listed in Table 7.3. This table shows that the initial fuel of S1 is approximately 3000kg more than S3. Therefore, for this experiment, the formation flight induced drag fraction is applied on aircraft A.

Table 7.3: Initial and final fuel weights of the solo flights

Route	**London - Atlanta**		**Madrid - New York City**	
Aircraft type	**S1: B733**	**S3: B744**	**S2: B733**	**S4: B744**
Initial fuel [kg]	17475	87373	14696	74215
Final fuel [kg]	900	8170	900	8170

In Figure 7.3 the horizontal flight paths of both aircraft are presented. The dotted lines represent the great circle routes from London to Atlanta (red) and from Madrid to New York City (blue). To join in formation both aircraft deviate from their corresponding individual optimal path. In Figures 7.4a and 7.4b, the vertical flight path and velocity of the flights are displayed. Although these figures show reasonably smooth trajectories, there are some "jumps" in the altitude and velocity. These jumps, which also recur in some of the other experiments, are elaborated upon in Chapter 8. Figure 7.4c gives the weights of the aircraft over time. The red line represents the weight of aircraft A, the blue line represents the weight of aircraft B and the dotted green line represents the earlier mentioned pseudo weight W_n of aircraft A. Table 7.4 summarizes the results of the optimization.

Table 7.4: Results for two B733 aircraft from London to Atlanta and Madrid to New York city that join formation (Experiment 1)

Results	**Aircraft A**	**Aircraft B**	**Total**
Fuel consumption [kg]	15961	13975	29937 (-1.48%)
Flight time [hr]	10.46	8.95	19.4 (+0.67%)
Distance flown [km]	6839	5847	12685 (+1.04%)

The individual fuel consumption for the leading aircraft B increases compared to the solo flights, but the total fuel consumption of both flights is less than the sum of the fuel consumption of the solo flights. Together the two solo flights consumed 30386kg of fuel, while in formation the combined fuel consumption is 29937kg. This is a reduction of approximately 1.5% on the total fuel burn.

Experiment 2: Boeing 747-400 from London to Atlanta and from Madrid to New York City

In this experiment two Boeing 747-400 fly the same routes as the Boeing 737-300 in Experiment 1:

1. Aircraft A: A B744 from London to Atlanta
2. Aircraft B: A B744 from Madrid to New York City

Aircraft A is the aircraft on which the induced drag reduction is applied. The resulting horizontal flight paths are similar to those of the Experiment 1 (Figure 7.3). The vertical flight path and velocity profiles, however, are different as the B744 has different performance characteristics compared to the B733. The B744 has a higher speed and altitude, is heavier and consumes more fuel. The vertical flight paths, velocity profiles and variation in aircraft weight are shown in Figures 7.5a, 7.5b and 7.5c, respectively.

The results for this experiment are given in Table 7.5. As was the case for Experiment 1, the individual fuel consumption of aircraft B increases compared to the solo flight, but the total fuel consumption of both flights decreases. The two solo flights consume 145512kg and in formation they consume 142785kg, which is a reduction in fuel burn of approximately 1.9%.

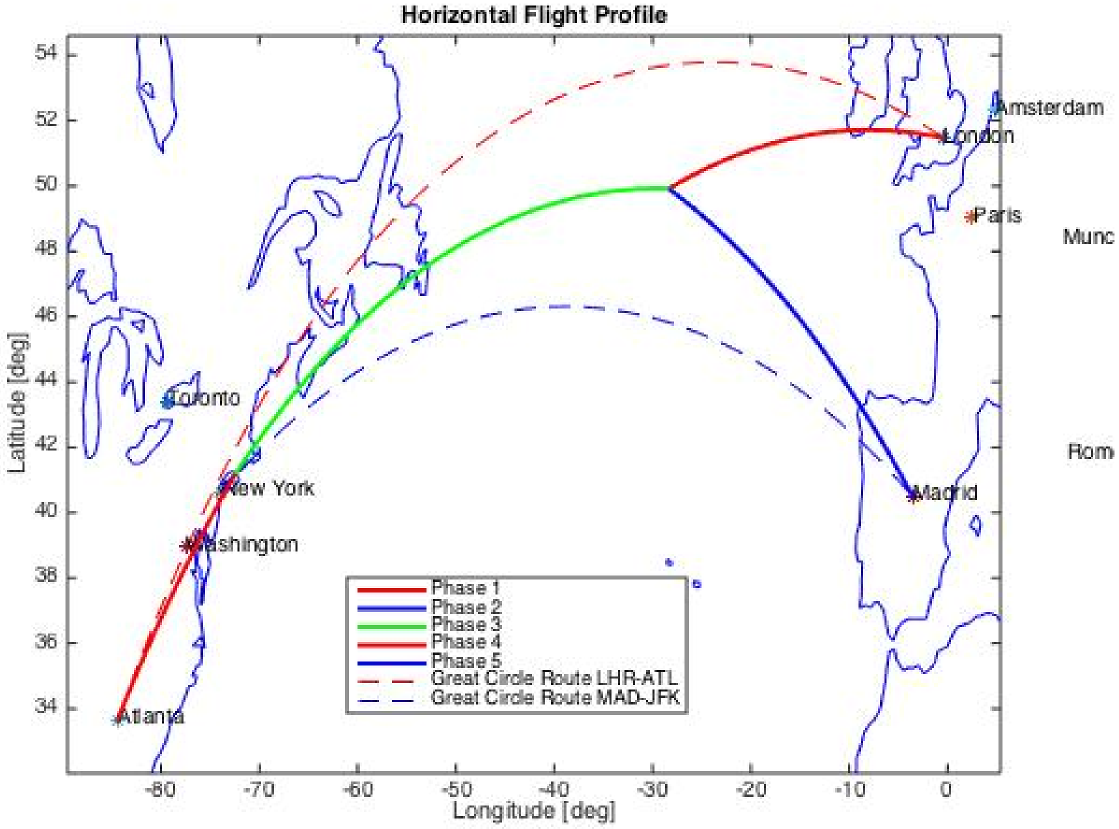
Horizontal Flight Profile
Latitude [deg]
Longitude [deg]
54
52
50
48
46
44
42
40
38
36
34
-80
-70
-60
-50
-40
-30
-20
-10
0
Amsterdam
London
Paris
Munc
Rom
Madrid
Toronto
New York
Washington
Atlanta
Phase 1
Phase 2
Phase 3
Phase 4
Phase 5
Great Circle Route LHR-ATL
Great Circle Route MAD-JFK

Figure 7.3: Horizontal Flight Paths of Aircraft A (London - Atlanta) and Aircraft B (Madrid - New York) when joining in formation and their corresponding optimal great circle paths

Table 7.5: Results for two B744 aircraft from London to Atlanta and Madrid to New York city that join formation (Experiment 2)

Results	**Aircraft A**	**Aircraft B**	**Total**
Fuel consumption [kg]	75515	67270	142785 (-1.87%)
Flight time [hr]	8.09	6.90	15 (+2.11%)
Distance flown [km]	6845	5853	12698 (+1.15%)

7.1.2. Experiments 3 & 4: Real-Life Scenarios

Two experiments are conducted to show what the benefits in real-life could be, one for KLM and one for SkyTeam.

Experiment 3: Real-Life Scenario: KLM

The Dutch airline KLM is a legacy carrier that operates mainly from its hub Schiphol Amsterdam. KLM operates with a so called ”seven wave system” [11]. This wave system concentrates the pattern of arriving and departing KLM aircraft into seven daily peaks (Figure 7.6).

These waves are linked with the arrival and departure patterns of feeder flights in Western Europe, meaning that many KLM flights depart around the same time. This provides a good starting point for formation flight. The flights presented in Figure 7.7, for example, could be suited to join in formation.

These are existing flights that operate on a daily basis. These flights are often carried out with long-haul aircraft like the Boeing 747-400. Hence, the next experiment is to have one B744 fly from Amsterdam to Washington and one B744 from Amsterdam to New York City, departing 30 minutes later:

1. Aircraft A: A B744 from Amsterdam to Washington at 13:00 (KLM)
2. Aircraft B: A B744 from Amsterdam to New York City at 13:30 (KLM)

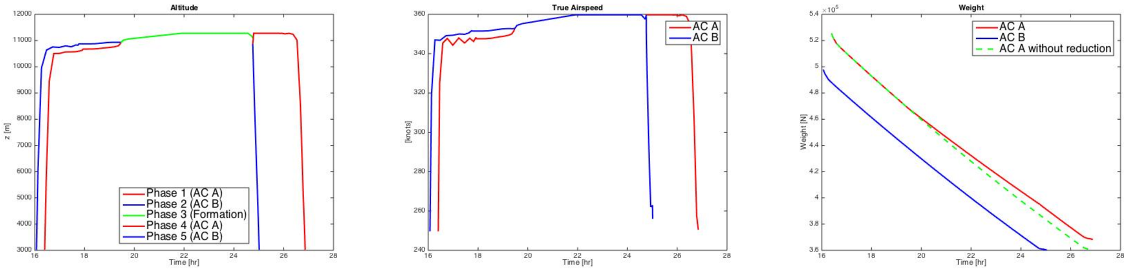

(a) Vertical Flight Paths (b) True airspeeds of both Aircraft (c) Aircraft Weights

Figure 7.4: Results of the Boeing 737-300 two-aircraft formation from London to Atlanta and Madrid to New York City

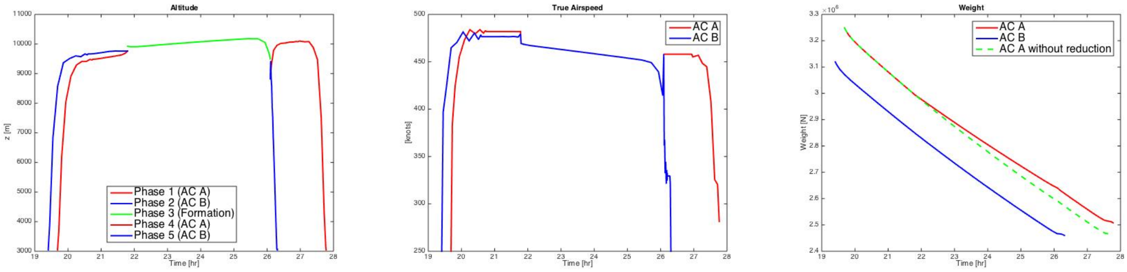

(a) Vertical Flight Paths (b) True airspeeds of both Aircraft (c) Aircraft Weights

Figure 7.5: Results for the Boeing 747-400 two-aircraft formation from London to Atlanta and Madrid to New York City

The experiment will be performed twice, once with aircraft A as trailing aircraft and once with aircraft B as trailing aircraft, to see if this matters for the results. In order to fly in formation aircraft B (which departs 30 minutes later) will have to speed up, aircraft A will have to slow down or a combination of these two most occur. Besides the variation in speed it could also be possible that aircraft A must perform a detour in order for aircraft B to catch up. The results for this experiment are summarized in Table 7.6 and for comparison, also the corresponding solo flights are added. Formation 1 (F1) has aircraft A as trailing aircraft and Formation 2 (F2) has aircraft B as trailing aircraft.

Table 7.6: Results for two KLM flights, one from Amsterdam to Washington (aircraft A) and one from Amsterdam to New York City (aircraft B) flying solo and in formation (Experiment 3)

Results	**2 Solo Flights**	**Formation 1**		**Formation 2**	
Total fuel consumption [kg]	139394	136020	*- 2.42%*	136100	*- 2.36%*
Total flight time [hr]	14.15	14.60	*+ 4.95%*	14.60	*+ 3.18%*
Total distance flown [km]	12086	12090	*+ 2.44%*	12090	*+ 0.03%*

The rendezvous times for Formation 1 and 2 are at $t_{RV} = 8231s$ and $t_{RV} = 8277s$, respectively. It is interesting to see that for formation 1 the rendezvous point is much earlier than for formation 2. In Appendix C the results for this experiment are presented in more detail. The optimization shows, that when formation flight is applied for these two flights, which fly on a daily basis, KLM can save a significant amount of fuel without causing too much delay for the passengers. If KLM changes its operations slightly and implements Formation 2, they can save approximately 3300kg (more than 2% for these two flights) daily. If this amount is saved on a daily basis, it sums up to over 1.2 million kg of fuel per year. With the current fuel prices of 2.77 dollar per gallon [48], KLM can save over €970,000,- per year just by combining these two flights.

Experiment 4: Real-Life Scenario: SkyTeam

As for KLM, the concept of formation flight can also be beneficial for alliances such as SkyTeam. Currently airlines that are part of an alliance benefit from cost reductions by sharing of, for example, sales offices, maintenance facilities and operational facilities. A next step could be to have aircraft of the same

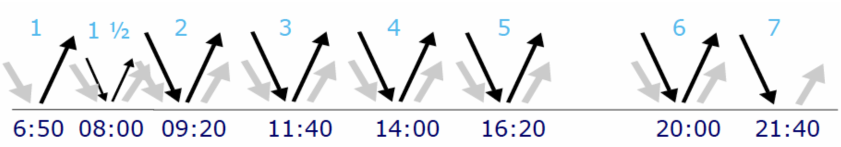

Figure 7.6: KLM seven wave system [11]

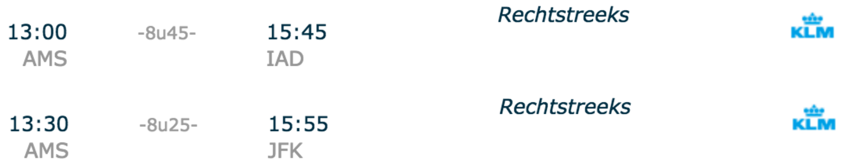
13:00 AMS -8u45- 15:45 IAD *Rechtstreeks* KLM

13:30 AMS -8u25- 15:55 JFK *Rechtstreeks* KLM

Figure 7.7: Real KLM flights [12]

alliances join in formation to reduce their fuel cost.

A good candidate for such a real-life alliance scenario could be a set of flights performed by SkyTeam. SkyTeam members KLM and Delta have many daily flights between Europe and North-America and often these daily flights depart within minutes of each other. The next experiment is to have two aircraft fly from Amsterdam to New York City departing a couple of minutes after one another. None of the aircraft has to perform a detour in order to join this formation, which means that almost zero extra fuel has to be taken on-board.

For this experiment, two fully loaded Boeing 747-400 aircraft will fly from Amsterdam to New York city, but one of them will start at $t_0 = 0s$ and the other will start at $t_0 = 300s$ (5 minutes). The experiment will be performed twice, once with an aircraft A as trailing aircraft (F1) and once with aircraft B as trailing aircraft (F2):

1. Aircraft A: A B744 from Amsterdam to New York City at 13:25 (Delta)
2. Aircraft B: A B744 from Amsterdam to New York City at 13:30 (KLM)

In Table 7.7 the results are summarized and in Appendix D the results are presented in more detail.

Table 7.7: Results for two SkyTeam flights from Amsterdam to New York City flying solo and in formation (Experiment 4)

Results	**2 Solo Flights**	**Formation 1**		**Formation 2**	
Total fuel consumption [kg]	134810	128300	*- 4.84%*	128320	*- 4.82%*
Total flight time [hr]	13.75	14.03	*+ 1.96%*	14.04	*+ 2.11%*
Total distance flown [km]	11727	11727	*+ 0.00%*	11752	*+ 0.21%*

For Formation 1 (aircraft A trailing) and Formation 2 (aircraft B trailing) the rendezvous times are at $t_{RV} = 1669s$ and $t_{RV} = 1097s$, respectively and for both formations the rest of their missions is in formation. The most beneficial formation in this case is Formation 1.

When a fully loaded Boeing 747-400 flies from Amsterdam to New York City it consumes approximately 67400kg of fuel and when two of these aircraft fly the same route independent of each other this sums up to 134810kg. When the aircraft join in formation, this sum can be reduced to 128300kg. This is a reduction of more than 6500kg or a little over 4.8% of the total fuel consumption of the two aircraft. In Figure 7.8a the airspeed of both aircraft are plotted. Here it can be seen that aircraft B has a higher speed in order to catch up with aircraft A. The weight of both aircraft is shown in Figure 7.8b. The aircraft start with the same weight at the beginning of the flights and from the moment they join in formation the weight of the aircraft A (the trailing aircraft) decreases less than that of aircraft B. For Formation 2, where aircraft B is the trailing aircraft, the distance covered increases a little. In Figure 7.9 the horizontal flight path is shown, zoomed in at the starting point (Amsterdam). Note, that the increased distance covered by aircraft A, is due to the small detour it makes after taking-off. It does so in order to have aircraft B join as soon as possible.

The savings for these flights can accumulate to over €1,900,000,- per year. These savings are for KLM and Delta combined. Normally, two different airlines will have to find a way to fairly split these

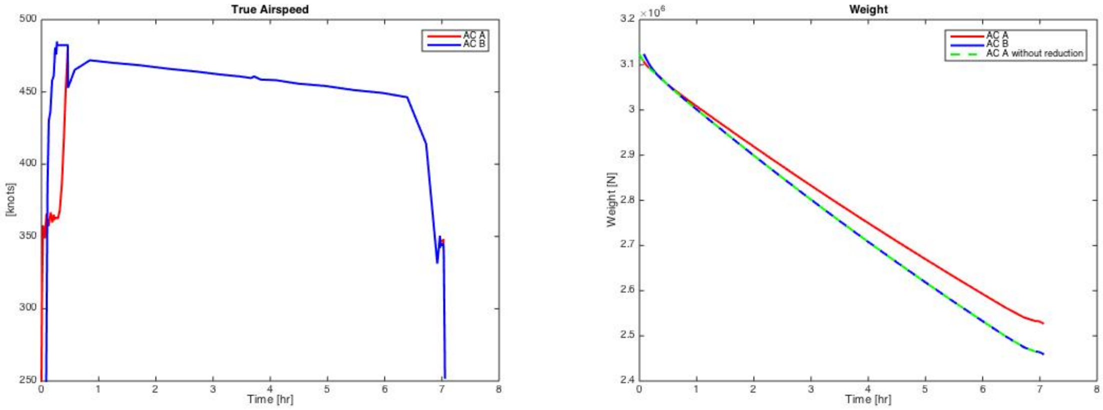

(a) Airspeed of aircraft A and B in Formation 1

(b) Weights of aircraft A and B in Formation 1

Figure 7.8: Results for the SkyTeam experiment

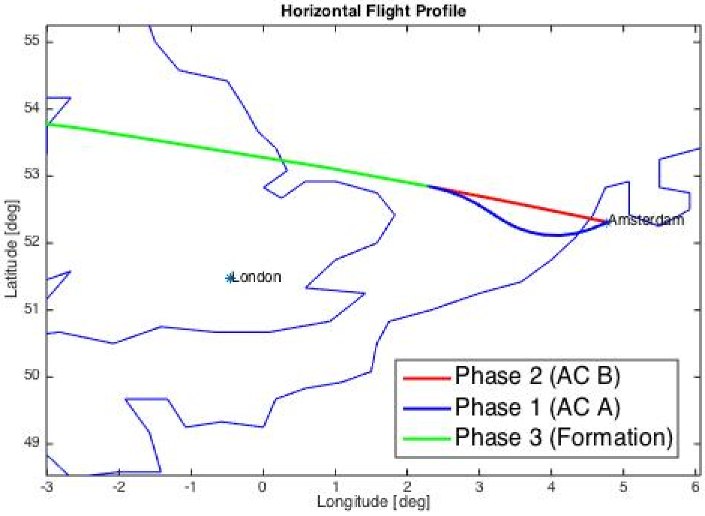
Horizontal Flight Profile
55
54
53
52
51
50
49
Latitude [deg]
London
Amsterdam
Phase 2 (AC B)
Phase 1 (AC A)
Phase 3 (Formation)
-3
-2
-1
0
1
2
3
4
5
6
Longitude [deg]

Figure 7.9: Small detour of aircraft A in Formation 2 for the SkyTeam experiment

savings. This can be done by, for example, daily alternating which of the two airlines has to provide the aircraft that leads the formation. For this case however, as Delta and KLM have a joint-venture over the Atlantic and split all their costs and revenues for transatlantic flights, these complications are not valid.

7.1.3. Experiments 5 & 6: Different Aircraft Types and Weights

Usually, aircraft that might join in a formation are not all of the same type, so it would be interesting to see what kind of effect different aircraft types have on formation flight. As mentioned in Chapter 4, the sequence of the aircraft is of importance when different aircraft join in formation. In this section, first, two flights with different aircraft types will be optimized and then, two flights with similar aircraft types, but with different weights will be optimized.

Experiment 5: Different Aircraft Types

The following two flights will be investigated:

1. Aircraft A: A MD-11 from London to New York City
2. Aircraft B: A B744 from Paris to Washington

Of these two aircraft, the Boeing 747-400 is the heavier aircraft. In Formation 1, aircraft A is the trailing aircraft and in Formation 2, aircraft B is the trailing aircraft. For Formation 1 the weight ratio between lead and trailing aircraft is approximately 0.72 and for Formation 2 this is approximately 1.39. According to Xue et al. [8], when in formation, these lead-trail weight ratios lead to a 35% and 20% induced drag reduction for the trailing aircraft of Formation 1 and Formation 2, respectively. In Table 7.8 the results for these two formations are summarized.

Table 7.8: Fuel consumption of the formations with different aircraft types (Experiment 5)

Results	**Solo**	**Formation 1**	**Formation 2**
Total fuel consumption [kg]	116800	120760 (+3.39%)	117150 (+0.30%)

The results in Table 7.8 show, that not only the different types of aircraft that join in formation have a large impact on the formation, but the sequence in which they fly also plays a major role. The optimization shows, that for both formations it is not beneficial to join in formation compared to the corresponding solo flights (Figure 7.10). Also, the formation time of Formation 1 is only five seconds (caused by a constraint), which indicates that flying in this formation is disadvantageous for the total fuel consumption. This is caused by the different performance characteristics of the aircraft (e.g. cruise speed and cruise altitude).

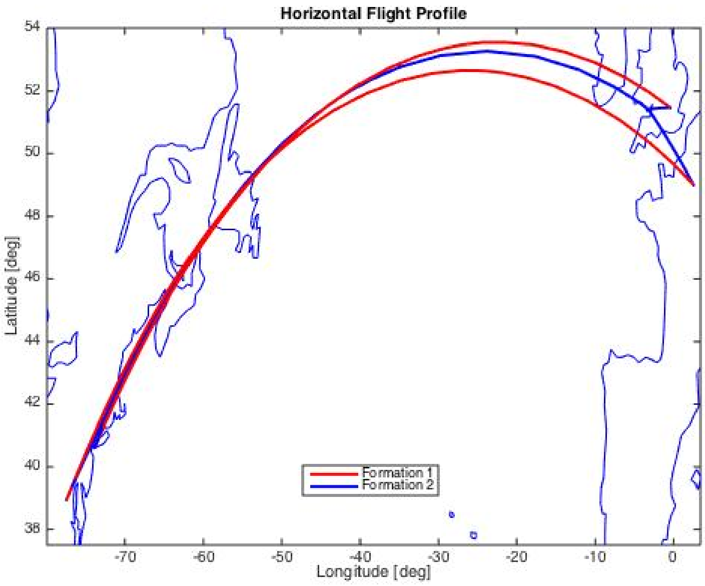

Figure 7.10: Different aircraft types in different lead-trail order (Experiment 5)

As seen before, when in formation, the optimal airspeed for the aircraft is lower than when flying solo. When the B744 is the trailing aircraft and thus has a lower induced drag, the aircraft wants to decrease its speed. The standard cruise speed of the B744 is higher than that of the MD-11 and therefore the decreased B744 speed is not a problem for the MD-11. The other way around, however, seems to be more tedious. When the MD-11 will be the trailing aircraft, the B744 has to slow down significantly to reach the decreased optimal speed of the MD-11. This seems to lead to more fuel consumption than the MD-11 saves and therefore, is not optimal.

Experiment 6: Different Aircraft Weights

The experiment with different aircraft types (Experiment 5) did not give the desired results. Although the results for the different aircraft types are interesting, because they showed that combining certain aircraft types will not give beneficial formations, this was not the desired outcome. The aim of this experiment was to explore what effect the sequence of the formation would be on the total fuel consumption. In this research, only three aircraft types are considered and none of these three are eligible to combine.

The question: ”is it more profitable to have the heavier aircraft fly as trailing or as leading aircraft?” remains. To answer this question, an extra experiment consisting of two B744s is set-up:

1. Aircraft A: A B744 from London to Washington with no payload
2. Aircraft B: A B744 from Madrid to New York with full payload

In Formation 1 aircraft A is the trailing aircraft, which gives a lead-trail ratio of 1.5 and in Formation 2 when aircraft B is the trailing aircraft this ratio is 0.67. These ratios correspond with a reduction of induced drag on the trailing aircraft of 32% and 18% for Formations 1 and 2, respectively. The results for both formations are summarized in Table 7.9.

Table 7.9: Results for formation flight for similar aircraft with different weights (Experiment 6)

Results	**Solo**	**Formation 1**	**Formation 2**
Fuel [kg]	128317	128120 (-0.15%)	126950 (-1.07%)

In this experiment, both formations are beneficial with regard to the total fuel consumption. Formation 2, however, where the heavier aircraft is the trailing aircraft, is the most profitable formation. It consumes approximately 1% less fuel than Formation 1. More results for this experiment are presented in Appendix E.

7.1.4. Experiment 7: Delay

Delay is a common phenomenon in the aviation industry and it would be interesting to see the effect of delay on formation flights. The tool is built to minimize the fuel consumption for the aircraft and therefore it automatically finds the optimal initial, rendezvous, split-up and final times of all aircraft that join the formation. In this experiment, the earlier conducted Experiment 2 will be compared with the same set of flights, but now with fixed initial times. Experiment 2 shows that the lowest total fuel consumption is obtained when aircraft A starts 1008 seconds later than aircraft B. So, for this set of flights the optimal initial times are $t_{A_0} = 1008s$ and $t_{B_0} = 0s$. For this experiment, a delay of 30 minutes is assigned to aircraft B, resulting in the following set of flights:

1. Aircraft A: A B744 from London to Atlanta with fixed initial time $t_{A_0} = 1008s$
2. Aircraft B: A B744 from Madrid to New York with fixed initial time $t_{B_0} = 1800s$

The results for this experiment are summarized in Table 7.10. In this table also the results for the corresponding solo flights and the optimal formation are presented for comparison.

Table 7.10: Results for formation flight when one aircraft has a delayed departure (Experiment 7)

Results	**Solo flights**			**No delay**			**AC B: 30min delay**		
	AC A	**AC B**	**Total**	**AC A**	**AC B**	**Total**	**AC A**	**AC B**	**Total**
Fuel [kg]	79181	66331	**145512**	75515	67270	**142785**	76391	66835	**143770**
Time [hr]	7.91	6.78	**14.69**	8.09	6.90	**15.00**	8.39	6.71	**15.10**

According to the results, the fuel consumption for the delayed set of flights is higher than for the optimal case, but still lower than the corresponding solo flights and the total flight time increased slightly compared to the optimal case. However, the flight time of aircraft B decreased compared to the flight time of the corresponding solo flight. This shorter flight time is partly due to the increase in velocity (Figures 7.11a and 7.11b) and partly due to the change in horizontal flight path (Figure 7.12). The change in the horizontal flight paths of the flights is discussed in Chapter 8.

7.1.5. Experiment 8: Wind - Eastbound vs. Westbound

As mentioned in Chapter 4, over the North-Atlantic Ocean there are jet-streams present. The amount of fuel saved by flying in formation depends on the length of the formation segment and the length of the formation segment depends on the origins and destinations of the aircraft. However, in the presence of wind the routes of the aircraft will most likely deviate from their optimal path, even when not in formation. During this experiment, the effects of wind on formation flight will be investigated.

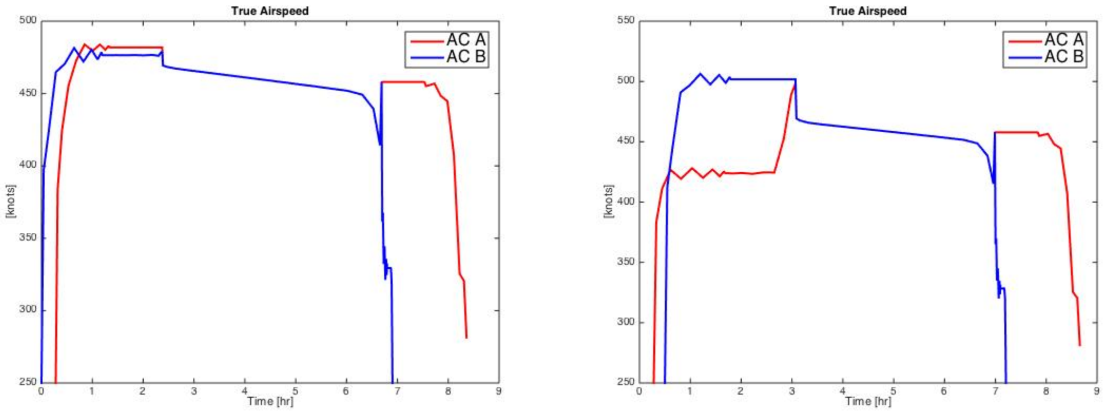

(a) No delay

(b) 30 minutes departure delay for Aircraft

Figure 7.11: Velocity profiles for the delay experiment (Experiment 7)

In the previous experiments all flights were from Europe towards North-America (westbound). To compare the effects of wind, two sets of flights will be compared: a set of Westbound flights:

1. Aircraft A: A B744 from London to Atlanta
2. Aircraft B: A B744 from Madrid to New York City

and a set of Eastbound flights (which are the same as above but in opposite direction):

1. Aircraft A: A B744 from Atlanta to London
2. Aircraft B: A B744 from New York City to Madrid

Data for the wind is taken for the 24^{th} of May 2016. For both cases, Formation 1 has aircraft A as trailing aircraft and Formation 2 has aircraft B as trailing aircraft. The results for the east and westbound flights are summarized in Table 7.11.

Table 7.11: Results for the Eastbound and Westbound flights (Experiment 8)

Results	**Eastbound**		**Westbound**	
	Formation 1	**Formation 2**	**Formation 1**	**Formation 2**
Total fuel consumption [kg]	136380	136380	148040	148300
Total flight time [hr]	14.65	14.65	15.32	15.32
Total distance flown [km]	12761	12758	12800	12795

For the eastbound flight the results for Formation 1 and 2 are more or less the same, but for the westbound flight Formation 1 has a lower fuel consumption. In Figure 7.13 both eastbound Formation 1 and westbound Formation 1 are shown. More results of this experiment are presented in Appendix F.

From the results in Table 7.11, it can be seen that the eastbound flights burn less fuel than the westbound flights. This is because the wind over the North-Atlantic Ocean is mainly eastbound. Because of this wind, the horizontal flight paths and flight times of the aircraft are also different. The eastbound formation has a shorter flight time, because these aircraft fly with a tailwind. Looking at the horizontal flight paths of the aircraft it can be noted that the westbound flights (blue dotted lines) fly further north than the optimal flight paths for no wind and the eastbound flights (green lines) fly further south. Also noteworthy is the difference in duration of the formation segments. The eastbound flights fly in formation for 13178 seconds and the westbound flights for 17057 seconds.

7.2. Experiment 9: Three-Aircraft Formation Flight

Up until now only two-aircraft formations have been explored. When more aircraft join a formation it will likely result in higher savings, because more aircraft benefit from a reduced induced drag. In a

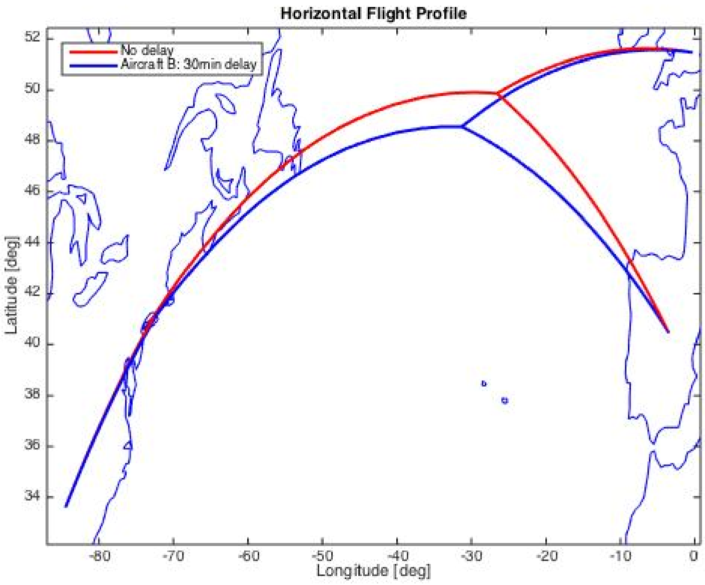

Figure 7.12: The rendezvous point of the formation shifts when one of the aircraft is delayed (Experiment 7)

two-aircraft formation there is one leading aircraft and one trailing aircraft and only the trailing aircraft benefits. When more aircraft join in formation, the number of trailing aircraft increases while the number of leading aircraft remains one. Next to this, as described in Chapter 4, the induced drag reduction also increases when the formation becomes larger. The intention of this experiment is to show that the tool is able to optimize formations larger than two. To show this, a three-aircraft formation will be examined. For this three-aircraft formation experiment, the formation factor on the second aircraft will remain 25%, but for the third aircraft it will increase to 50%. When adding a third flight to the model, the number of phases increases from 5 to 9. This is schematically shown in Figure 7.14. When the number of phases increase, the computational time also increases significantly.

The order in which the aircraft meet is implemented manually. In this example, three flights from Europe to North-America will join in formation:

1. Aircraft A: A B733 from London to Atlanta
2. Aircraft B: A B733 from Amsterdam to New York City
3. Aircraft C: A B733 from Madrid to Toronto

Aircraft A will first join with aircraft B and subsequently aircraft C will join the formation. Then, after completing the formation segment, first aircraft C leaves the formation and then aircraft A and aircraft B separate. In Figure 7.15 the resulting horizontal flight paths are presented. In this experiment, aircraft A is the trailing aircraft during the two-aircraft formation phases, aircraft B is the leading aircraft during all formation phases and aircraft C is the trailing aircraft in the three-aircraft formation phase (there are three formation phases). In other words, during the formation phases, aircraft A has a 25% reduction, aircraft B has no reduction and aircraft C (which only joins in the three-aircraft formation) has a 50% reduction in induced drag.

The joining sequence during this experiment is also convenient from an operational point of view, because this way only aircraft C has to manoeuvre itself behind aircraft A and B, while they can continue their current flight. The results for this experiment are summarized in Table 7.12 and are presented in more detail in Appendix G.

Compared to their optimal great circle routes, aircraft A, aircraft B and aircraft C fly an additional distance of 43, 94 and 222 kilometres, respectively. The largest detour is flown by aircraft C. The benefits of formation flight are the highest when all three aircraft fly together and because aircraft A and B join quite fast, aircraft C should try to join them as fast as possible as well. For a three-aircraft formation it would also be possible to have the aircraft join in 3 other sequences (first aircraft B and

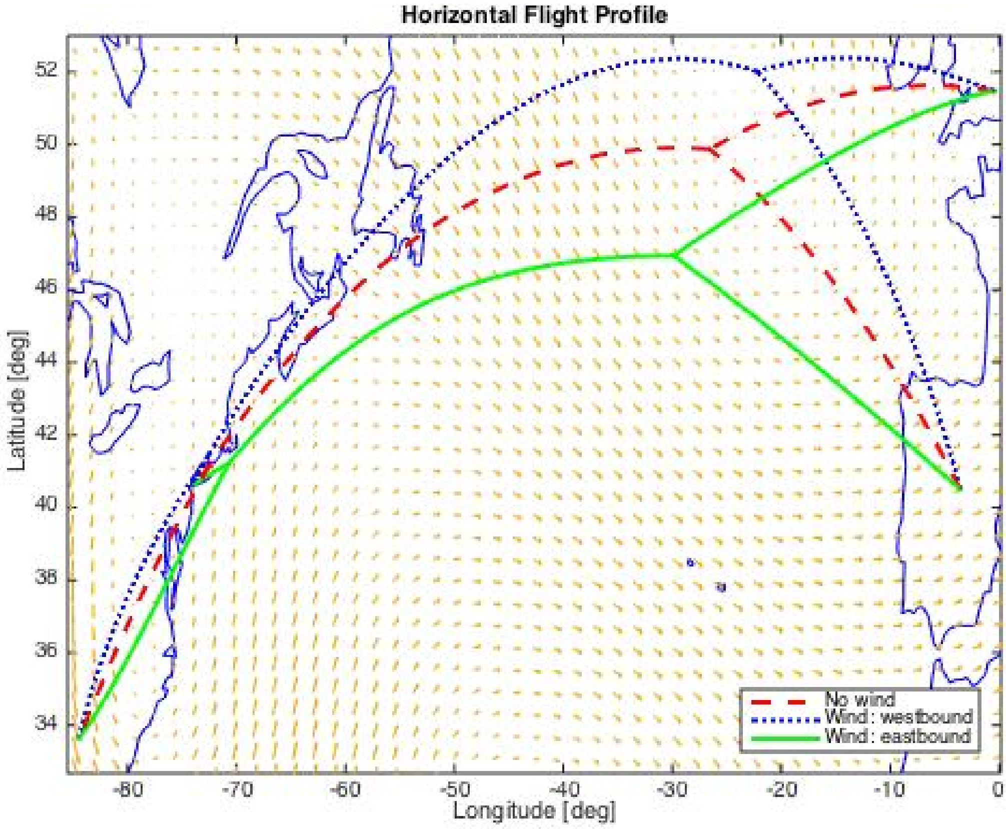

Figure 7.13: Horizontal flight paths of an Eastbound and a Westbound formation (Experiment 8)

Table 7.12: Results for the three-aircraft formation (Experiment 9)

Results	**Solo**	**Three-Aircraft Formation**
Fuel [kg]	45203	42445 (-6.08%)
Flight time [hr]	28.73	28.99 (+0.90%)
Distance [km]	18709	19061 (+1.88%)

C and then aircraft A, first aircraft A and C and then B or have them all join at the same time) and it can also split-up in three different sequences. Therefore, there are 8 potential options to join and split-up. The assembling and disassembling sequence of this experiment is chosen random, but for future investigations it would be interesting to see what the effects of different sequences are. The results of this experiment will not be discussed further.

7.3. Experiment 10: Direct Operating Cost

Up until now, all experiments were optimized to minimize the total fuel consumption of the aircraft that join in formation. This is done because the fuel cost is a significant contributor to the Direct Operating Cost and the cost for fuel can be calculated. But as mentioned in Chapter 4, another contributor to the DOC is the flight time, which means that an increase in flight time also leads to an increase in cost. The next experiment is set-up in order to show what the effect on the performance of the aircraft in the formation would be when the optimization is shifted from optimize for fuel consumption to optimize for flight time.

$$Mayer_{DOC} = \alpha \cdot \sum_{i=1}^{n} t_{f_i} + (1-\alpha) \cdot \sum_{i=1}^{n} \left(W_i(t_0) - W_i(t_f)\right) \tag{7.1}$$

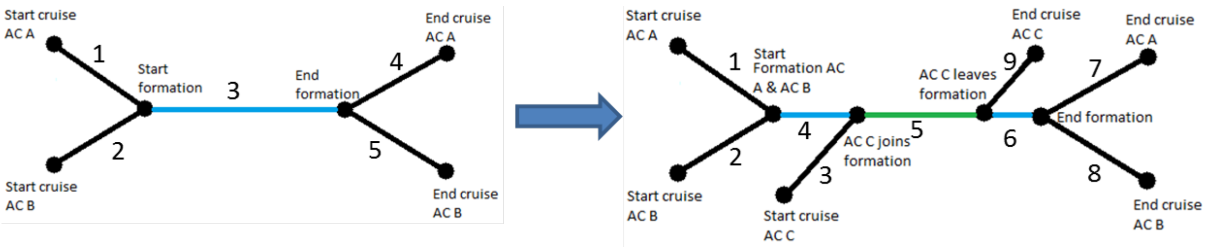
Start cruise
AC A
1
Start
formation
3
End
formation
4
End cruise
AC A
2
5
Start cruise
AC B
End cruise
AC B
Start cruise
AC A
1
Start
Formation AC
A & AC B
AC C leaves
formation
End cruise
AC C
9
End cruise
AC A
7
End formation
4
AC C joins
formation
5
6
2
3
8
Start cruise
AC B
Start cruise
AC C
End cruise
AC B

Figure 7.14: Schematic overview of how the number of phases increases from a two-aircraft formation to a three-aircraft formation

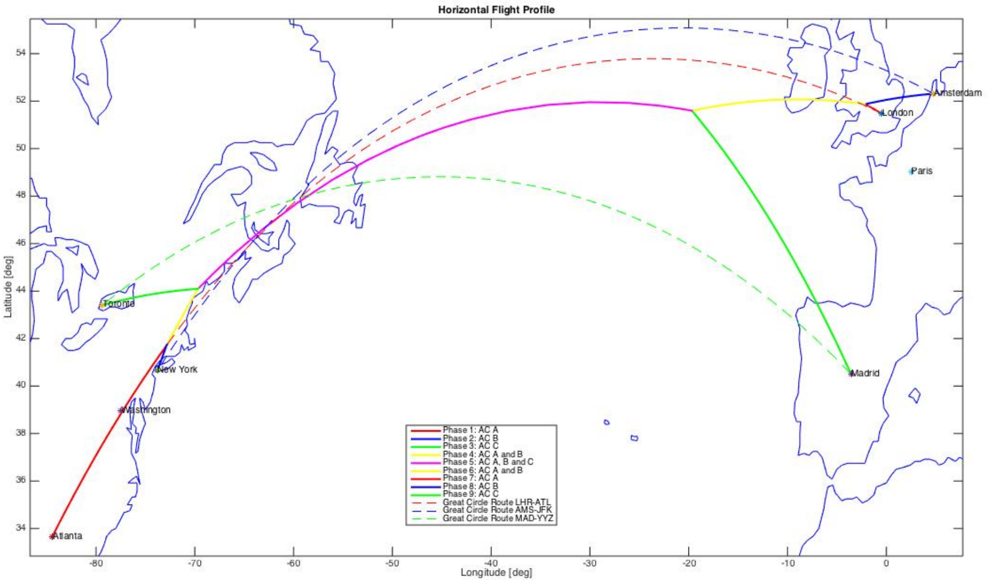
Horizontal Flight Profile
Latitude [deg]
Longitude [deg]
54
52
50
48
46
44
42
40
38
36
34
-80
-70
-60
-50
-40
-30
-20
-10
0
Amsterdam
London
Paris
Madrid
Toronto
New York
Washington
Atlanta
Phase 1: AC A
Phase 2: AC B
Phase 3: AC C
Phase 4: AC A and B
Phase 5: AC A, B and C
Phase 6: AC A and B
Phase 7: AC A
Phase 8: AC B
Phase 9: AC C
Great Circle Route LHR-ATL
Great Circle Route AMS-JFK
Great Circle Route MAD-YYZ

Figure 7.15: The horizontal flight path of a three-aircraft formation from Europe to North-America (Experiment 9)

For this experiment the cost function from Equation 7.1 is minimized, where the α is shifted from 0 to 0.9 in steps of 0.1. As $\alpha = 1$ results in a cost function that optimizes purely for flight time, and this is not relevant as it is not the purpose of formation flight, $\alpha = 1$ is not considered in this experiment. The set-up of Experiment 2 is considered, where one B744 flies from London to Atlanta and another B744 flies from Madrid to New York City. In Figure 7.16 the results for this shifting cost function are shown.

From Figure 7.16, it can be derived that when shifting the optimization from fuel to time, this affects the results. The blue dots represent the results for formation flight, where the dot in the upper left corner represents $\alpha = 0$ (optimized for minimum total fuel consumption). When α increases (and thus the cost function shifts to optimize for minimum total flight time), the figure shows that the total flight time indeed decreases and the total fuel burn increases. In the figure, also the results for the corresponding solo flights are shown (represented by the red dot). As can be seen, the corresponding solo flights consume significantly more compared to when flying in formation, while the flight time is not much lower (note that the solo flights are optimized for minimum fuel consumption and not for minimum flight time). When α is set to $\alpha \approx 0.78$ in the cost function, the total flight time of the formation equals the total flight time of the corresponding solo flight, while the total fuel consumption decreases with 2300kg (1.58%). This shows that, compared to flying solo, formation flight can lead to a significant reduction in fuel burn, without losing time.

Only when α is near 1 (the dot would be in the bottom right corner of the figure), the total fuel consumption would exceed the total fuel consumption for the corresponding solo flights. However, this means that the flights are optimized purely for time and it is obvious that aircraft are not appointed to join in formation to achieve lower flight times. It should be kept in mind, though, that this analysis is

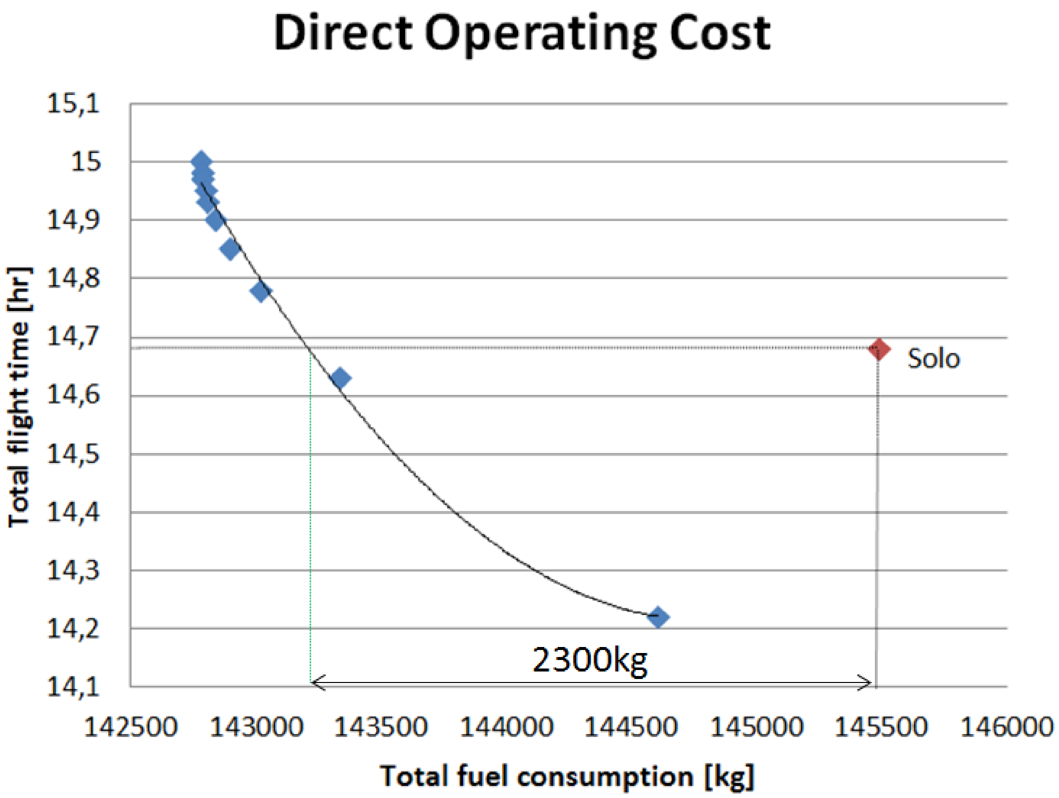

Figure 7.16: Direct Operating Cost: shift cost function from optimize for minimum total fuel consumption to optimize for minimum total flight time

purely for this particular set of flights and aircraft type combination. For other origin and destination pairs or aircraft type combinations, the results can deviate from the results obtained for this scenario.

8

Discussion

In this chapter, the performed research will be discussed. First, a sensitivity analysis is performed to explore what the influence of different values for the induced drag reduction is on the results of the optimization tool. Second, the results obtained in the previous chapter are evaluated. Finally, the employed methodology is discussed.

8.1. Sensitivity Analysis

From other research it is not immediately clear what the precise benefit of formation flight is in terms of drag. Some sources indicate much higher reductions in fuel flow and drag than others. In this study, a standard of 25% induced drag reduction on the trailing aircraft of a two-aircraft formation has been adopted, but it would be interesting to see how the results of the developed optimization tool react, when the formation flight induced drag fraction ϵ changes. In other words, how robust is the model and how beneficial is formation flight when the induced drag reduction caused by formation flight is modified? To answer this question a sensitivity analysis is performed.

Experiment 2, where the two Boeing 747-400 aircraft fly from London and Madrid to Atlanta and New York City, will be used to investigate the sensitivity of the model. The induced drag reduction on the trailing aircraft will be varied from 0% to 50%, in steps of 5% (this corresponds to the formation flight induced drag fraction ϵ that will be varied from 0.5 to 1, in steps of 0.05). In Figure 8.1 the trajectories of the different outputs of the model (green lines) and the corresponding optimal solo flights are shown (white lines). The flights are westbound and depart from London and Madrid. From this figure it can be seen that, when varying the formation flight induced drag reduction, the rendezvous point location for this set of flights changes significantly. The highest reduction in induced drag (50%) results in the easternmost rendezvous point location and this location shifts in western direction when the induced drag reduction decreases.

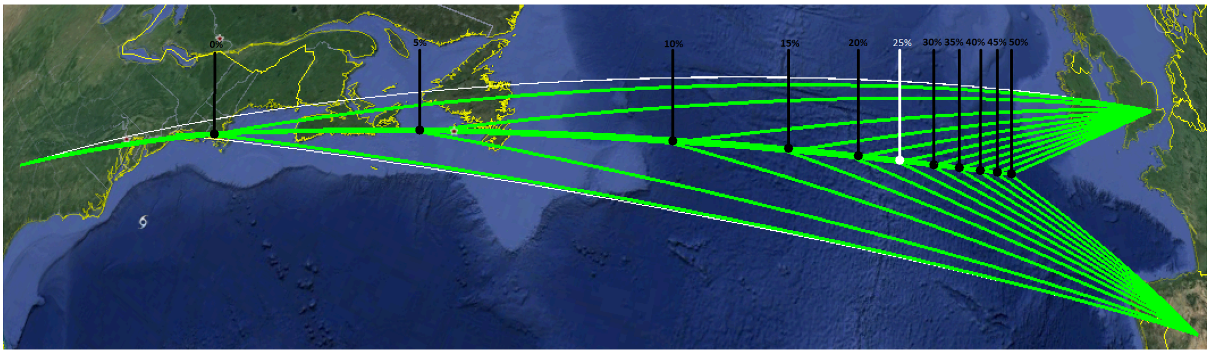

Figure 8.1: Shifting rendezvous point for two flights from Europe to North-America for different values of induced drag reduction

The resulting fuel consumptions and flight times are plotted in Figures 8.2a, 8.2b, 8.3a and 8.3b. In Figure 8.2a the fuel burn is plotted against the percentage of induced drag for the aircraft individually, while in Figure 8.2b the total fuel burn is plotted. From the fuel burn of the individual aircraft one can see that fuel consumption of the leading aircraft (aircraft B) increases almost linearly while the fuel consumption of the trailing aircraft seems to be decreasing exponentially. This linear increase in consumption is caused by the increasing distance this aircraft most overcome. The exponential decrease of the trailing aircraft can be attributed to the fact that not only the formation segment increases, but also the reduction in induced drag. The sum of the fuel consumptions of the two aircraft shows that, for this particular set of flights, it would be beneficial to join in formation (with regard to fuel consumption) if the reduction in induced drag is higher than 5% ($\epsilon < 0.95$).

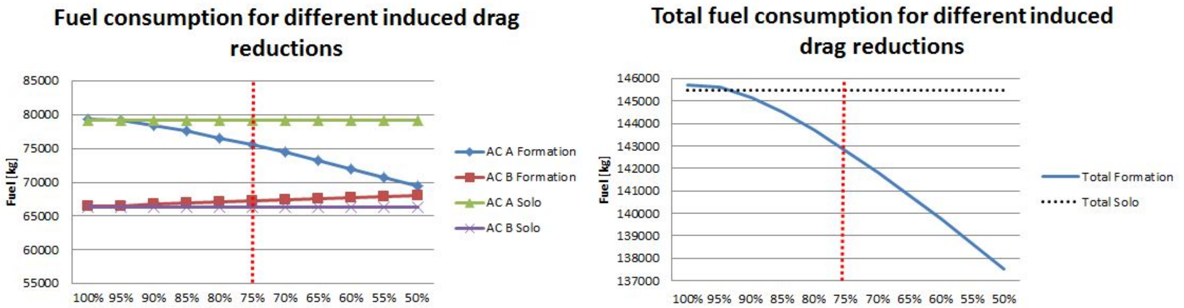

(a) The fuel consumption for different percentages of induced drag reduction per aircraft

(b) The total fuel consumption for different percentages of induced drag reduction

Figure 8.2: Sensitivity analysis: fuel consumption

In Figures 8.3a and 8.3b the flight times are plotted. In Figure 8.3a the time per aircraft is plotted for the different values of induced drag reduction, while in Figure 8.3b the total flight time is plotted for the different induced drag reductions. For comparison, the corresponding flight times of the solo flights are shown as well in these graphs. As expected, the flight time for joining aircraft is larger than for the solo flights and increases even further when the formation flight induced drag fraction decreases. This is because, as the aircraft need to meet at some point, they both deviate from their optimal solo path, resulting in a detour. This detour increases when the aircraft fly together for longer periods, which results in a linearly increasing total flight time (as shown in the results).

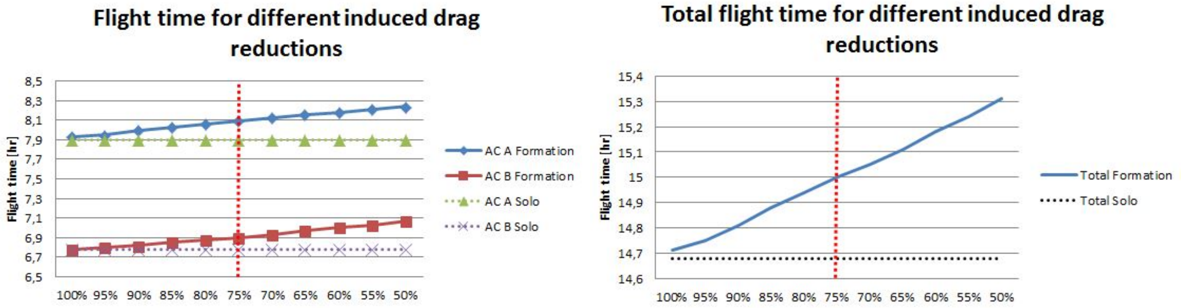

(a) The flight time for different percentages of induced drag reduction for per aircraft

(b) The total flight time for different percentages of induced drag reduction

Figure 8.3: Sensitivity analysis: flight time

In Figures 8.2a - 8.3b, the vertical red dotted lines highlight the results for a reduction in induced drag of 25% which is used as standard during the experiments. Decreasing or increasing this reduction will give slightly different results, but the difference will not be significant. Changing the reduction will change the results with just a few percent. Increasing the reduction to 50% will give a decrease in total fuel consumption and an increase in flight time of 3.61% and 2.11%, respectively, and when a 5% reduction is taken the increase in total fuel consumption and decrease in total flight time will be, respectively, 1.41% and 1.57%. These small changes show that the model is robust when it comes to different percentages of reduction. This sensitivity analysis is performed for this specific set of flights, which makes it only valid for this set of flights. For origin and destination pairs that have a favourable position with regard to formation flight the results might deviate, but the trends will be similar.

8.2. Results

A tool has been developed that optimizes mainly the minimal fuel consumption for the trajectories of multiple aircraft that will join in formation. To determine the benefits of formation flight, in this section the results of the experiments are analyzed further. During the experiments, a couple of issues were noted. First of all, it seems that, apart from the technical challenges, formation flight can lead to substantial lower fuel consumption for the aviation industry. Secondly, when aircraft plan to join in formation the travelled distance increases. Next, also the flight time of the aircraft seems to increase when in formation. And finally, there are many factors that influence the shaping of the trajectories.

8.2.1. Fuel Consumption

All experiments have shown that applying formation flight (assuming the reduction in induced drag for the trailing aircraft is not too small) to a set of suitable flights offers potential benefits in terms of fuel burn. The results indicate that the leading aircraft will have a slightly higher fuel consumption, but the savings of the trailing aircraft more than make up for this when looking at the total fuel consumption of the two aircraft combined. The longer the formation flight segment is, the higher the savings in fuel are.

8.2.2. Distance Flown

The distances the aircraft fly increase when the aircraft join in formation. In other research, investigators sometimes let one aircraft fly its optimal path and a second aircraft join it, resulting in a detour only for the second aircraft. The tool in this study changes both trajectories to get an optimal total result. This means that both aircraft will deviate from their original optimal path, with the effect that additional distance must be covered.

8.2.3. Flight Time

From the results it can be seen, that the total flight time of the aircraft generally increases when implementing formation flight. In contrast to the total fuel consumption, where one aircraft uses more fuel and the other less, the flight time increases for both aircraft when flying in formation. This can be partly traced back to the additional distance flown by the aircraft. Obviously, an increase in distance, with no increase in velocity, also leads to an increase in flight time. Another part of the increase in flight time can be assigned to the change in velocity. When looking closer at the velocity profiles of the aircraft it can be seen that (in most cases) the velocity of the aircraft when in formation is lower than when flying solo. This can be explained by looking at Figure 8.4. When the induced drag is reduced, not only the total drag reduces accordingly, but its minimum also shifts to the left. So, the minimum total drag with a reduced induced drag is at a lower airspeed than it would be without the reduction. Ning et al. also state another positive effect of slowing down in their research. They state that when slightly reducing the speed, also the formation-induced compressibility penalties are eliminated [26] (these penalties are not considered for this study though).

8.2.4. Formation Trajectory

Apart from a change in total fuel consumption and total flight time, the change of the flight trajectories should be noted as well. The horizontal flight paths of all aircraft joining in formation changes, because in order to fly in formation, the aircraft need to rendezvous and the rendezvous point is generally not on their optimal original flight path. The detour caused by this change in route is already discussed in the sections above, but the optimal velocities and altitudes of aircraft flying in formation also differs from the corresponding optimal solo flights. From observing the results of the experiments, it can be often noted that there is a small jump in altitude and velocity at the moment the formation is formed. As mentioned in the previous section, the minimum total drag is achieved at a lower velocity (Figure 8.4), which results in the aircraft flying at a slightly lower airspeed. Also, the altitude of aircraft flying in formation is slightly higher compared to when flying solo. Looking at, for example, the SkyTeam case (Experiment 4), these changes in altitude and airspeed in formation with regard to the solo flights are easily visible. In Figures 8.5a and 8.5b, respectively, the altitude and airspeed of aircraft A of the formation is compared with its

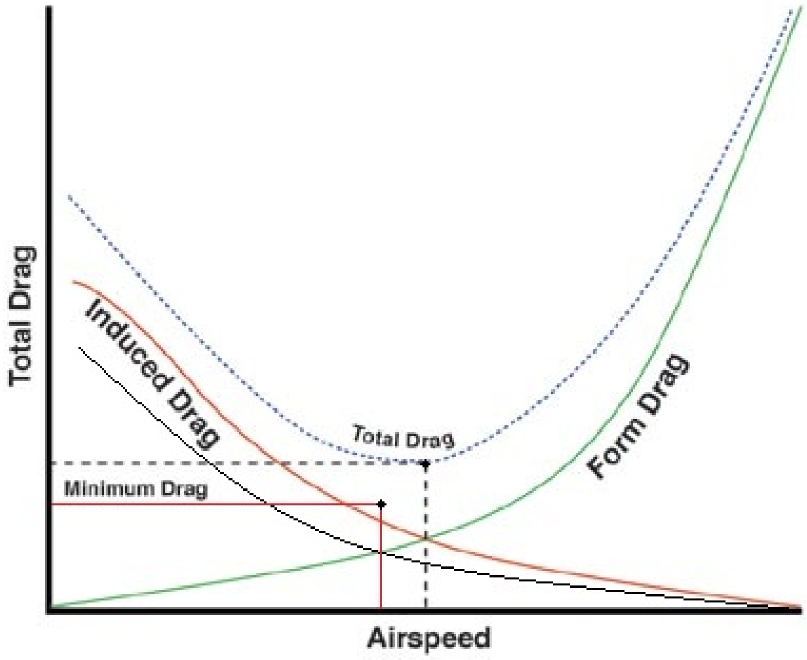

Figure 8.4: Change in induced and total drag due to formation flight, minimum total drag point shifts to bottom left

corresponding original solo flight. The green lines in the figures represent the segment of the aircraft in formation, while the blue dotted lines represent the corresponding original solo flight.

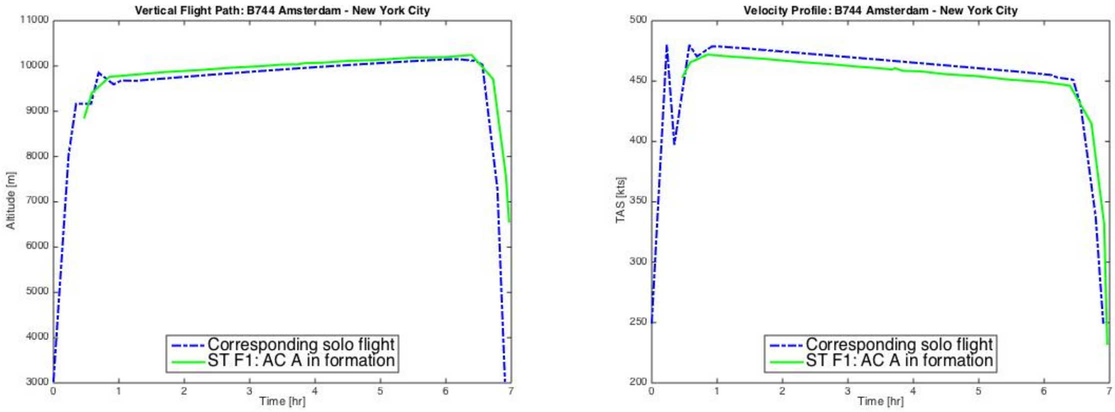

(a) Comparison of the vertical flight path of an aircraft in formation against an aircraft flying solo

(b) Comparison of the airspeed of an aircraft in formation against an aircraft flying solo

Figure 8.5: Trajectory comparison of a flight from the SkyTeam formation experiment (Experiment 4) to its corresponding solo flight

The increase in altitude is actually in contradiction with the research of Ning et al., who state that when aircraft join in formation the reduction in speed requires an altitude drop [26]. The results of this research, however, imply that the optimal altitude increases when aircraft fly in formation.

8.2.5. Factors influencing the Formation

With some experiments the influences of several factors were tested.

Aircraft Types

The idea of testing different aircraft types in a formation is interesting because there are many aircraft types in the transatlantic market. Two topics were of interest during this experiment: is it beneficial for different aircraft types to join in formation and if so, what is the effect of the sequence in which they fly. Experiment 5, with the different aircraft types (a MD-11 from London to New York City and a B744 from Paris to Washington), showed that it is not beneficial to join in formation as both formations gave a higher fuel consumption than the corresponding solo flights. What also is interesting to see is that when the larger B744 is set to lead the formation, the trajectories only join for 5 seconds (due to the constraint) and then part again. This shows that it is undesired for the faster and heavier B744 to slow down to the (due to formation even lower) speed of the MD-11. The other way around however, when the MD-11 is set to lead the formation, the trajectories do join for a longer period. From these results it can be concluded that the effect of the sequence of which type of aircraft is set to fly at what position in the formation has a big impact on the resulting trajectories and fuel consumption. In this study three aircraft types are investigated with very different performance characteristics. It would be interesting to further investigate these effects by adding more different aircraft types to the developed tool.

Experiment 6, with one empty and one fully loaded B744 joining in formation, shows that the sequence in which the aircraft fly makes a difference as well. Formation 2 (with the lighter aircraft leading) seems to be the better option, while in Formation 1 (where the heavier aircraft is leading), the reduction on induced drag for the trailing aircraft was higher. This experiment shows that for identical aircraft types, the couple of percent extra on induced drag reduction does not outweigh the higher fuel consumption of the heavier aircraft. It also shows that for Formation 1, even though there is a higher reduced drag, the formation duration is much shorter than for Formation 2. The formation duration is 11753 seconds for Formation 1 and 15056 seconds for Formation 2. The speed of the fully loaded aircraft is much higher than the empty aircraft, which is in line with the experiment with different aircraft types. This could be the reason why in Formation 1 the heavier aircraft doesn't like to join in formation as the leading aircraft.

Delay

The results of Experiment 7, where the effects of delay are investigated, are very interesting. As in previous research the optimal trajectories of the aircraft have not been really investigated, many different assumptions were made. Some researchers assumed that when one aircraft is delayed, the other aircraft would have to wait at the predefined rendezvous point. Others assumed that the rendezvous point would shift in the direction of the destination, but purely over the predefined optimal path. Others again assumed that when one aircraft is delayed, the formation should be cancelled and both aircraft should continue solo. This study, however, shows something different. From Experiment 7, it is clear that the rendezvous point location shifts and not only over the predefined optimal route. In Figure 8.6 the resulting rendezvous points of several formations with one delayed aircraft are presented. This figure shows the movement of the rendezvous point location when aircraft A and B are delayed by 10, 15 and 30 minutes.

Next to this shift in the rendezvous point location, also the velocities of the aircraft change compared with the optimal flight. The airspeed for the delayed aircraft increases and that of the on-time aircraft decreases until the aircraft meet. This leads to an even further increase in flight time for the on-time aircraft, but the flight time of the delayed aircraft decreases. The resulting fuel consumption in this particular delayed case is still approximately 2% lower than the fuel consumption for the corresponding solo flights. It should be kept in mind, however, that these results are based on the assumption that the magnitude of the delay is known beforehand. This is not often the case (e.g. sometimes a couple of minutes delay for an aircraft lead to the loss of its take-off slot, which leads to more delay) and could lead to non-optimal trajectories.

Wind

Wind always has an impact on aircraft trajectories. In Experiment 8, the effect of wind on formation flight is investigated. This experiment showed that it is possible to implement wind in the developed tool and to assess its influence on the results. The results show that the eastbound flights have a much lower and the westbound flights have a much higher fuel consumption and flight time, compared to the no-wind case. This is due to the tail- and head winds. The optimal flight paths look for the most beneficial route in terms of wind and therefore deviate from the optimal no-wind paths. Also, it should be

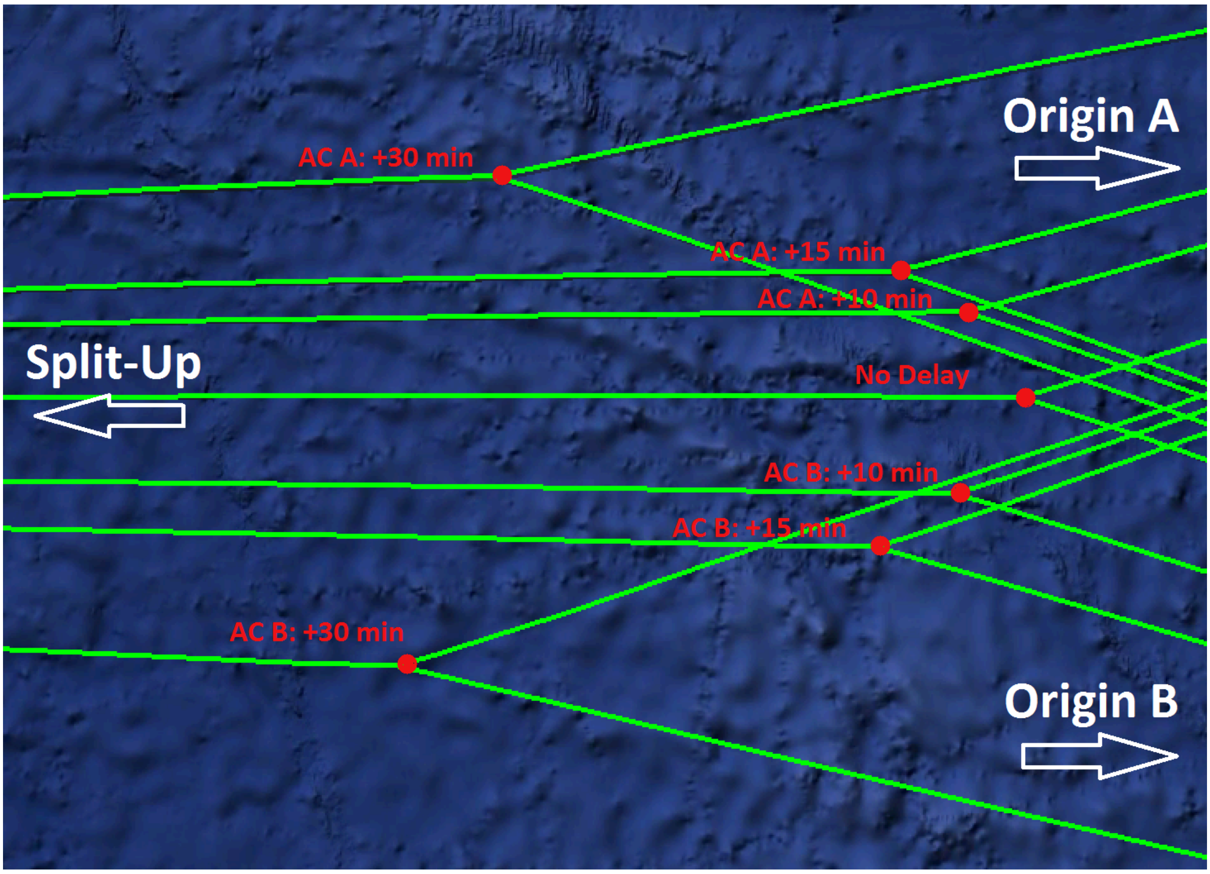

Figure 8.6: Shift of rendezvous point when aircraft A or B is delayed

noted that the formation segment for the westbound flight is much longer than for the eastbound flight. At first sight, the results of this experiment do no show that the effect of wind on a formation is different from the effect of wind on solo flights. Aircraft flying solo also experience a decrease in fuel burn and flight time when flying eastbound and an increase when flying westbound and the optimal solo wind trajectories also deviate from their optimal corresponding no-wind trajectories (the optimal trajectories of the solo flights are presented in Appendix F). However, when comparing the tailwind (eastbound), no-wind and headwind (westbound) formation flights with the corresponding solo flights (Table 8.1), the results show that the relative reduction in fuel burn increases with more unfavorable wind. These results imply that formation flight becomes relatively more beneficial with increased headwinds.

Table 8.1: Resulting fuel consumption for the experiment on which the influence of wind is taken into account (Experiment 8) compared with corresponding solo flights

Fuel consumption [kg]	**Solo**	**Formation**
Tailwind (eastbound)	138600	136400 (-1.59%)
No wind	145500	142800 (-1.86%)
Headwind (westbound)	151500	148000 (-2.31%)

8.3. Methodology

Now that the results are discussed, it is time to evaluate the methodology used in this research. The developed optimization tool seems to work well, but some parts could be improved or further investigated.

8.3.1. Jumps in the Results

When looking at the results of certain experiments, one of the first things that could be noticed is that sometimes there are ”jumps” in the course of the altitude and the velocity variables. These jumps can be due to several reasons. In Figures 8.7a and 8.7b, the results for the experiment in which delay was examined are presented once more (Experiment 7). In these two graphs, the jumps in altitude and velocity are clearly visible.

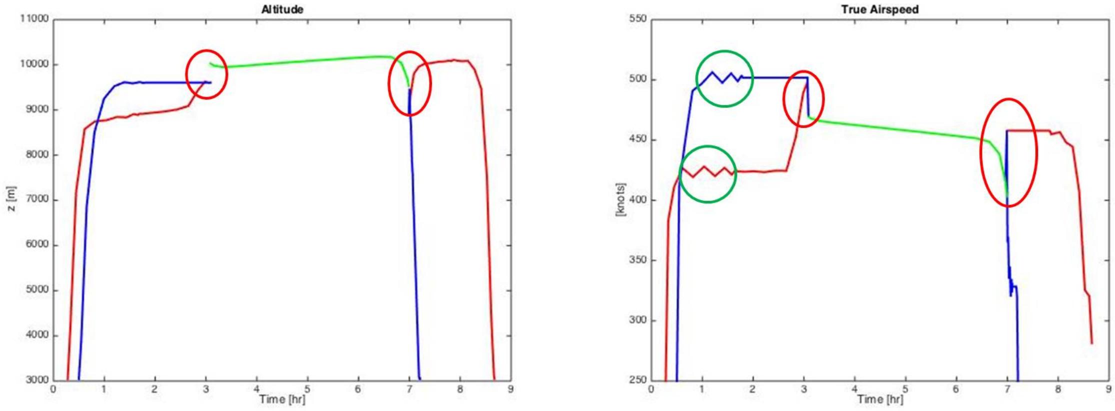

(a) Jumps in altitude

(b) Jumps in velocity

Figure 8.7: Examples of jumps in the results

Two reasons are distinguished for the jumps in this research. Jumps occurring during the solo phases, which are indicated by the green circles in Figures 8.7a and 8.7b, and jumps occurring at the transition point between the solo and formation phases, which are indicated by the red circles. The jumps that occur during the solo phases (green circles) are caused by a ”bang-bang” solution of the optimal engine thrust setting η. A bang-bang solution implies that the optimal control switches from one extreme to the other. Due to the optimal engine thrust setting control that fluctuates at the nodes and the large time steps in this problem, the resulting velocity oscillates. These oscillations, however, hardly affect the results and are therefore not further considered. The jumps that occur at the transition points between the phases (red circles) are due to the fact that at the transition from one dynamic aircraft performance model to the other, the specific energy of the phases is set to be equal, while this is not possible for the altitude and velocity of the phases. During the energy-state model, the altitude and velocity are no longer state variables and can therefore not be linked with the intermediate point-mass model.

8.3.2. Cost Function

The initial idea of this study was to develop an optimal control formulation of formation flight with the aim to minimize the overall fuel consumption or Direct Operating Cost (DOC). The developed optimization tool is able to optimize both minimum fuel consumption and minimum DOC, however, as the DOC are not easy to formulate, the results of the tool are not in cost, but in fuel consumption and flight time. When the cost components for fuel and flight time are specified, the results of the tool can be expressed in DOC. As these cost components were not further investigated in this research, most conducted experiments were optimized for minimum fuel consumption. In other words, this research is mainly focused on the fuel consumption of formation flight and not on the DOC. The benefits in DOC could be further investigated ans as the DOC is different for all airlines, it would be interesting to do this with reference to a specific airline.

8.3.3. Aircraft Dynamic Performance Models

In the model two different aircraft dynamic performance models are combined: the intermediate point-mass model and the energy-state model. This is done because during the formation phase it was assumed that the altitude would not vary much (as this happens during cruise) and the energy-state model would therefore suffice. This leads to difficulties when linking the different models implemented in the different phases. As mentioned before, when switching from the intermediate point-mass model to the energy-state model, the state variables altitude z and Velocity V combine into the specific energy E. This did not cause many problems, but the trajectory altitudes and velocities would sometimes make a jump at the transition point between the phases, which is not realistic. This could be solved by implementing a pseudo state variable during the energy-state phase that defines the altitude or velocity or by implementing the intermediate point-mass model for all phases. However, the latter has been attempted during the research and it resulted in much larger computational time. For this reason, the energy-state model was retained in this study.

8.3.4. Initial Guess

A drawback of the developed tool is that it requires an initial guess that is close to the optimal solution in order to converge to the optimal results. When, for example, new route points are introduced and there are no initial guesses that are close to the optimal result, the tool might encounter numerical difficulties solving the problem and fail to converge. During this research, the initial guesses used were the results of earlier performed optimizations for slightly different problems and therefore could be solved rather fast. When a new experiment was performed and the initial guess led to problems, the transition from the previous experiment to the new experiment was done in small steps. This means that, to get from one experimental set-up to another, many experiments were often performed in between and this way the new experiment was performed step-by-step.

8.3.5. Aircraft Types

Different aircraft types were considered in this research and an experiment was conducted to investigate the effect of different aircraft types on formation flight. This experiment gave a good impression of the significant effect of different aircraft types aircraft have on the formation, as well as the large impact of the sequence in which the aircraft fly. It would be interesting to investigate this further with more aircraft types.

8.3.6. Wind

In this study a wind-field is used which does not change with altitude. The wind components, in north-south and east-west direction, are represented by two polynomials. These polynomials, however, don’t give a perfect representation of the real wind. The vertical wind component has been disregarded as well. However, the experiment proved that the model is able to optimize a set of flights when a wind-field is added and this was the main purpose of the experiment. A more realistic wind-field and atmospheric data from other days can be implemented to investigate the influences of wind further.

9

Conclusions & Recommendations

The aviation industry is growing rapidly and airlines, to stay lucrative, are compelled to keep costs as low as possible. A significant contributor to the airline costs are the Direct Operating Costs (DOC). Reducing the fuel consumption of the aircraft can cut these costs significantly and at the same time it will also lead to fewer emissions. This is why airlines are looking into ways of reducing their fuel consumption, and introducing formation flight could be a solution. Much research has been done into formation flight, but not into the optimal trajectories of the aircraft that will join in the formation. This research focuses on developing a tool that optimizes the multiple-phase trajectories of commercial aircraft that will join in formation. In this final chapter, the research will be concluded and recommendations on future research are given.

9.1. Conclusions

Firstly, some background information on formation flight has been treated and the pros and cons of formation flight have been reviewed. From previous research and performed flight tests it was clear that formation flight can lead to significant reductions in fuel burn. Investigating the current state-of-the-art research on the topic of formation flight and the optimization of the trajectories the aircraft follow, revealed that there is a gap in the body of knowledge and that actually no research has been done in the topic of trajectory optimization for formation flight. This led to the research question: ”is it possible to develop a tool that optimizes the multiple-phase trajectories for two or three commercial aircraft flying in formation weighing the reduced fuel consumption, due to induced drag reduction, versus economic factors using a dynamic optimization technique?”

This led to the main goal of this research to develop an optimal control formulation optimizes the trajectories of multiple commercial aircraft joining in formation for minimum fuel consumption or DOC. The tool developed in this study finds the trajectories of all aircraft that will join the formation and the resulting cost of the flights.

The optimization structure can be split up into of three main parts: the optimization framework, the input and the output. For the optimization framework a cost functional needs to be defined. The tool should be able to minimize the total fuel burn or DOC of the formation. Furthermore, the problem that needs to be solved contains multiple aircraft that first fly solo from their starting point to the rendezvous point, then fly in formation to the split-up point and from there continue their missions solo to their end points. All these segments are considered as separate phases. This means that for a two-aircraft formation, five phases are distinguished. The optimization software that is used to optimize this problem is GPOPS, which is a MatLab based software that solves multiple-phase optimal control problems using pseudospectral methods. The developed tool combines two dynamic aircraft performance models to define the aircraft: the intermediate point-mass model and the energy-state model. The intermediate point-mass model, which is a simplification of the full point-mass model, is applied to all solo phases and the energy-state model, which in its turn is a simplification of the intermediate point-mass model, is applied to the phases where multiple aircraft are joined in formation. At the transition point between the phases, the state variables of the phases are linked to each other. During this research three different aircraft types are considered: the short-range Boeing 737-300, the long-range Boeing 747-400 and the medium- to long range McDonnell Douglas MD-11. When the aircraft fly in formation, a reduction in induced drag is applied on the trailing aircraft. A reduction in induced drag of 25% is assumed for the trailing aircraft of a two-aircraft formation. Other required inputs for the tool are the atmospheric data (which is a function of altitude only), several constraints and a well estimated initial guess. When the tool finds an optimal solution, the output yields the state and control variables for all points in time and the final cost of the problem is obtained. The trajectories for all phases can be replicated with the resulting state and control variables. Furthermore, the fuel burn, flight time and distance flown per aircraft per phase can be derived and these can be aggregated to find the total of all aircraft that join in the formation.

To make the developed tool more versatile and more realistic, delay and wind can also be taken into account. To account for delay, first, the optimal departure times should be found and then the initial time per aircraft can be altered to mimic a delayed flight. As for the wind, atmospheric data is found which contains the wind components in north-south and east-west direction for a worldwide grid. This data is interpolated using polynomial functions to obtain a continuous wind speed surface. The wind components are added to the atmospheric data and are a function of latitude and longitude. The differential-algebraic equations are also modified to incorporate the effects of wind in the dynamic aircraft performance models.

The developed multiple-phase optimization tool is validated by comparing the results of the developed tool for the intermediate point-mass model and energy-state model in combination with all three aircraft types, to the performance manuals of the corresponding aircraft and an online flight planner. This validation showed that the tool gives accurate results for solo flights. To validate that the tool gives reliable results for formation flight as well, an optimization is ran replicating the FedEx case study performed by Bower et al. in their research. In this case study, Bower et al. demonstrate a total fuel saving for a two-aircraft formation between 1.17% to 7.85% and the results from the developed tool from this study show a reduction in fuel burn between 1.09% and 7.68% (these percentages depend on the amount of reduction on induced drag assumed for formation flight).

During this study several experiments are conducted. From these experiments, it can be concluded that formation flight could lead to significant fuel savings without too much delay. When two or more aircraft have similar flight missions (similar flight directions, aircraft and fly more or less around the same time), it would be beneficial for aircraft to rendezvous and continue a part of their flight together. For two identical aircraft that perform similar transatlantic flights and join in formation a total fuel burn reduction of around 1.5% can be obtained, while not increasing the flight distance and time significantly (both increase with 1-2%). Looking at the individual aircraft, it should be noted that the leading aircraft has an increased fuel consumption, but the trailing aircraft has a higher reduction resulting in a lower total fuel consumption for both flights compared to the total fuel consumption of the corresponding solo flights. Two real-life scenarios are replicated: a set of flights operated by KLM and a set of flights operated by SkyTeam members. The results of these experiments showed that the airlines can yearly save millions of dollars when applying formation flight. Other experiments showed that combining different aircraft types or combining aircraft of the same type but with different weights have a significant effect on the results. And the sequence in which the aircraft fly in formation influences the results as well. From these experiments it can be concluded that it is more beneficial when the heavy aircraft is the trailing aircraft in the formation. As departure delay often occurs in reality, also the effects of departure delay on formations were examined. This showed, that for the formation on which a delay was assigned, apart from the increase in fuel consumption compared with the non-delay formation, the rendezvous point location shifted. Unlike what prior research stated, the rendezvous point location will not just shift over the predefined optimal route, but it will actually also deviate from this optimal predefined path to the side of the delayed aircraft to relatively shorten that route compared to the on-time aircraft. Another finding is that the on-time aircraft slows down and the delayed aircraft speeds up in order to rendezvous quickly, resulting in an increase and decrease in the flight times of the on-time and delayed aircraft, respectively. In the presence of wind, the optimal trajectories of the aircraft that join in formation deviate from their optimal corresponding no-wind trajectories and the eastbound formation consume less fuel than the westbound formation, which is also the case for aircraft that fly solo. However, it is found that the relative reduction in fuel burn increases when a formation flies in western direction in comparison with a formation that flies in eastern direction. From this it can be concluded, that flying in formation becomes relatively more beneficial, in terms of fuel consumption, when the formation encounters more headwinds. An experiment containing three aircraft that join in formation has been conducted as well.

The results of this experiment are not elaborated upon further, however, this experiment proves that the developed tool can be expanded to implement more aircraft.

All experiments are optimized for fuel burn and not for DOC, therefore a final experiment is performed shifting the optimization from optimal for minimum fuel burn to minimum flight time. This experiment concluded that, compared to the corresponding solo flights, formation flight can lead to a significant reduction in fuel consumption, while maintaining the same flight time. The results change per set of flights (origin and destination locations, aircraft types, departure time, etc.), however, for a set of eligible flights, this conclusion generally remains. Finally, a sensitivity analysis is conducted to check the robustness of the optimization tool. The impact of a changing reduction in induced drag due to formation flight is analyzed. From this analysis it can be concluded that the output of the optimization, in terms of fuel burn and trajectory, changes for different amount of drag reductions. However, these changes are within the lines of expectation and do not demonstrate any abnormal results. The results of this sensitivity analysis can, just as the DOC optimization before, vary per case, but this conclusion in general remains true as well.

9.2. Recommendations

In this study, a tool is developed to optimize the multiple phases of commercial aircraft that join in formation. Not much research on this subject is yet performed and as such there is much to further investigate. In this section some recommendations are made on the methodology and on future research.

First of all, the optimization in this research mainly focused on minimizing the total fuel burn. For airlines this is interesting, but what also is important is to find the optimal trajectories for the minimal DOC. As the DOC might be different for different situations (flights, aircraft, airlines, etc.), it might be interesting to investigate what the effect of formation flight would be on the DOC for a specific airline.

During the research, two different dynamic aircraft performance models are implemented. The energy-state model is used during the formation phases in order to keep the computational time within limits. In some experiments, the link between the intermediate point-mass model and the energy-state model resulted in a jump in altitude and velocity. In future research, the method could contain only the intermediate point-mass model in order to avoid these disruptions. This will result in a higher computational time, but, as during this research the computational time was not very high, this could remain within limits.

Experiment 5, in which different aircraft types joined in formation, gave good results in the sense that different aircraft types do have a large impact on the results. However, only three aircraft types are included in this research and these three have very different performance characteristics. The effects of different aircraft types could be explored further by adding more aircraft types to the model.

Two real-life scenarios were replicated and optimized and the results showed that there is much to gain for airlines or alliances. The experiments only optimized two flights joining in formation. As many airlines use a ”wave” system (patterns for arriving and departing aircraft from a hub), there are probably many more flights per airline that are eligible to join in formation. Future research could look into applying formation flight to an entire daily schedule of an airline to see what kinds of savings are available on a large scale. It would even be conceivable to investigate how these savings can be further increased by slightly changing the schedule of the airlines to gain more flights that are eligible to join in formation.

As formation flight can lead to a significant reduction in fuel burn, it would be a waste to only fly in formation with aircraft from the same airline. There are probably more and better options when aircraft of all airlines join in formation together. When two aircraft from different airlines (and even different alliances) join in formation there is much to gain, but only for one of the two aircraft. As only the trailing aircraft benefits from formation flight, it should be interesting to see how formation flight can be applied from an operational point of view. It would be interesting to investigate how different airlines can split the savings fairly.

In this research also the effects of wind are taken into account. This is done in order to see what effect wind has on formation flight. However, the replicated wind-field is not very realistic. The wind is assumed to be constant over time and altitude and also the vertical wind component is disregarded. Next to this, the wind data, which is distributed over a large grid, is interpolated with polynomial functions. These polynomials function don’t give a very accurate representation of the real wind. And finally, the wind for only one day is investigated. To get a more realistic view of the effects of wind on formation or even to check if formation flight is beneficial or not at certain days, it is important to replicate the wind more accurately in the tool.

Based on the origins and destination, the aircraft types and the weights of the aircraft, the tool developed in this study can investigate whether it is beneficial for aircraft to join in a formation or not. It does so by finding the optimal trajectories of the flights and comparing the resulting fuel consumption with the fuel consumption of the corresponding original solo flights. This process, however, is time-consuming and especially when entire flight schedules are to be analyzed. Future research can be conducted, to investigate the possibilities of generalizing flights for which formation flight can be beneficial. A generalization that indicates if aircraft should join in formation or not, based on the routes and aircraft types, would allow for a quick evaluation of entire flight schedules and would therefore be very interesting for airlines.

Finally, in this research a three-aircraft formation experiment (Experiment 9) showed that the developed tool is able to handle more aircraft than two. By increasing the number of aircraft joining, also the number of phases increases and this leads to significantly higher computational times. When more than two aircraft join each other in a formation also the joining order, the formation configuration and the aircraft sequence are of great importance for the outcome. In this research only one test was performed to proof that the tool is capable of handling more than two aircraft, but in future research an entire study can be conducted to larger formations and all related matters.

A

Polynomial representation of the wind field

The following polynomial is considered to replicate the wind field that is added in this research:

$$\begin{aligned} wind = {} & p00 + p10 \cdot \lambda + p01 \cdot \phi + p20 \cdot \lambda^2 + p11 \cdot \lambda \cdot \phi + p02 \cdot \phi^2 \\ & + p30 \cdot \lambda^3 + p21 \cdot \lambda^2 \cdot \phi + p12 \cdot \lambda \cdot \phi^2 + p03 \cdot \phi^3 + p40 \cdot \lambda^4 \\ & + p31 \cdot \lambda^3 \cdot \phi + p22 \cdot \lambda^2 \cdot \phi^2 + p13 \cdot \lambda \cdot \phi^3 + p04 \cdot \phi^4, \end{aligned} \tag{A.1}$$

which is only valid for the North Atlantic area, which implies:

$$30 \leq \phi \leq 60 \tag{A.2}$$

$$-85 \leq \lambda \leq 50, \tag{A.3}$$

where ϕ is the latitude, λ is the longitude and the constants of p vary for north-south and east-west wind. For the wind "U" component that represents east-west wind (eastern direction positive), the constants are:
p00 = -1919
p10 = -10.04
p01 = 150
p20 = 0.08874
p11 = 0.7957
p02 = -4.078
p30 = -0.0004509
p21 = -0.005785
p12 = -0.02144
p03 = 0.04516
p40 = 3.464e-06
p31 = 2.535e-05
p22 = 0.0001006
p13 = 0.0001955
p04 = -0.0001648

and for the wind "V" component that represents the north-south wind (northern direction positive), the constants are:
p00 = -234.2
p10 = 3.032
p01 = 19.89
p20 = 0.09329
p11 = -0.09254

p02 = -0.6044
p30 = -7.36e-05
p21 = -0.003115
p12 = 0.001215
p03 = 0.007992
p40 = -1.308e-05
p31 = -4.396e-05
p22 = -2.373e-05
p13 = -2.672e-05
p04 = -4.015e-05

In Figure A.1 the wind field considered in this research is presented.

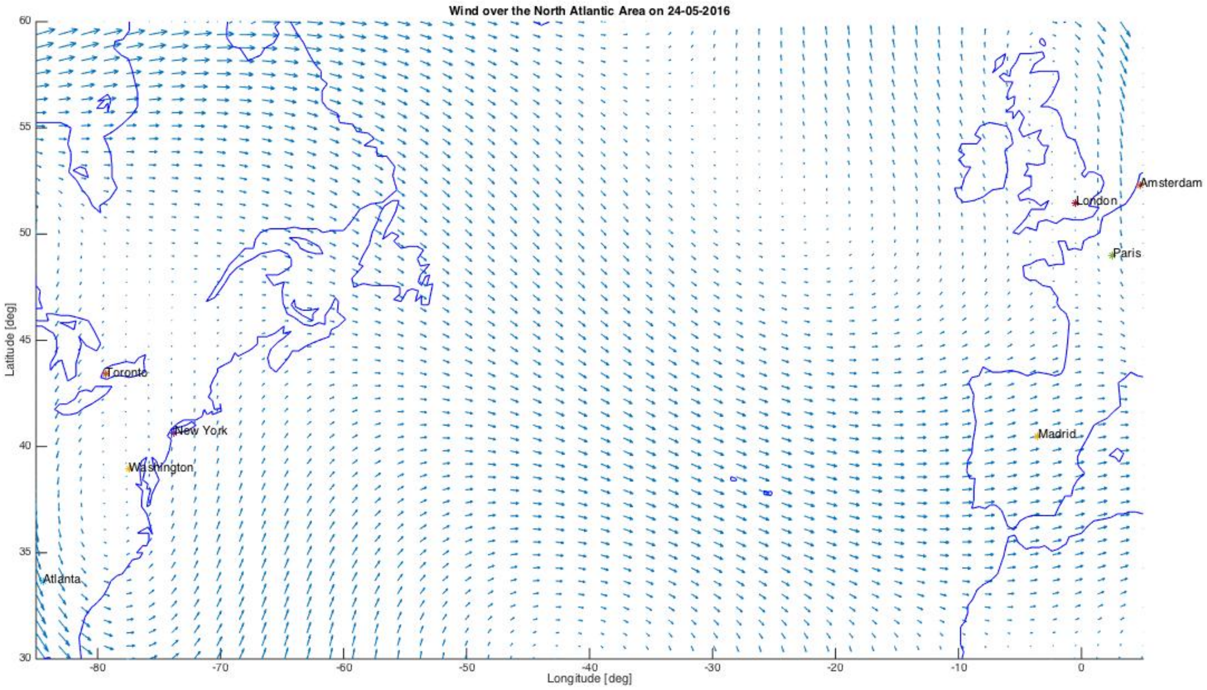
Wind over the North Atlantic Area on 24-05-2016
Latitude [deg]
Longitude [deg]
60
55
50
45
40
35
30
-80
-70
-60
-50
-40
-30
-20
-10
0
Amsterdam
London
Paris
Madrid
Toronto
New York
Washington
Atlanta

Figure A.1: Considered wind-field for this research (May 24^{th} 2016)

B

Solo Flights for Benchmarking

In this appendix the results of four solo flights are presented. The four solo flights are the following:

1. Solo flight 1 (S1): A Boeing 737-300 that flies from London to Atlanta
2. Solo flight 2 (S2): A Boeing 737-300 that flies from Madrid to New York City
3. Solo flight 3 (S3): A Boeing 747-400 that flies from London to Atlanta
4. Solo flight 4 (S4): A Boeing 747-400 that flies from Madrid to New York City

As all four solo flights only consist of one phase (because they fly solo), they are all optimized twice: once with the intermediate point-mass model and once with the energy-state model. The average of these two results are used to benchmark during the research. In Tables B.1 - B.4 the results are presented.

Table B.1: S1: Solo flight from London to Atlanta for the Boeing 737-300 with a payload of 3142kg

Results	**LHR-ATL: PM**	**LHR-ATL: ES**	**LHR-ATL: Average**
Fuel consumption [kg]	16575	16571	16588
Flight time [s]	37521	37504	37489
Distance [km]	6778	6778	6778

Table B.2: S2: Solo flight from Madrid to New York City for the Boeing 737-300 with a payload of 3142kg

Results	**MAD-JFK: PM**	**MAD-JFK: ES**	**MAD-JFK: Average**
Fuel consumption [kg]	13799	13796	13798
Flight time [s]	31897	31880	31889
Distance [km]	5776	5776	5776

Table B.3: S3: Solo flight from London to Atlanta for the Boeing 747-400 with a payload of 63916kg

Results	**LHR-ATL: PM**	**LHR-ATL: ES**	**LHR-ATL: Average**
Fuel consumption [kg]	79183	79179	79181
Flight time [s]	28453	28462	28458
Distance [km]	6778	6778	6778

In Figures B.1a - B.1d and B.2a - B.2d, graphs containing the true airspeeds, vertical flight paths, specific energies and aircraft weights of, respectively, solo flights 1 and 2 and solo flights 3 and 4 are presented.

Table B.4: S4: Solo flight from Madrid to New York City for the Boeing 747-400 with a payload of 63916kg

Results	**MAD-JFK: PM**	**MAD-JFK: ES**	**MAD-JFK: Average**
Fuel consumption [kg]	66305	66357	66331
Flight time [s]	24392	24408	24400
Distance [km]	5776	5776	5776

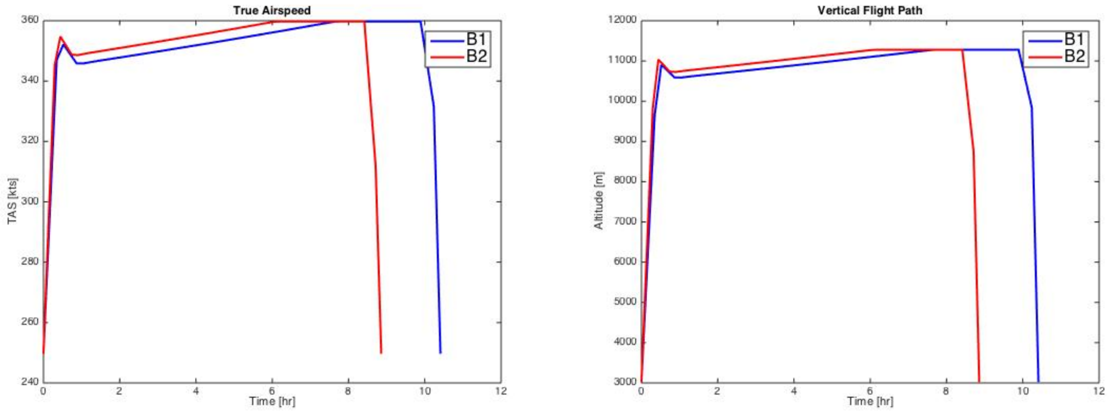

(a) True airspeed

(b) Vertical flight profile

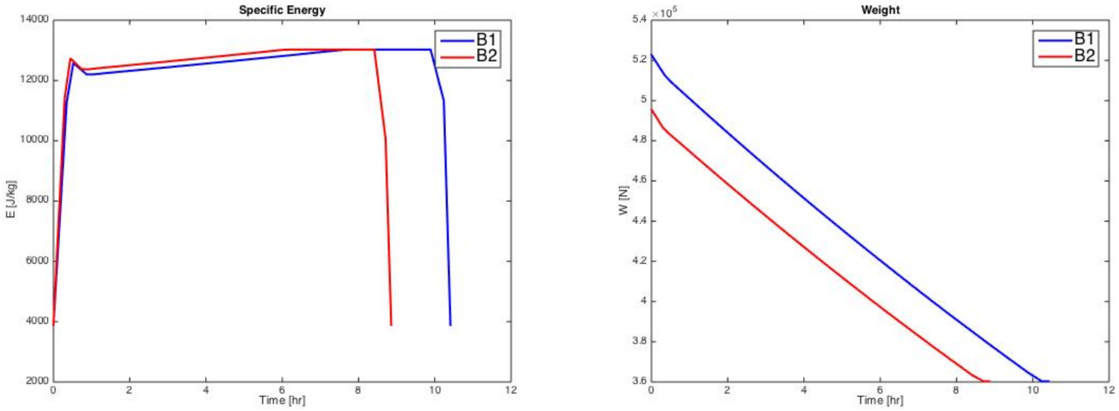

(c) Specific energy

(d) Aircraft weights

Figure B.1: Results for solo flights 1 and 2

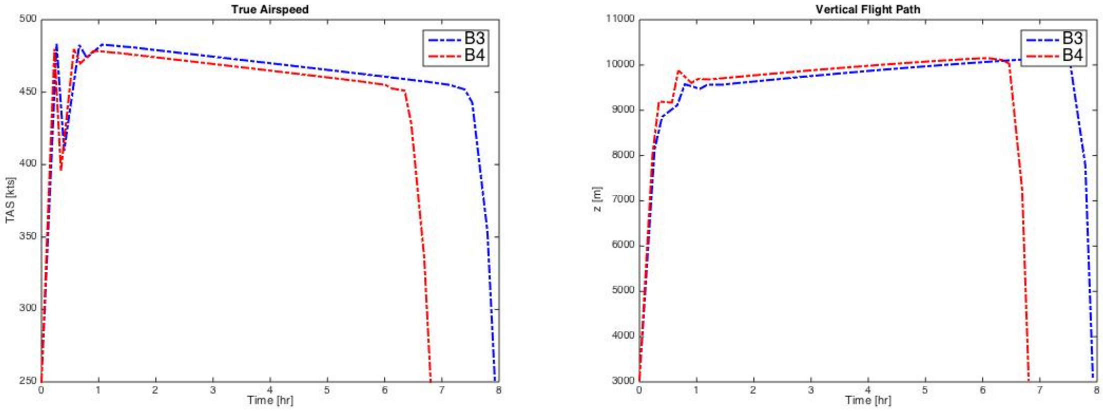

(a) True airspeed (b) Vertical flight profile

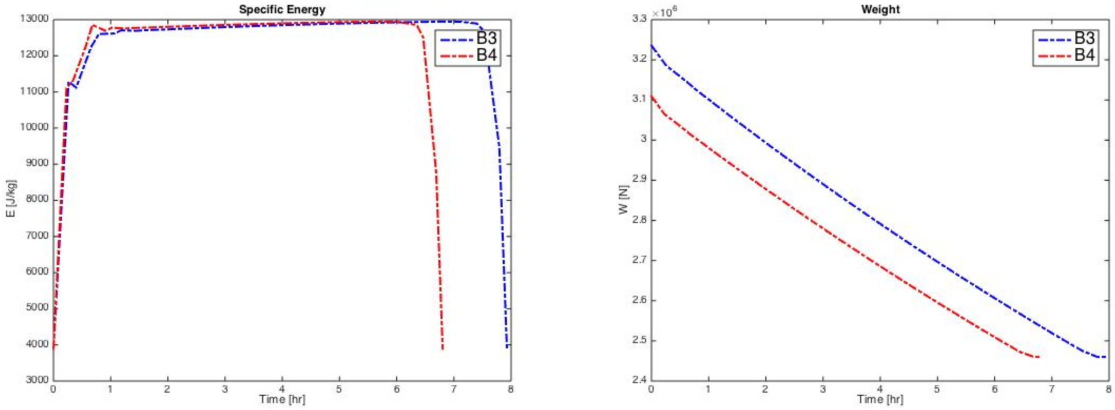

(c) Specific energy (d) Aircraft weights

Figure B.2: Results for solo flights 3 and 4

C

Results for the KLM Scenario (Experiment 3)

In this appendix the results for the KLM experiment (Experiment 3) are presented in more detail. In Table C.1 the results for the individual aircraft and for the total formation of both formations are presented.

Table C.1: Results for the KLM experiment

Results	**Formation 1**			**Formation 2**		
	AC A	**AC B**	**Total**	**AC A**	**AC B**	**Total**
Fuel [kg]	68283	67740	136020	73364	62738	136100
Flight time [hr]	7.78	6.83	14.60	7.78	6.82	14.60
Distance [km]	6226	5864	12090	6226	5864	12090

More results are presented in Figures C.1a - C.1f and C.2a - C.2f for Formations 1 and 2, respectively.

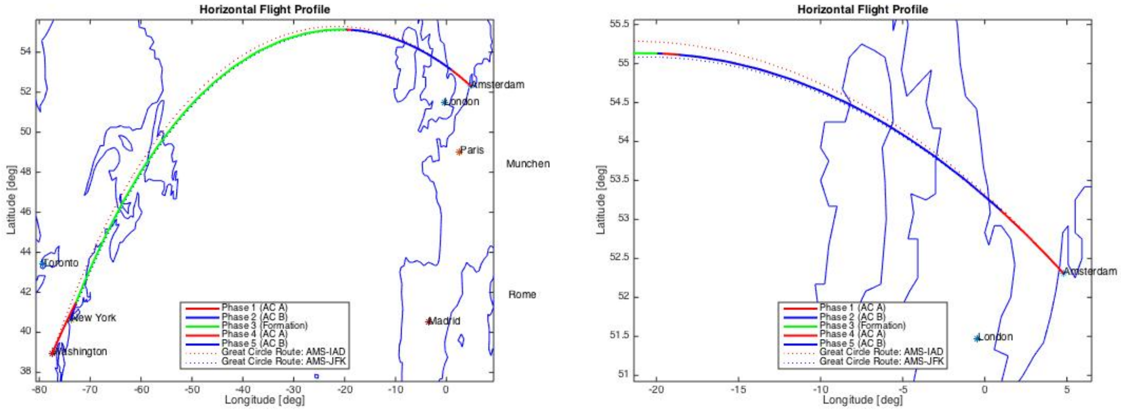
Horizontal Flight Profile
Latitude [deg]
Longitude [deg]
Amsterdam
London
Paris
Munchen
Rome
Madrid
Toronto
New York
Washington
Phase 1 (AC A)
Phase 2 (AC B)
Phase 3 (Formation)
Phase 4 (AC A)
Phase 5 (AC B)
Great Circle Route: AMS-IAD
Great Circle Route: AMS-JFK
Horizontal Flight Profile
Latitude [deg]
Longitude [deg]
Amsterdam
London

(a) Horizontal flight path

(b) Horizontal flight path at origin

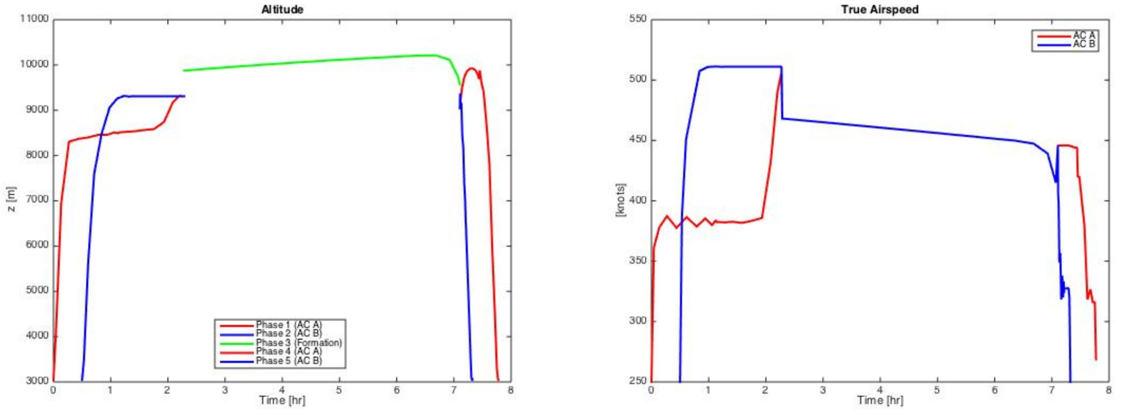

(c) Vertical flight profile

(d) True airspeed

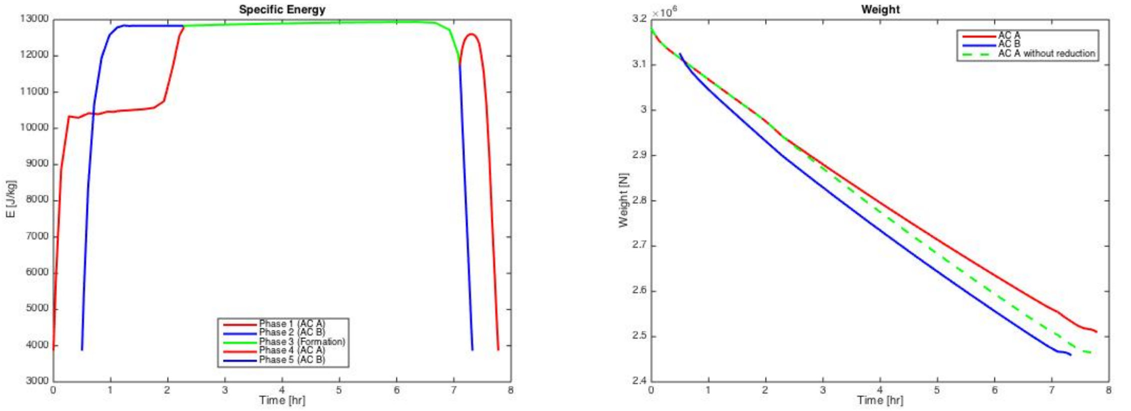

(e) Specific energy

(f) Aircraft weighs

Figure C.1: Results for Formation 1 of the KLM experiment (Experiment 3)

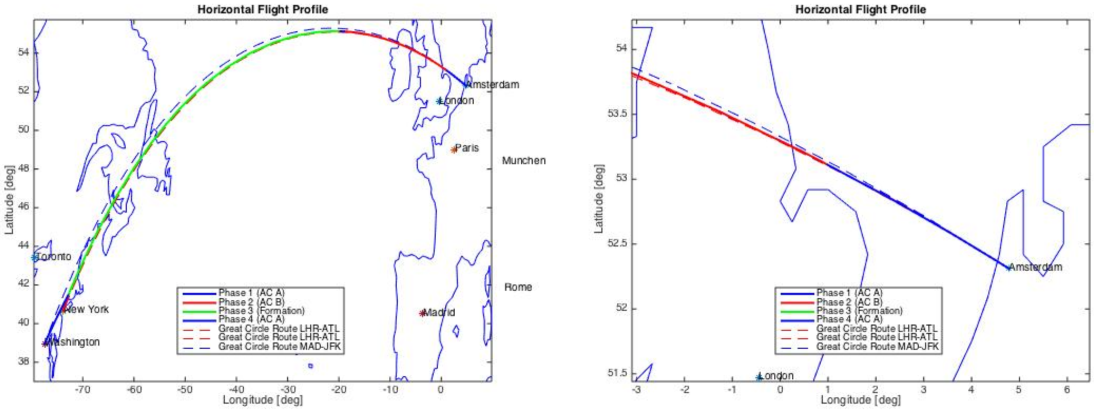
Horizontal Flight Profile
Latitude [deg]
Longitude [deg]
Amsterdam
London
Paris
Munchen
Rome
Madrid
Toronto
New York
Washington
Phase 1 (AC A)
Phase 2 (AC B)
Phase 3 (Formation)
Phase 4 (AC A)
Great Circle Route LHR-ATL
Great Circle Route LHR-ATL
Great Circle Route MAD-JFK
Horizontal Flight Profile
Latitude [deg]
Longitude [deg]
Amsterdam
London
Phase 1 (AC A)
Phase 2 (AC B)
Phase 3 (Formation)
Phase 4 (AC A)
Great Circle Route LHR-ATL
Great Circle Route LHR-ATL
Great Circle Route MAD-JFK

(a) Horizontal flight path

(b) Horizontal flight path at origin

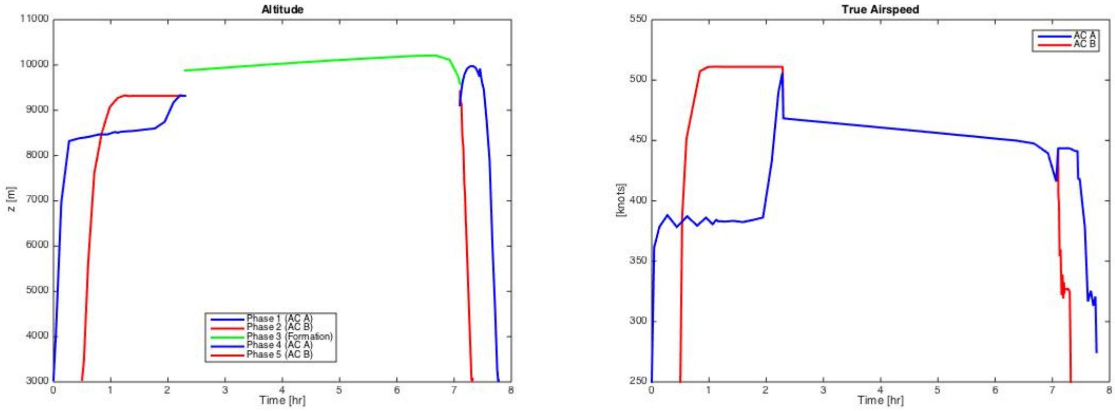

(c) Vertical flight profile

(d) True airspeed

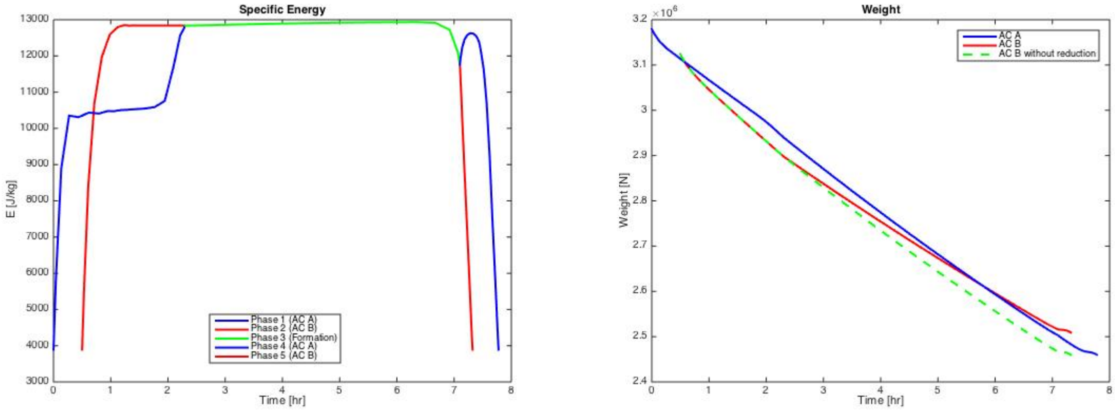

(e) Specific energy

(f) Aircraft weight

Figure C.2: Results for Formation 2 of the KLM experiment (Experiment 3)

D

Results for SkyTeam Scenario (Experiment 4)

In this appendix the results for the SkyTeam experiment (Experiment 4) are presented in more detail. In Table D.1 the results for the individual aircraft and for the total formation of both formations are presented.

Table D.1: Results for the SkyTeam experiment

Results	**Formation 1**			**Formation 2**		
	AC A	**AC B**	**Total**	**AC A**	**AC B**	**Total**
Fuel [kg]	60787	67510	128300	67954	60365	128320
Flight time [hr]	7.05	6.97	14.03	7.06	6.98	14.05
Distance [km]	5863	5863	11727	5889	5863	11752

More results are presented in Figures D.1a - D.1f and D.2a - D.2f for Formations 1 and 2, respectively.

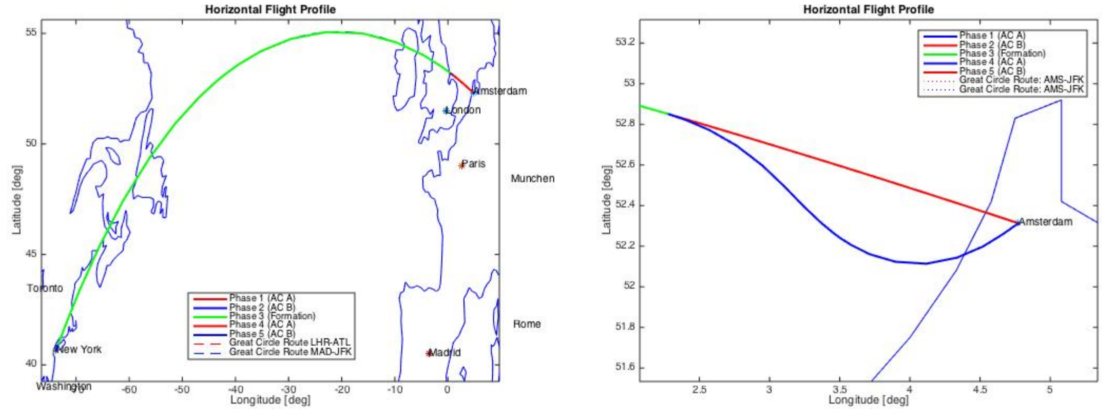
Horizontal Flight Profile
Latitude [deg]
Longitude [deg]
Amsterdam
London
Paris
Munchen
Toronto
Rome
New York
Madrid
Washington
Phase 1 (AC A)
Phase 2 (AC B)
Phase 3 (Formation)
Phase 4 (AC A)
Phase 5 (AC B)
Great Circle Route LHR-ATL
Great Circle Route MAD-JFK
Horizontal Flight Profile
Great Circle Route: AMS-JFK
Great Circle Route: AMS-JFK
Latitude [deg]
Longitude [deg]
Amsterdam

(a) Horizontal flight path

(b) Horizontal flight path at origin

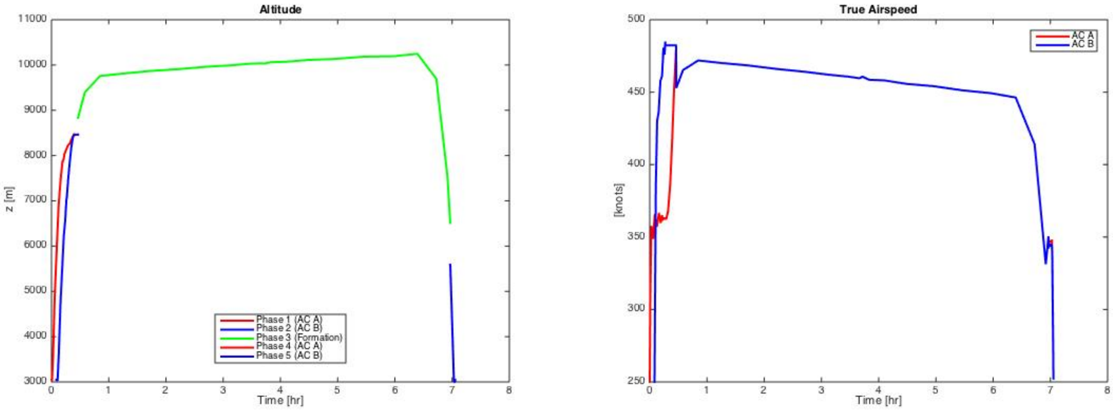

(c) Vertical flight profile

(d) True airspeed

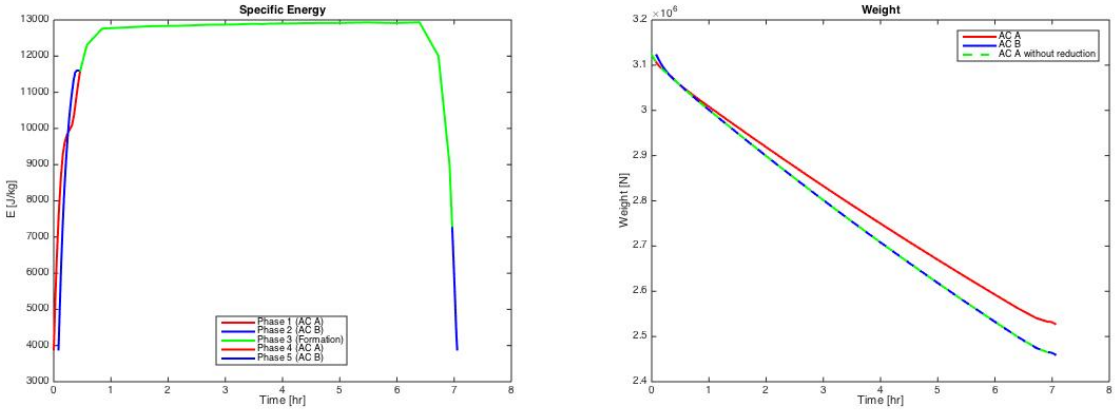

(e) Specific energy

(f) Aircraft weight

Figure D.1: Results for Formation 1 of the SkyTeam experiment (Experiment 4)

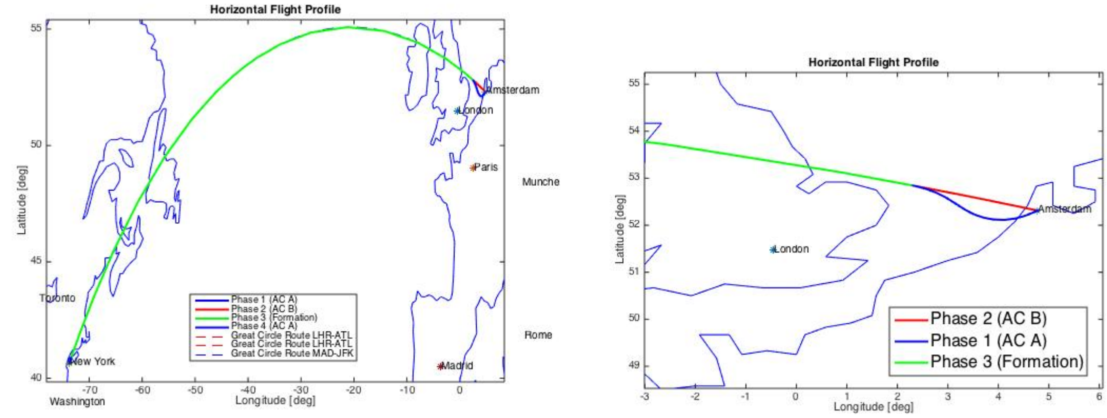
Horizontal Flight Profile
Latitude [deg]
Longitude [deg]
Amsterdam
London
Paris
Munche
Rome
Madrid
Toronto
New York
Washington
Phase 1 (AC A)
Phase 2 (AC B)
Phase 3 (Formation)
Phase 4 (AC A)
Great Circle Route LHR-ATL
Great Circle Route LHR-ATL
Great Circle Route MAD-JFK
Horizontal Flight Profile
Latitude [deg]
Longitude [deg]
Amsterdam
London
Phase 2 (AC B)
Phase 1 (AC A)
Phase 3 (Formation)

(a) Horizontal flight path

(b) Horizontal flight path at origin

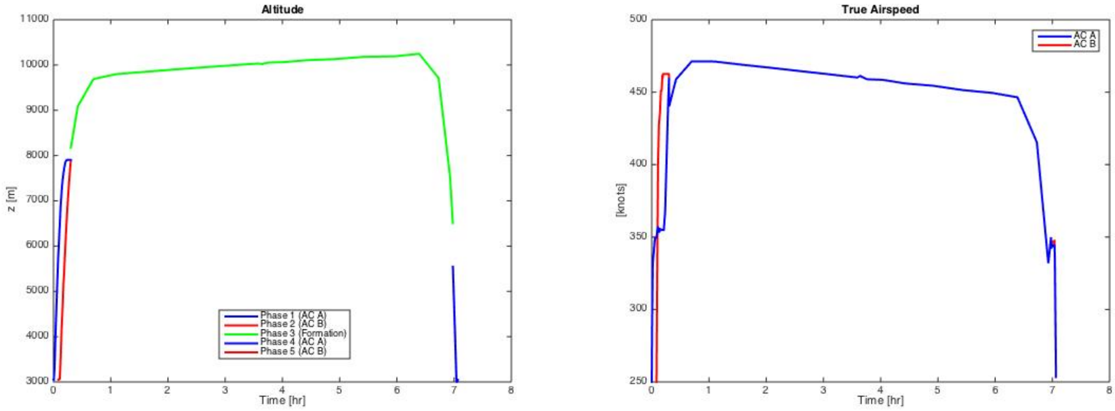

(c) Vertical flight profile

(d) True airspeed

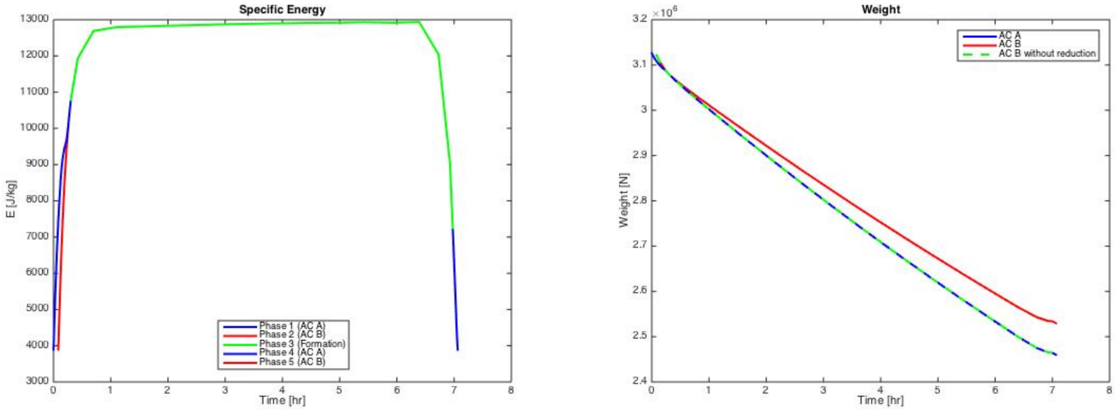

(e) Specific energy

(f) Aircraft weight

Figure D.2: Results for Formation 2 of the SkyTeam experiment (Experiment 4)

E

Results for the experiment with Different Aircraft Weights (Experiment 6)

In this appendix the results for the experiment with similar aircraft, but with different weights (Experiment 6) are presented in more detail. In Figure E.1, the horizontal flights paths for both formations are shown, where Formation 1 has the heavy aircraft as leading aircraft and Formation 2 has the heavy aircraft as trailing aircraft.

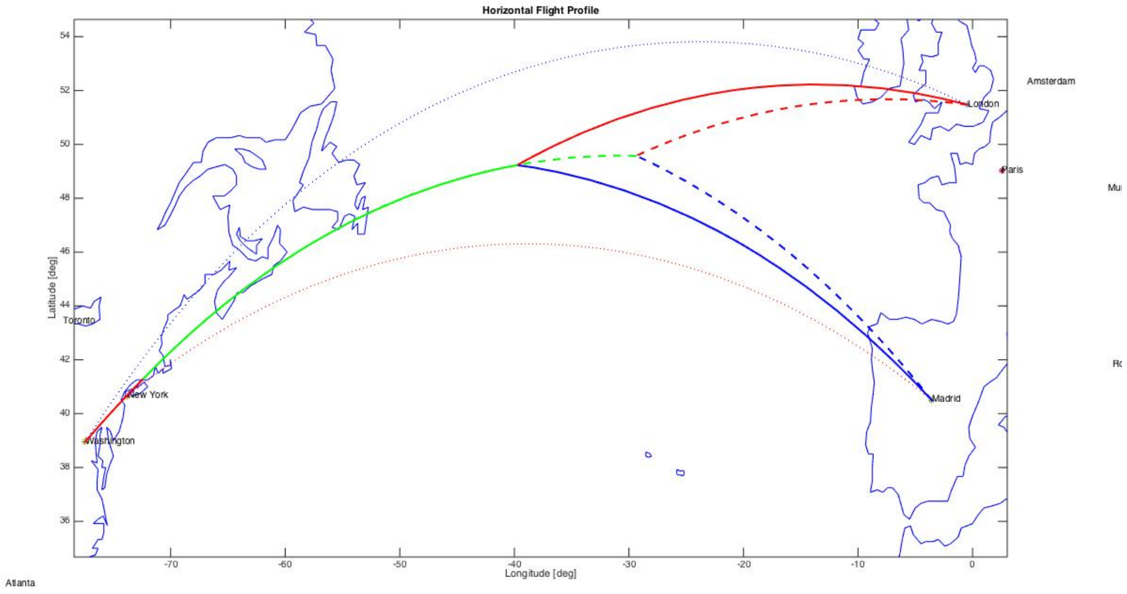
Horizontal Flight Profile
Latitude [deg]
54
52
50
48
46
44
42
40
38
36
Longitude [deg]
-70
-60
-50
-40
-30
-20
-10
0
Amsterdam
London
Paris
Mu
Toronto
New York
Washington
Madrid
Ro
Atlanta

Figure E.1: Horizontal flight paths of Formation 1 (solid line) and Formation 2 (dashed line)

In Figures E.2a - E.2d, more results for this experiment are presented. In the graphs the solid lines represents Formation 1 and Formation 2 is represented by the dashed lines. Formation 2 with the heavy aircraft trailing the aircraft shows the highest reduction in total fuel consumption.

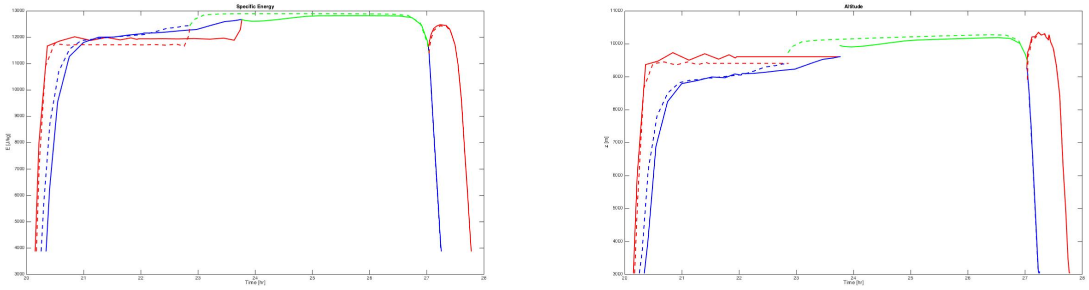

(a) Specific energy

(b) Vertical flight path

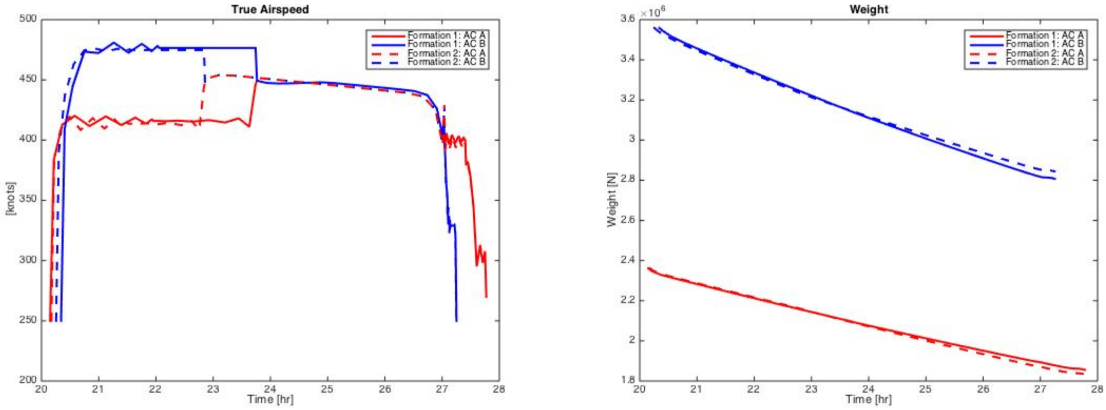

(c) True airspeed

(d) Aircraft weight

Figure E.2: Results for the experiment with one empty (aircraft A) and one full (aircraft B) B744. Formation 1 has aircraft A as trailing aircraft (solid line) and Formation 2 where aircraft B is the trailing aircraft (dashed line).

F

Results for the experiment with wind (Experiment 8)

In this appendix, the results for the eastbound and westbound flights, on which the effects of the presence of wind is examined, are presented in more detail (Experiment 8). In Figures F.1 and F.2 the horizontal flight paths for the sets of, respectively, eastbound and westbound flights are shown.

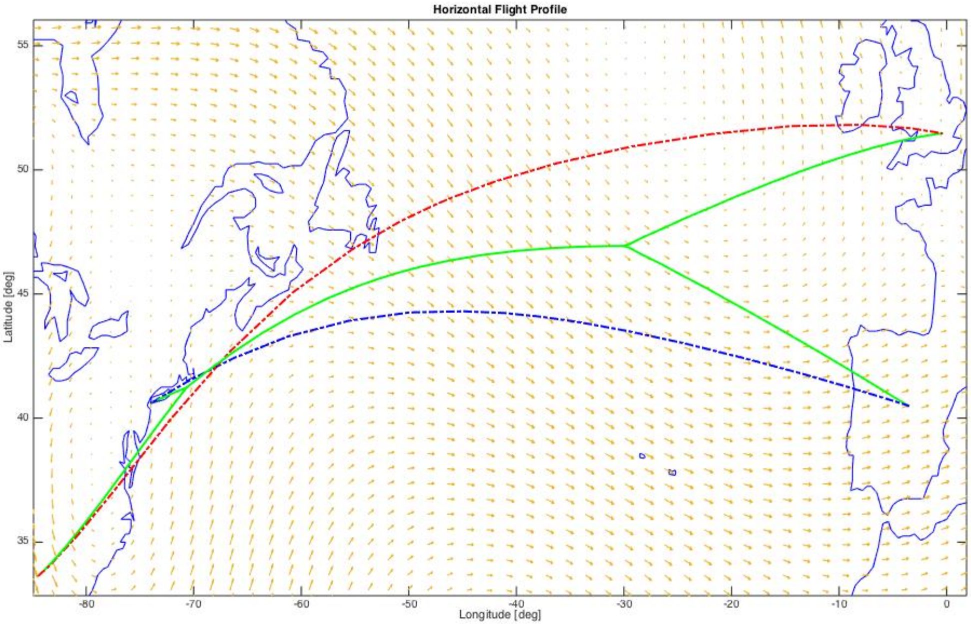
Horizontal Flight Profile
Latitude [deg]
55
50
45
40
35
Longitude [deg]
-80
-70
-60
-50
-40
-30
-20
-10
0

Figure F.1: Horizontal flight paths of the set of eastbound flights. The dashed lines represent the optimal trajectories of the aircraft when flying solo and the solid green lines represent the optimal trajectories for the same flights that join in formation.

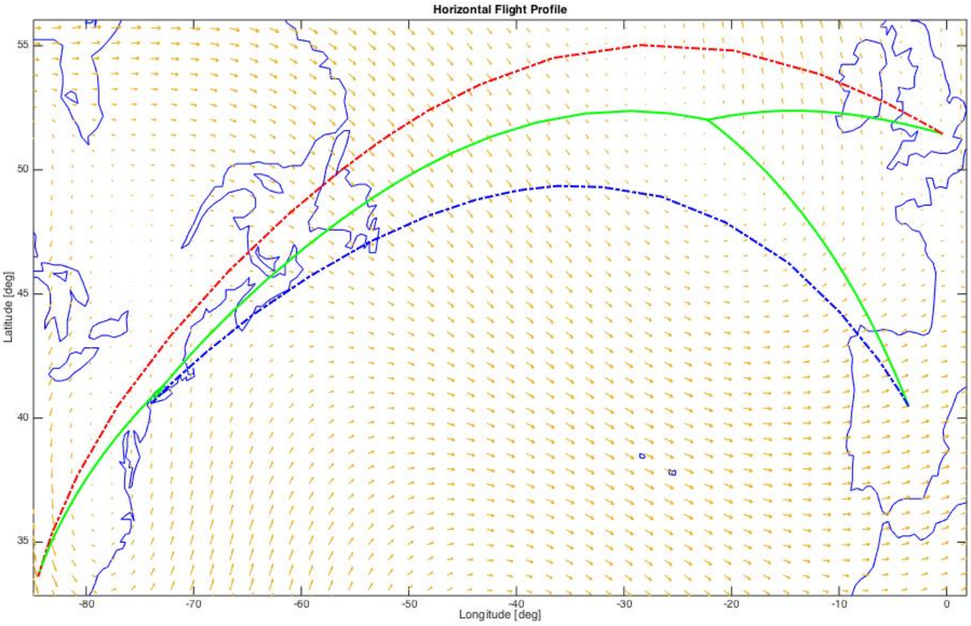
Horizontal Flight Profile
55
50
45
40
35
Latitude [deg]
-80
-70
-60
-50
-40
-30
-20
-10
0
Longitude [deg]

Figure F.2: Horizontal flight paths of the set of westbound flights. The dashed lines represent the optimal trajectories of the aircraft when flying solo and the solid green lines represent the optimal trajectories for the same flights that join in formation.

G

Results for the Three-Aircraft Formation (Experiment 9)

In this appendix the results for the three-aircraft formation (Experiment 9) are presented in more detail. In Table G.1 the results for the individual aircraft and for the total formation of both formations are presented. When comparing the results for the aircraft in formation to the corresponding solo flight, it shows that larger formations can result into larger fuel reductions. The results for the aircraft in a three-aircraft formation relative to their corresponding solo flights are presented in Table G.2.

Table G.1: Results for a three-aircraft formation flown by three B733 aircraft. Aircraft A from London to Atlanta, aircraft B from Amsterdam to New York City and aircraft C from Madrid to Toronto (Experiment 9)

Results	**Solo**				**Three-Aircraft Formation**			
	AC A	**AC B**	**AC C**	**Total**	**AC A**	**AC B**	**AC C**	**Total**
Fuel [kg]	16575	14035	14593	**45203**	15029	14265	13151	**42445**
Flight time [hr]	10.42	9.00	9.31	**28.73**	10.35	9.06	9.58	**28.99**
Distance [km]	6778	5863	6068	**18709**	6819	5953	6289	**19061**

Table G.2: Results for the aircraft in a three-aircraft formation relative to their corresponding solo flights (Experiment 9)

	Aircraft A	**Aircraft B**	**Aircraft C**	**Total**
Fuel	-9.33%	+1.64%	-9.88%	**-6.08%**
Flight time	-0.67%	+0.67%	+2.90%	**+0.90%**
Distance	+0.60%	+1.54%	+3.64%	**+1.88%**

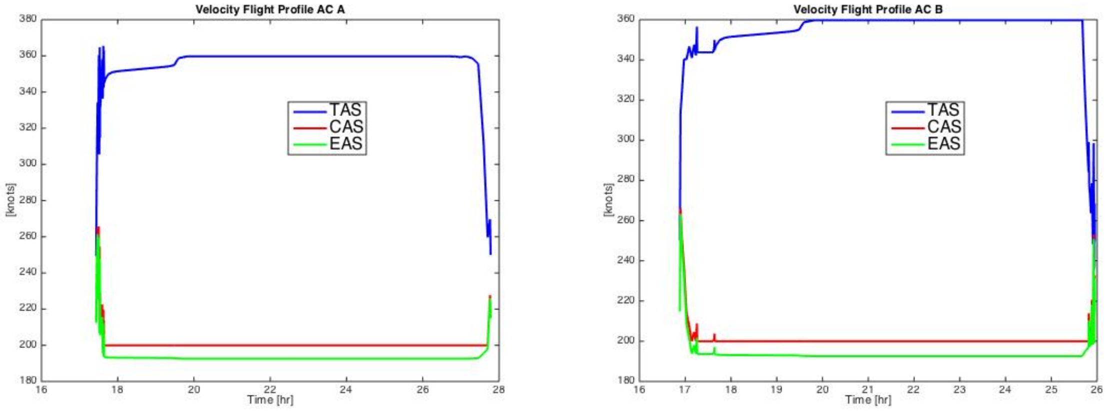

(a) Velocity profile of aircraft A

(b) Velocity profile of aircraft B

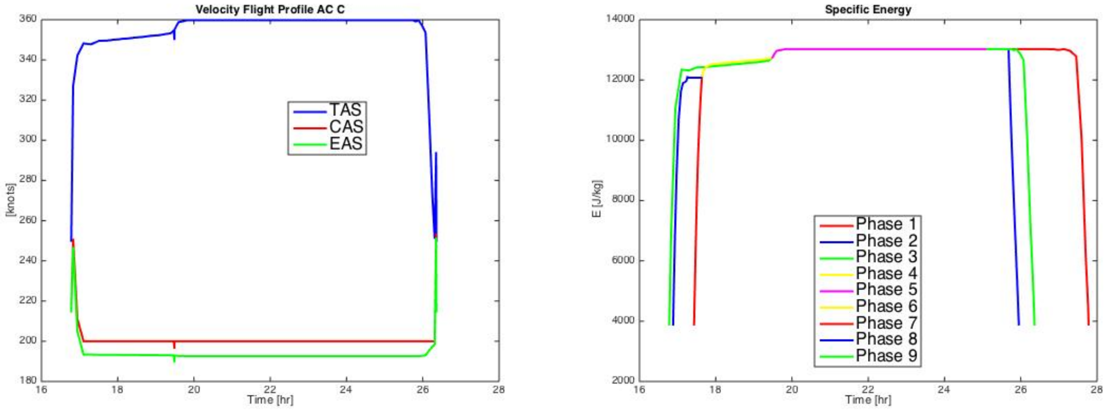

(c) Velocity profile of aircraft C

(d) Specific energies

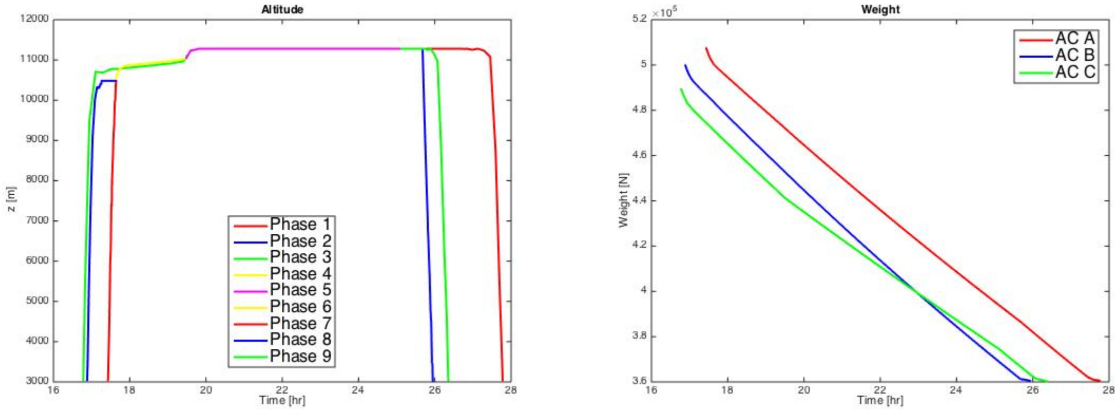

(e) Vertical flight profiles

(f) Aircraft weights

Figure G.1: Results for the three-aircraft formation experiment (Experiment 9)

Bibliography

[1] J. Pahle, D. Berger, M. Venti, C. Duggan, J. Faber, and K. Cardinal, *An Initial Flight Investigation of Formation Flight for Drag Reduction on the C-17 Aircraft,* AIAA Atmospheric Flight Mechanics Conference , 1 (2012).

[2] W. B. Blake, S. R. Bieniawski, and T. C. Flanzer, *Surfing aircraft vortices for energy,* The Journal of Defense Modeling and Simulation: Applications, Methodology, Technology **12**, 31 (2013).

[3] L. E. Herinckx, H. P. a. Dijkers, R. V. Nunen, D. a. Bos, T. L. M. Gutleb, H. Radfar, V. E. Rompuy, S. E. Sayin, D. J. Wit, and V. B. Blokland, *Formation flying as an innovative air transportation system for long-haul commercial flight: A focus on operational feasibility and potential gain,* 11th AIAA Aviation Technology Integration and Operations ATIO Conference , 1 (2011).

[4] S. A. Ning and I. Kroo, *Compressibility Effects of Extended Formation Flight,* 29th AIAA Applied Aerodynamics Conference , 1 (2011).

[5] C. Haissig, *Military formation flight as a model for increased capacity in civilian airspace,* The 23rd Digital Avionics Systems Conference , 1.C.4 (2004).

[6] J. Xu, S. Andrew Ning, G. Bower, and I. Kroo, *Aircraft Route Optimization for Formation Flight,* Journal of Aircraft **51**, 490 (2014).

[7] G. C. Bower, T. C. Flanzer, and I. M. Kroo, *Formation Geometries and Route Optimization for Commercial Formation Flight,* AIAA Journal (2009).

[8] M. Xue and G. S. Hornby, *An Analysis of the Potential Savings from Using Formation Flight in the NAS,* AIAA Guidance, Navigation, and Control Conference , 1 (2012).

[9] EUROCONTROL, *Coda digest q1 2015,* (2015).

[10] EUROCONTROL, *All-causes delay to air transport in europe,* (2016).

[11] KLM Corporate, *KLM Fact sheet network and hub systems,* (2014).

[12] *Royal dutch airlines,* `https://www.klm.nl/` (2016), [Online; accessed 24-06-2016].

[13] Boeing, *737 performance summary,* (2010).

[14] IATA, *New iata passenger forecast reveals fast-growing markets of the future,* `http://www.iata.org/pressroom/pr/Pages/2014-10-16-01.aspx` (2014), [Online; accessed 29-06-2016].

[15] IATA, *IATA ECONOMIC BRIEFING: Airline Fuel and Labour Cost Share,* , 2010 (2010).

[16] IATA, *IATA Carbon Offset Program Frequently Asked Questions,* (2014).

[17] P. B. S. Lissaman and C. A. Shollenberger, *Formation Flight of Birds,* Science **168**, 1003 (1970).

[18] T. E. Kent and A. G. Richards, *On Optimal Routing For Commercial Formation Flight,* AIAA Guidance, Navigation, and Control (GNC) Conference , 1 (2013).

[19] H. G. Visser, *A 4-D Trajectory Management and Guidance Technique for Terminal Area Traffic Management,* (1994).

[20] H. G. Visser and S. Hartjes, *Economic and environmental optimization of flight trajectories connecting a city-pair,* Proceedings of the Institution of Mechanical Engineers, Part G: Journal of Aerospace Engineering **228**, 980 (2014).

[21] W. B. Blake and D. Multhopp, *Design, Performance and Modeling Considerations for Close Formation Flight,* American Institute of Aeronautics and Astronautics, Inc. **2**, 476 (1998).

[22] S. Khan, *Flight trajectories optimization,* Science , 1 (2002).

[23] G. Ribichini and E. Frazzoli, *Efficient coordination of multiple-aircraft systems,* 42nd IEEE International Conference on Decision and Control (IEEE Cat. No.03CH37475) **1** (2003), 10.1109/CDC.2003.1272704.

[24] Z. a. Bangash, R. P. Sanchez, A. Ahmed, and M. J. Khan, *Aerodynamics of Formation Flight,* Journal of Aircraft **43**, 907 (2006).

[25] S. A. Ning, T. C. Flanzer, and I. M. Kroo, *Aerodynamic Performance of Extended Formation Flight,* Journal of Aircraft **48**, 855 (2011).

[26] S. A. Ning, I. Kroo, M. J. Aftosmis, M. Nemec, and J. E. Kless, *Extended Formation Flight at Transonic Speeds,* **51**, 1 (2014).

[27] Federal Aviation Administration, *APPENDIX A: NATIONAL AIRSPACE SYSTEM OVERVIEW,* `https://www.faa.gov/air_traffic/nas/nynjphl_redesign/documentation/feis/media/Appendix_A-National_Airspace_System_Overview.pdf` (2016), [Online; accessed 27-06-2016].

[28] J. Xu, S. A. Ning, and G. Bower, *Aircraft Route Optimization for Heterogeneous Formation Flight,* 53rd AIAA/ASME/ASCE/AHS/ASC Structures, Structural Dynamics and Materials Conference (2012), 10.2514/6.2012-1524.

[29] T. E. Kent and a. G. Richards, *A geometric approach to optimal routing for commercial formation flight,* AIAA Guidance, Navigation, and Control Conference 2012 , 1 (2012).

[30] T. E. Kent and A. G. Richards, *Analytic Approach to Optimal Routing For Commercial Formation Flight,* AIAA Guidance, Navigation, and Control (GNC) Conference , 1 (2015).

[31] S. Gueron and R. Tessler, *The Fermat-Steiner Problem,* **109**, 443 (2015).

[32] M. D. de Villiers, *A Generaliztion of the Fermat-Torricelli Point,* **79**, 374 (1995).

[33] W. B. Blake and T. C. Flanzer, *Optimal Routing for Drag-Reducing Formation Flight: A Restricted Case,* Journal of Guidance, Control, and Dynamics , 1 (2015).

[34] R. Ray, B. Cobleigh, M. J. Vachon, and C. St. John, *Flight Test Techniques used to Evaluate Performance Benefits During Formation Flight,* AIAA Atmospheric Flight Mechanics Conference (2002), 10.2514/6.2002-4492.

[35] E. Wagner, D. Jacques, W. Blake, and M. Pachter, *Flight Test Results of Close Formation Flight for Fuel Savings,* AIAA Atmospheric Flight Mechanics Conference and Exhibit , 1 (2002).

[36] O. Rodionova, M. Sbihi, D. Delahaye, and M. Mongeau, *North atlantic aircraft trajectory optimization,* IEEE Transactions on Intelligent Transportation Systems **15**, 2202 (2014).

[37] ICAO, *International civel aviation organization,* `http://www.icao.int/Pages/default.aspx`, [Online; accessed 24-06-2016].

[38] C. M. A. Verhagen, *Formation flight in civil aviation*, Ph.D. thesis, TU Delft (2015).

[39] S. Hartjes, *An Optimal Control Approach to Helicopter Noise and Emissions Abatement Terminal Procedures* (2015).

[40] A. V. Rao, C. L. Darby, and M. Patterson, *User's Manual for GPOPS Version 3.3: A MATLAB Software for Solving Optimal Control Problems Using Pseudospectral Methods,* Control (2010).

[41] D. Garg, M. A. Patterson, C. L. Darby, C. Francolin, G. T. Huntington, W. W. Hager, and A. V. Rao, *Direct Trajectory Optimization and Costate Estimation of State Inequality Path-Constrained Optimal Control Problems Using a Radau Pseudospectral Method,* , 1 (2012).

[42] F. Fahroo and I. Ross, *Advances in Pseudospectral Methods for Optimal Control,* AIAA Guidance, Navigation and Control Conference and Exhibit , 1 (2008).

[43] G. of Canada, *GDPS data in GRIB2 format: 66 km,* `http://weather.gc.ca/grib/grib2_glb_66km_e.html` (2016), [Online; accessed 25-05-2016].

[44] G. Evans, *Fuelplanner - advanced fuel planner for microsoft flight simulator,* `http://fuelplanner.com/index.php` (2016), [Online; accessed 24-06-2016].

[45] *Planes utilize most fuel during takeoff | worldwatch institute,* `http://www.worldwatch.org/planes-utilize-most-fuel-during-takeoff` (2013), [Online; accessed 24-06-2016].

[46] W. Roberson and J. Johns, *Fuel Conservation Strategies: Takeoff and Climb,* Aero Quarterly , 25 (2008).

[47] Boeing, *747-400 performance summary,* (2010).

[48] *Nyserda, "new york home kerosene price monitoring program",* `http://www.nyserda.ny.gov/Cleantech-and-Innovation/Energy-Prices/Kerosene/Average-Kerosene-Prices` (2016), [Online; accessed 24-06-2016].